AECL
TECHNOLOGIES INC.

June 15, 2003

Our File: 108US-013210-021-001
Your File: Project No. 722

U.S. Nuclear Regulatory Commission,
Document Control Desk,
Washington, D.C. 20555

Attention: Ms. B. Sosa
Project Manager, ACR

Reference:

1. Letter from B. Sosa to V. Langman, "Requests for Additional Information – ACR-700 Pre-application Review (TAC No. MB5765)", May 13, 2003.

Re: **RAI for ACR-700 Physics and Fuel Related Data**

In response to an NRC staff request (Reference 1) and in support of the NRC's pre-application review of the ACR (i.e., specifically focus topic # 9), please find enclosed the report: "ACR-700 Reactor Physics Design", AECL Report No. 10810-03300-ASD-001 by M. Ovanes.

If you have any questions on this letter and/or the enclosed report please contact the undersigned at (905) 823-9060 extension 6543.

Yours sincerely,

V. J. Langman for

Vince J. Langman
ACR Licensing Manager

/Enclosures:
1. Report: "ACR-700 Reactor Physics Design", AECL Report No. 10810-03300-ASD-001, by M. Ovanes.A

D070

481 North Frederick Avenue, Suite 405, Gaithersburg, MD, 20877 U.S.A., Tel. 301-228-8240, Fax. 301-417-0746

AECL
TECHNOLOGIES INC.

April 15, 2003

Our File: 108US-013210-021-001
Your File: Project No. 722

Ms. Belkys Sosa
ACR Project Manager
US NRC – M/S 0-4D9A
11555 Rockville Pike
Rockville, MD 20852-2738
U.S.A.

Dear Ms. Sosa,

Re: **AECL Copyright Notice**

During the current pre-application review for the ACR AECL Technologies will be transmitting documents to the NRC that bear an AECL copyright notice. The NRC is permitted to make the number of copies of these reports which is necessary for NRC's internal use in connection with the ACR pre-application review, subject to the requirements of 10CFR 2.790 regarding restrictions on public disclosure to the extent that such information has been identified as proprietary by AECL, copyright protection not withstanding. For the non-proprietary versions of these reports, where they exist, the NRC is permitted to make additional copies (i.e., beyond those necessary for its internal use) in order to have one copy available for public viewing in the appropriate record retrieval system, ADAMS or from the Public Document Room as may be required by NRC regulations. All copies made by the NRC of any AECL documents must include any copyright and/or proprietary notices that are present in the copies sent to the NRC.

If you have any questions with regards to this letter please contact the undersigned at (905) 823-9060 extension 6543.

Yours sincerely,

for Vince J. Langman
ACR Licensing Manager

481 North Frederick Avenue, Suite 405, Gaithersburg, MD, 20877 U.S.A., Tel. 301-228-8240, Fax. 301-417-0746

AECL EACL

Assessment Document

ACR-700
Reactor Physics Design

ACR-700

10810-03300-ASD-001
Revision 2

2003 June

CONTROLLED - Licensing

2251 Speakman Drive
Mississauga, Ontario
Canada L5K 1B2

Juin 2003

CONTRÔLÉ - Permis

2251, rue Speakman
Mississauga (Ontario)
Canada L5K 1B2

AECL EACL

Assessment Document

ACR-700 REACTOR PHYSICS DESIGN

ACR-700

10810-03300-ASD-001

Revision 2

Prepared by
Rédigé par

Ovanes Michaela

Reviewed by
Vérifié par

Chan Peter

Approved by
Approuvé par

Bonechi Massimo

2003/06/06
Controlled
Licensing

2003/06/06
Contrôlé
Licensing

2251 Speakman Drive
Mississauga, Ontario
Canada L5K 1B2

2251 rue Speakman
Mississauga (Ontario)
Canada L5K 1B2

AECL EACL

Release and Revision History / Liste des documents et des révisions

0939B Rev. 13

Document Details / Détails sur le document

Title / Titre	Total no. of pages / Nbre total de pages
ACR-700 Reactor Physics Design	

CONTROLLED – Licensing – CONTRÔLÉ - Permis

Release and Revision History / Liste des documents et des révisions

Release Document No./N°	Date	Revision Révision No./N°	Date	Purpose of Release; Details of Rev./Amendement Objet du document; détails des rév. ou des modif.	Prepared by Rédigé par	Reviewed by Examiné par	Approved by Approuvé par
1		D1	2002/06/25	Issued for Review and Comment.	M. Ovanes	P. Chan	M. Bonechi
2		0	2002/06/28	Issued as "Approved for Use".	M. Ovanes	P. Chan	M. Bonechi
3		1D1	2002/09/04	Issued for Review and Comment.	M. Ovanes	P. Chan K.S. Kozier B. Rouben I. Love E. Choy A. Josefowicz J. Millard K. Hau	
4		1	2002/09/30	Issued as "approved for use". The document number has changed from 108-03300-TD-001 to 10810-03300-ASD-001.	M. Ovanes	P. Chan	M. Bonechi
5		2D1	2003/04/24	Issued for Review and Comment.	M. Ovanes	P. Chan P.G. Boczar B. Rouben G.B. Wilkin A.G. Lee K. Kozier	M. Bonechi

DCS/RMS Input / Données SCD ou SGD

Rel. Proj. Proj. conn.	Project Projet	SI	Section	Serial Série	Sheet Feuille No. N°	Of De	Unit No.(s) Tranche n°
	10810	03300	ASD	001	1	1	

AECL EACL

Release and Revision History / Liste des documents et des révisions

0939B Rev. 13

Document Details / Détails sur le document

Title / Titre	Total no. of pages / Nbre total de pages
ACR-700 Reactor Physics Design	

CONTROLLED – Licensing – CONTRÔLÉ - Permis

Release and Revision History / Liste des documents et des révisions

Release Document		Revision Révision		Purpose of Release; Details of Rev./Amendement Objet du document; détails des rév. ou des modif.	Prepared by Rédigé par	Reviewed by Examiné par	Approved by Approuvé par
No./N°	Date	No./N°	Date				
6		2	2003/06/09	Issued as "Approved for Use".	M. Ovanes	P. Chan	M. Bonechi

DCS/RMS Input / Données SCD ou SGD

Rel. Proj. Proj. conn.	Project Projet	SI	Section	Serial Série	Sheet Feuille No. N°	Of De	Unit No.(s) Tranche n°
	10810	03300	ASD	001	2	2	

ABSTRACT

ACR™ (Advanced CANDU Reactor™)[1] is the "Next Generation" CANDU®[2] reactor, aimed at producing electrical power at a capital cost significantly less than that of the current reactor designs. The ACR achieves substantial reduction in capital cost by using H_2O coolant, Slightly Enriched Uranium (SEU) fuel, in a compact D_2O-moderated lattice. Full-core coolant-void reactivity is slightly negative. The use of the CANFLEX®[3] fuel-bundle design and the flat flux and power distributions enable ACR to operate at higher channel and bundle powers with improved safety margins. The tight neutronic coupling in a small core results in excellent stability, which is further enhanced by a moderately negative power coefficient.

The ACR is easily scalable to accommodate various reactor power output requirements by adjusting the number of fuel channels in the reactor design. The current reference ACR design is the ACR-700 which features 284 channels and has a reactor thermal-power output of 1982 MW(th).

This reactor-physics assessment document reflects the computer codes, nuclear-data libraries, and the design of the ACR core used in the conceptual physics design and safety analyses up to April 2003.

---

1 ACR™ (Advanced CANDU Reactor™) is a trademark of Atomic Energy of Canada Limited (AECL).

2 CANDU® (CANada Deuterium Uranium) is a registered trademark of Atomic Energy of Canada Limited (AECL).

3 CANFLEX® is a registered trademark of AECL and the Korea Atomic Energy Research Institute (KAERI)

TABLE OF CONTENTS

TABLE OF CONTENTS

TABLE OF CONTENTS

TABLES

TABLE OF CONTENTS

SECTION PAGE

FIGURES

TABLE OF CONTENTS

TABLE OF CONTENTS

TABLE OF CONTENTS

SECTION PAGE

APPENDICES

1. INTRODUCTION

The present document reflects the state of the analysis and ACR core design for the conceptual physics design and preliminary safety analysis. In parallel with this analysis, an assessment of the adequacy of the physics computer codes and reactor modeling techniques used for ACR physics applications is currently being conducted. The results of this assessment may result in changes to either the codes used in ACR physics analysis, or the modelling of the ACR. Thus, this report represents a snapshot in time of the ACR core design and analysis up to April 2003.

The ACR is characterized by the traditional CANDU fuel channel design, but featuring light-water coolant, heavy-water moderator and reflector, slightly-enriched uranium (SEU) fuel, and a reduced lattice pitch (distance between fuel channels). This core design retains important benefits of the previously well-established CANDU design concept, but introduces additional benefits.

Standard CANDU benefits include:

- Separate low pressure low-temperature moderator circuit, which is available as an inherent emergency heat sink
- Reactivity mechanisms and instrumentation located in low pressure and low temperature moderator environment
- On-power refuelling enables improved plant performance

Additional ACR benefits include:

- Flat and stable core flux and power distributions, with minimal requirement for reactivity mechanisms
- Core and fuel designs are optimised to achieve benign neutronic characteristics such as moderately negative power and coolant-void reactivity coefficients
- SEU fuel enables much higher burnup than Natural Uranium (NU) fuel
- CANFLEX fuel bundle design increases reactor power output by reducing element ratings and improving safety margins

The ACR core design is very adaptable to varying configurations. For example, the reference reactor design is optimised for base-load operation, but if deep load-following capability is desired, additional absorber rods can be added to the core configuration with no adverse effect on reactor operation. Within the reference SEU fuel cycle, as experience is gained with fuel performance, burnup can be increased in a stepwise manner, again with very little effect on reactor operating characteristics.

Similarly, the ACR core can be readily adapted to different power outputs. This can be done by increasing or decreasing the number of fuel channels, while maintaining identical fuel and fuel-channel characteristics. Reactivity-mechanism configuration is adjusted, using the same individual mechanism and flux detector design as for the reference ACR-700. The specific number of fuel channels and reactivity control devices depends on the size of the reactor, but the basic neutronic characteristics are similar for all sizes of the ACR currently under consideration.

2. DESIGN REQUIREMENTS

2.1 Physics-Design Basis

Power is produced in the core of a nuclear reactor by the neutron-induced fission of the fissile isotopes of uranium and plutonium contained in the fuel. Continuous power production is only possible if the materials in the core are chosen and arranged in such way as to produce a sustained nuclear chain reaction. This means that the number of neutrons produced by the fission process is sufficient to balance the number of neutrons lost in various removal processes. The main physics-design requirement for the ACR is, therefore, to sustain a controlled chain reaction within the reactor core for the production of power.

The overall physics-design requirements considered in the development of the ACR concept can be broken down into the following categories:

- Retain the basic proven characteristics of the CANDU reactor, while optimising the design by utilizing SEU fuel to use light-water coolant and reduce the amount of heavy-water moderator in the lattice cell.
- Target the coolant-void reactivity at a slightly negative value.
- Increase the core-average discharge fuel burnup to at least 20 MWd/kgU.
- Enhance the reactor safety and control characteristics.
- Maintains the traditional CANDU advantage of fuel-cycle flexibility.

2.1.1 Reactor Type and Total Power Output

The ACR adopts an evolutionary approach, incorporating significant design changes while retaining the traditional CANDU features:

- Modular horizontal fuel-channel core design
- Proven-technology of simple and economical fuel-bundle design
- On-power refuelling
- Separate low-pressure and low-temperature moderator with back-up heat sink capability
- Heavy-water moderator.

The reference ACR-700 design has 284 fuel channels producing 731 MW(e) inside a 5.20-metre diameter calandria shell. The total reactor thermal output is 1982 MW(th).

2.1.2 Type of Fuel

The ACR is designed to operate with Slightly-Enriched Uranium (SEU) fuel using the 43-element CANFLEX bundle design. Each fuel channel contains 12 bundles. Each bundle is 49.53 cm long.

In order to maximize the fuel utilization and fuel burnup, the number of neutrons lost in parasitic (non-fissionable) materials must be minimized. This is accomplished by using materials of low neutron-absorption cross section, such as zirconium alloys, for structural components. On-power fuelling also improves the overall fuel efficiency.

2.1.3 Definitions of Moderator and Coolant

The ACR is a channel-type reactor. Coolant is defined as the liquid inside the fuel channel. Moderator is defined as the liquid outside the fuel channel. The pressure tube, the calandria tube and the gas gap between them provide physical separation of the pressurized, high-temperature coolant from the low-pressure and temperature moderator. The ACR is designed to operate with light-water (H_2O) coolant and heavy-water (D_2O) moderator.

2.1.4 Coolant-Void Reactivity and Fuel Burnup

The ACR is designed to operate with a slightly negative coolant-void reactivity for nominal operating conditions. The current design target is –3 milli-k (mk), which includes an uncertainty of ± 2 mk. The design target for the core-average discharge fuel burnup is at least 20 MWd/kgU.

2.1.5 Major Reactivity Effects

The ACR is designed to operate with:

- Negative power feedback coefficient
- Negative temperature feedback coefficients for the moderator, coolant, and fuel.

3. ANALYTICAL METHODS AND REACTOR-PHYSICS CODES

The full set of nuclear cross sections required to solve the finite-difference neutron-diffusion equation for a CANDU reactor is evaluated by means of a three-step process:

- First, the bare-lattice cross sections are generated for each basic lattice cell in the core, through a cell-code calculation. Since reactivity devices are not present everywhere in the core, they do not affect every lattice cell, and are therefore not included in the cell calculations.
- The second step refers to the representation of reactivity devices, which, in CANDU reactors, are placed vertically or horizontally at some locations in the moderator, interstitially between fuel channels. In a three-dimensional reactor model, the reactivity devices are usually represented with incremental cross sections generated through a supercell calculation.
- In the last step, these incremental cross sections are added to the unperturbed lattice-cell properties to represent the effects of the device on neutron-flux distributions and system reactivity.

This entire process of finite-reactor physics analysis relies on a suite of computer codes, each one part of the Industry Standard Toolset (IST) for CANDU reactor analysis. The bulk of results presented here were obtained using:

i) the transport code WIMS-IST [1] for the calculation of lattice-cell properties (WIMS-AECL release 2.5d, with the 89-energy-group ENDF/B-VI ver. 1a1 nuclear-data library [2])

ii) the transport code DRAGON ver. 3.04 [3] for three-dimensional (3D) modelling of reactivity devices

iii) the Reactor Fuelling Simulation Program (RFSP-IST) [4] code for core design and fuel management simulations.

3.1 Lattice Calculations

Lattice cell calculations are required to generate most of the information required in CANDU core physics analyses for design, operation, and accident assessment. The cell code used for the design of the ACR-700 is WIMS-IST.

The program has the following capabilities:

a) It calculates diffusion coefficients, lattice reactivity, multi-group cell-averaged cross sections, and isotopic composition as a function of fuel irradiation.

b) It calculates the two-energy-group lattice parameters which are used in detailed reactor core simulations and fuel-management studies with two-group diffusion codes, such as RFSP-IST. The basic information required for this is the detailed distribution of the neutron flux in space and energy throughout the lattice cell, the configuration and composition of all materials in the lattice cell, and the neutronic properties of all those materials.

c) Using the perturbation feature, the program can be used to calculate the reactivity effect of changes in the fuel temperature and changes in the temperature and density of the coolant and moderator. Such calculations are performed to predict various reactivity coefficients and other important quantities such as the loss-of-coolant reactivity. Moreover, the variation of reactivity coefficients with fuel irradiation can also be calculated.

The basic approach of the WIMS-IST code is to set up and solve the steady-state neutron transport equation in two-dimensions for a lattice cell where the microscopic cross sections of each nuclide in the cell are available from an external nuclear-data library. The standard AECL multigroup cross-section library used for CANDU lattice calculations is the 89-energy group ENDF/B-VI library.

Although several options are available, the neutron distribution is usually found by the method of collision probabilities. The cross sections incorporate corrections for resonance reactions in pin cell and cluster geometries, both scattering and absorption. To maintain a steady state distribution of neutrons, an outer iteration (between energy groups) on the neutron multiplication factor *k-eff* is placed around the inner iteration of the neutron-flux distribution convergence within the group. Burnup step calculations are performed, altering the appropriate number densities of nuclides and the transport equations are solved again for the cell with the new composition. WIMS-IST outputs include, among others, reaction rates by material or by region, few-group diffusion-theory parameters for full-core reactor studies, nuclide densities upon irradiation, power production by region, and activation of experimental foils, if any, that are introduced into the lattice cell.

3.2 Supercell Calculations

Reactivity devices such as zone controllers, shutoff units, mechanical control absorbers, etc., are represented in core simulations by the use of incremental cross sections derived through three-dimensional supercell calculations. These incremental cross sections are added to the basic lattice-cell properties to evaluate the effect of the device on neutron-flux distributions and system reactivity. Three-dimensional calculations are required because reactivity devices are transverse to fuel channels.

The supercell models the fuel channel, reactivity device and associated moderator. The supercell methodology [5, 6, 7] that has recently been adopted for performing incremental-cross-section calculations for CANDU reactivity devices is based on the DRAGON code. This method uses explicit three-dimensional neutron-transport theory to calculate the macroscopic neutron-flux distribution in and around CANDU reactor fuel channels and reactivity-control devices. One of the main advantages that DRAGON offers is the possibility to couple inside a single code detailed multi-group neutron-transport calculations for 2- and 3-dimensional geometries (such as mixed Cartesian and r-θ-z geometries) in a collision-probability formalism.

3.3 Core Design and Fuel-Management Calculations

3.3.1 Steady-State Reactor Simulations

For steady-state reactor simulation, the most frequent method to obtain global flux distributions is by solving the finite-difference form of the neutron-diffusion equations. The solution in the RFSP-IST code is based on 2-energy group diffusion theory using the three-dimensional finite-difference method.

The finite-difference spatial grid is constructed with sufficient detail to limit the solution error and to represent the heterogeneities in the reactor model. As an example, a typical grid interval in the reference ACR RFSP full-core model is 11.0 cm (one half of a lattice pitch). This grid-structure is needed to represent the neutron-absorber devices placed between fuel channels.

The RFSP-IST code is used to study the effects of different fuel-management schemes on reactor flux-and power distributions. This code is capable of calculating time-averaged and instantaneous flux, power, burnup, and irradiation distributions. RFSP-IST is also used to simulate various reactor operations including channel refuellings. The code is flexible enough that it may be used for a variety of core design and safety-analysis calculations in addition to fuel management.

RFSP is also used for dynamic simulations involving xenon transients. Xenon transients are simulated as a series of steady-state cases with the flux, xenon, and iodine levels assumed constant over short time intervals. The response of the spatial-control system to xenon redistribution and reactivity-device movements can also be simulated in the "quasi-dynamic" approximation. RFSP can also solve the time-dependent neutron-diffusion equation for use in fast transients such as loss-of-coolant accident (LOCA) transients, where the delayed-neutron effects are important.

The flux harmonics (higher-order eigenfunctions of the diffusion equation) are used for flux mapping and also in the study of spatial stability and reactor control. The *MONIC module of RFSP is used to numerically calculate the flux harmonics of the steady-state neutron-diffusion equation, again using a three-dimensional, two-group, finite-difference neutron diffusion method. It solves for the flux harmonics by use of a Fourier expansion technique, whereby known harmonics are subtracted out from the unconverged flux, and convergence is forced on the highest harmonic remaining in the unconverged flux.

RFSP also has the capability to perform flux mapping based on in-core-detector readings and pre-calculated flux modes generated by the *MONIC module.

The diffusion-theory modelling in RFSP has been enhanced by the addition of the local-parameter methodology. In the traditional "uniform-parameter" method, "effective" values for fuel flux and fuel temperature, coolant density and coolant temperature are used for every bundle when calculating the lattice cross sections. The local-parameter method accounts for local conditions at each bundle. The fuel flux and fuel temperature are made consistent with the bundle power for each bundle. The coolant temperature and coolant density at each bundle location are obtained from a thermal-hydraulics code such as NUCIRC [8].

3.3.2 Space-Time Kinetics Calculations

To calculate space-dependent neutronic transients on a time-scale where delayed-neutron effects are important, *CERBERUS, the space-dependent kinetics module of RFSP-IST, is used. The most typical application of this is the evaluation of the power transient resulting from a hypothetical LOCA event, and the performance of the shutdown system in terminating a power excursion under accident conditions. The CERBERUS module employs the Improved Quasi-Static (IQS) method [9] to analyse space- and time-dependent neutronic transients. In this method, the space-time flux is factored into an amplitude function, which is only time-dependent, and a space function, which is only weakly dependent on time. A backward difference approximation is used for the time derivatives. The space function is calculated in three dimensions and two energy groups, using finite-difference diffusion methods. Generally, six delayed-neutron precursor groups are used, although more groups (to accommodate photo-neutrons explicitly) may be used. The code can accurately simulate flux-shape retardation effects in space and time from delayed-neutron holdback following asymmetric coolant voiding, shutdown system action, etc. Point-kinetics codes are used to analyse situations where spatial effects are unimportant.

4. LATTICE-CELL DESIGN

4.1 Negative Coolant-Void Reactivity

One of the key parameter that determines the coolant-void reactivity (CVR) in the ACR is the moderator-to-fuel volume ratio in the lattice cell. At the CANDU-6 lattice pitch of 28.575 cm, a CANDU reactor with H_2O coolant would have a highly positive CVR. The lattice of existing CANDU reactors has a large moderator-to-fuel volume ratio of 16.4, resulting in a well-moderated lattice that is optimized for the natural uranium fuel cycle. An effective way of reducing the coolant-void reactivity, for a CANDU reactor using H_2O coolant and SEU fuel, is to reduce the lattice pitch until an under-moderated lattice condition is reached.

The lattice becomes under-moderated when the D_2O moderator volume alone cannot provide sufficient moderation to achieve maximum reactivity. The H_2O inside the fuel channel then functions as both coolant and moderator. Coolant-void reactivity is determined by the net result due to the loss of absorption (a positive reactivity change) and the loss of moderation (a negative reactivity change). Spatial and spectral changes of the neutron flux in the lattice cell due to voiding of the coolant, as well as the nuclide composition in the fuel, also affect the coolant-void reactivity.

Coolant-void reactivity in the ACR is a design parameter; lower values can be achieved mainly by reducing the lattice pitch. The current design target of ACR coolant-void reactivity is –3 mk, which includes an uncertainty allowance of ± 2 mk. The relationship between coolant-void reactivity and the moderator-to-fuel volume ratio was studied using the lattice code WIMS-IST and the more rigorous Monte Carlo code MCNP [11] with the ENDF/B-VI nuclear data library. It was determined that a moderator-to-fuel volume ratio of less than 6.0 is required to achieve a slightly negative coolant-void reactivity. This would require the reduction of the lattice pitch from the CANDU-6 value of 28.575 cm to about 20 cm.

From a physics point of view, reducing the lattice pitch to about 20 cm would be sufficient to achieve a slightly negative coolant-void reactivity, however, how much it can possibly be reduced is dictated by mechanical and manufacturing constraints. The space requirements between feeders in adjacent fuel channels in a CANDU reactor determine the minimum lattice pitch that is permissible. A detailed engineering assessment recommended a minimum lattice pitch of 22 cm, giving a moderator-to-fuel volume ratio of 8.4.

This ratio can be further reduced to 7.1 by displacing more moderator from this lattice cell by increasing the calandria tube outer radius from the current value of 6.6 cm to 7.8 cm. This is considered to be the maximum calandria tube size that still retains the necessary tube-sheet ligament strength required for a robust core mechanical design. The separation between adjacent calandria tubes is adequate for the installation of interstitial in-core reactivity control devices. However, there is still too much D_2O moderator in this lattice cell, resulting in a coolant-void reactivity significantly higher than the design target of –3 mk.

Using a small quantity of burnable poison in the central pin of a CANDU fuel bundle can further reduce the coolant-void reactivity. There is an increase in the thermal-neutron flux towards the centre of the fuel bundle upon voiding of the coolant. Depending on the amount of burnable poison incorporated in the central fuel pin, the resulting increase in neutron absorption could

generate a negative reactivity component strong enough to reduce the overall coolant-void reactivity from a slightly positive value to a slightly negative value.

There are two consequences of using burnable absorbers for coolant-void reactivity reduction:

1. Higher fuel enrichment is required to overcome the parasitic load of the absorber, which also increases the fuel-fabrication cost, and
2. The relative power in the central element that contains neutron absorber is reduced, resulting in a small increase in the power rating of the other elements.

The fuel enrichment and the burnable poison concentration can be tailored to meet the design targets of fuel burnup and coolant-void reactivity. Uniform fuel enrichment is used in the reference ACR fuel design. However, differential enrichment schemes, which use different enrichment in individual fuel rings, can be used to reduce the element rating in the bundle, if required.

Figure 4-1 shows the dimensions of the lattice pitch (LP), pressure tube (PT), calandria tube (CT), and the moderator-to-fuel volume ratio (VM/VF) in NU CANDU and ACR lattices. The small ACR lattice results in a highly compact reactor core. The savings in D_2O inventory are clearly demonstrated in Figure 4-2, which compares the size of this compact ACR core with those for other CANDU designs.

The current reference ACR-700 core has 284 fuel channels producing 731 MWe inside a 5.20-metre diameter calandria shell. One version of the ACR-1000 has 456 fuel channels producing 1093 MWe inside a 6.2-metre diameter calandria shell. Both versions of the ACR are significantly smaller in size than the existing CANDU 6 reactor, which has 380 fuel channels producing 728 MWe inside a 7.6-meter diameter calandria shell.

The compact lattice and slightly negative coolant-void reactivity result in moderate negative power feedback, high stability, and other benign neutronic characteristics for all sizes of ACR reactors currently under consideration. These features are further discussed in Sections 5 to 7.

4.2 Fuel-Bundle Configuration and Uranium Enrichment

The fuel used in the ACR is uranium dioxide sintered in the form of cylindrical pellets and clad in a zircaloy sheath using the CANFLEX fuel bundle design. The central element is natural uranium (NU) mixed with 4.6 wt% dysprosium (relative to the total mass of uranium). The remaining 42 fuel elements contain SEU fuel with uniform enrichment of 2.0 wt% of ^{235}U. All 43 fuel elements are fastened together at each end to form a fuel bundle containing a total of 17.98 kg of uranium. Each channel contains twelve fuel bundles. The fuel bundles are replaced on-power at a rate that compensates for the reactivity loss due to the depletion of ^{235}U and the build-up of fission products in the core.

Dysprosium is the best candidate to be used as neutron poison in the ACR fuel because its absorption cross section is most compatible with that of ^{235}U. Also, its chemical and physical properties are similar to those of gadolinium, which is widely used as a burnable poison in LWR fuel. NU was chosen as the dysprosium carrier rather than graphite or depleted uranium, because it offers lower fuelling costs and higher uranium utilization.

This fuel design gives a core-averaged discharge burnup of 20.0 MWd/kgU and a coolant-void reactivity of –5 mk, based on full-core fuel-management simulations using the RFSP-IST code with WIMS-IST (WIMS-AECL 2-5d-3 with the ENDF/B-VI v.1a1 library) lattice parameters.

Figure 4-3 shows the 37-element fuel bundle inside a CANDU-6 fuel channel and the 43 fuel elements in a CANFLEX bundle inside an ACR fuel channel. The inner 8 fuel elements in the CANFLEX bundle have a slightly bigger radius than the outer 35 fuel elements. This arrangement compensates for the thermal-flux depression caused by the two outer fuel rings, resulting in an improved power profile across the bundle.

4.3 MCNP Simulations

The WIMS lattice code was originally developed as a general-purpose code for reactor lattice-cell calculations for a wide range of reactor systems, including both thermal and fast reactors. Various versions of the WIMS lattice code have been used successfully to design the SGHWR and the FUGEN reactors, where the reactor core physics characteristics are similar to those in ACR. While precise experiments will be required to determine the absolute accuracy of the WIMS-IST calculations, it is desirable to confirm some of the basic ACR lattice properties calculated by the WIMS-IST code by using a more rigorous code, such as the Monte Carlo code MCNP.

Figure 4-4 shows the neutron spectra averaged over the fuel and coolant regions inside the pressure tube with and without the H_2O coolant. These results were calculated with MCNP using nuclide densities calculated with WIMS-IST for an ACR lattice cell at mid-burnup. The neutron spectrum "hardens" when the coolant is lost and the dips at low epithermal neutron energies become more pronounced. Figure 4-5 shows a general increase in the fast and epithermal neutron flux in the moderator region as a result of increased escape of fast neutrons from the voided channel, and an associated decrease in the thermal neutron flux due to the lack of moderation.

The dips in the spectra in Figure 4-4 are attributed to absorption effects in different uranium and plutonium isotopes at specific neutron energies. Figure 4-6 shows the large resonance absorption cross section of ^{238}U between 1 eV and 1 keV, while Figure 4-7 shows the prominent broad resonance of ^{239}Pu fission cross section centred at 0.3 eV. The behaviours of these cross sections have a major influence on the coolant-void reactivity in the ACR lattice.

Both MCNP and WIMS-IST predict that the ACR lattice is undermoderated at the nominal operating conditions. Voiding of the H_2O coolant removes its moderation effect, which renders the lattice even more undermoderated. The shift in neutron spectrum upon coolant voiding increases the absorption in ^{238}U in the resonance region. There is also a significant reduction of the fission-yield in ^{239}Pu due to the decrease in neutron flux near the 0.3 eV resonance. In addition, ^{240}Pu has a prominent absorption resonance at about 1.0 eV, while ^{162}Dy has a similar absorption resonance near 5.5 eV. These negative reactivity effects reduce the overall coolant-void reactivity in the lattice cell that would be expected from the loss of substantial absorption in the H_2O coolant.

Survey calculations using MCNP and WIMS-IST indicated that the ACR is an effective plutonium burner and that slightly negative coolant-void reactivity could be achieved in ACR using various plutonium-driven fuel cycles without the need for burnable poison. The on-line

refuelling capability of ACR allows full-core implementation of these advanced fuel cycles with consistently benign physics characteristics, without requiring major modifications to the reference design.

4.4 WIMS-IST Lattice-Cell Calculations

The purpose of a cell calculation is to provide information on the variation of cross sections and isotopic composition with fuel burnup, on reactivity coefficients, on the power distribution within the fuel bundle and on cell-averaged lattice parameters to be used in core calculations. The methods and accuracy with which this information is produced is critical to the overall accuracy of the full-core analyses.

WIMS-IST (WIMS-AECL release 2-5d [1]) is used together with RFSP-IST for the reactor-core design and safety analysis of the ACR.

All the lattice-cell calculations presented in this report were carried out using the standard model for routine calculations of ACR–type lattices, which is based on the recommendations described in References [12] and [13]. The depletion data and the microscopic cross-section library used in the WIMS-IST calculations was the 89-energy-group ENDF/B-VI library, modified to include the burnable dysprosium isotopes (library patch titled e6lib-1a1 [14, 15]).

4.4.1 Standard WIMS-IST Model for ACR Lattice

4.4.1.1 Equilibrium-Core Fuel

The lattice conditions at which the design simulations were performed are representative of an ACR equilibrium core at the nominal operating conditions. The fuel-channel design specifications, common to all ACR designs under consideration, are presented in Table 4-1.

The geometrical specifications of the CANFLEX 43-element fuel bundle used to perform the WIMS-IST lattice-cell calculations are presented in Table 4-2. The standard WIMS-IST input deck for the reference fuel at nominal operating conditions, with and without coolant, is presented in Appendix A.

The compositions of the ACR fuel materials in the four fuel rings were calculated according to the specified dysprosium concentration, uranium enrichment, total mass of uranium and total zircaloy mass in the bundle. The ENDF/B-VI regular cross-section set using unshielded zirconium data and ^{238}U data, as recommended in Reference [12], was used in all the WIMS-IST calculations. The weight percent composition for the nuclides in each fuel type is shown in Table 4-3. The nuclide number densities for fresh, mid-burnup and discharged fuel are presented in Appendix B. The reflector properties were obtained from a WIMS-IST calculation where the nuclide densities used to represent the fuel compositions were specified to correspond to an average mid-burnup of about 10 MWd/kgU, or about 300 full-power-days irradiation.

In the WIMS-IST models, fuel parameters were specified to represent the bundle in its nominal configuration. The composition of the fuel end-region was not explicitly represented in the model. Therefore, the material densities of the UO_2 and the sheath in each fuel ring in the WIMS calculations were defined so as to preserve the total mass of UO_2 and zirconium alloy over the total bundle length of 49.53 cm, while preserving the geometry of the fuel and cladding in the two-dimensional transport calculation. The total mass of uranium in the fuel bundle is 17.98 kg.

The total mass of zirconium in the bundle is 2.3 kg. A detailed representation of the end-region model will be incorporated in the WIMS-IST lattice model at a later stage of the design work. The gap between the UO_2 and cladding is not explicitly represented in the sample input, since the configuration with the cladding crept down onto the UO_2 is more typical of the reactor operating conditions. The inner and outer radii of the cladding correspond to those in a fresh cold fuel bundle. The volume and mass of the material of the appendages mounted on the cladding along the fuel stack length, including spacers, bearing pads, buttons and end-plates, were also included in the cladding in the WIMS-IST models by using an "effective" cladding density. The effective densities and weight fractions of zirconium and other nuclides in the zirconium alloys used in the ACR are given in Table 4-4.

4.4.1.2 Cell Spatial Discretisation

The lattice cell is subdivided into a number of mesh regions in each of which a flat neutron flux is assumed. For each pair of mesh regions and each energy group, a related collision-probability matrix is computed by the code. The current standard WIMS-IST methods for CANDU analysis are based on two-dimensional transport theory applied over the region in and around the fuel, and one-dimensional transport theory applied outside of that region. The choice for the boundary between the two- and one-dimensional domains was taken to be the end of the spectral coolant region at the fuel rubber-band perimeter. White circular-boundary condition is applied at the outer surface of the cell, with a 14-fold reflection symmetry factor.

The spatial approximation of radial flux variation is very much dependent on the number of the annuli defined in the cell model, while the fuel-rod subdivision impacts on the calculation accuracy of the local flux variation inside the fuel.

In the standard WIMS-IST model for the ACR-lattice (see Appendix A), the fuel rod subdivision consists of 2 rod sub-annuli with no sectorial subdivision for the central pin, and 2 fuel annuli each of which is further subdivided into two radially opposite sectors (relative to the bundle centre) for the fuel elements in the inner, intermediate and outer rings. The material specifications within each fuel-rod region were defined as separate materials, to allow the different burnup rates in the different element subdivisions to be properly captured. Consequently, the central pin was specified as 2 different materials (fuel 1a and fuel 1b), while 4 different materials were specified for each one of the three other fuel rings in the cluster cell (for example: fuel 2a1, fuel 2a2, fuel 2b1 and fuel 2b2 materials were defined for fuel elements in the inner ring). For the region inside the pressure tube, a total of 63 coolant annuli were explicitly defined: 60 coolant annuli with a coolant-spectral type inside the fuel rubber band, and 3 other coolant annuli with a moderator-spectral type. The moderator region contains 14 annuli, each about 0.3 cm thick. The pressure tube was divided into 3 annular meshes of equal thickness, while a single annular mesh was considered adequate for the calandria tube. Two-dimensional (2-D) neutron-transport calculation is performed for the region inside the fuel rubber band, while one-dimensional neutron-transport calculation is performed for the lattice cell outside this region.

Pressure-tube creep was not modelled in the standard WIMS-IST model for ACR, because the core-design calculations were based on the nominal operating parameters.

Isotropic tracking was performed using an angular quadrature set to 5 solid angles and a tracking density of 100 lines/cm^2, for the region covering the rubber-band area. This is sufficient to ensure

a tracking error less then 1% for the most important zones. A radial integration using 4 lines and 1 angle was used for the area outside the rubber band, where 1-D annular geometry applies.

4.4.1.3 Leakage Treatment and Energy Condensation

The properties of the ACR bundle allow the global effects to be represented by relatively simple leakage models and reflective boundary conditions imposed on the surfaces of the lattice cell, although the homogenized properties and the local flux distribution within the cell are calculated using neutron-transport theory. In this method of neutron-flux calculation, the spatial domain of the lattice cell is subdivided into a set of regions, and collision probabilities are used to determine the distribution of neutron flux over the regions. For CANDU-reactor applications, these calculations are usually performed within WIMS-IST in two-dimensional geometry over the region inside the pressure tube, and in one-dimensional geometry elsewhere, including the moderator region. The neutron spectrum was calculated in 50 energy groups (condensed from the 89 groups in the nuclear data library), chosen according to the energy bounds of the major reaction rates that are expected in the ACR lattice. The simulation modelled the fuel elements discretely; the *Pij* method was used to compute the collision-probability matrix that is required for self-shielding calculations and flux evaluation. A B_1 homogeneous-leakage treatment was considered in all the neutron-transport calculations for the axial and radial neutron leakage. At each burnup step, the multi-group transport equation was solved using a critical-buckling search option. The variation of the lattice k-infinity (yields/absorption in the leakage spectrum) with burnup is presented in Table 4-5.

Following the transport calculation of the spatial flux distribution, a two-energy group condensation was done by weighting the cell-averaged cross sections using the 50-energy-group critical-spectrum flux, with the lower bound energy cut-off at 0.625 eV for the fast group.

4.4.1.4 Power and Burnup Range

Burnup calculations were performed to model the transformation of the fuel composition as a function of irradiation and time, assuming a constant power rating of 32.34 W/g of initial heavy elements. This power rating corresponds to an average bundle power of 581.5 kW in ACR-700. Bundle-averaged fuel burnup was calculated up to approximately 29 MW·d/kg U, which spans the expected fuel burnup range. A total of 59 burnup steps were used in the WIMS-IST calculations in order to properly account for the change in material composition due to fuel depletion. Short time steps of one day were used to increment the burnup in the first stage, when the level of saturating fission products, xenon-135 in particular, is building up. Time steps of 10 and 20 days were used at later stages in the burnup calculations. The power distribution and element rating in each fuel ring as a function of the bundle burnup are given in Table 4-6.

The use of the CANFLEX bundle design allows ACR to operate at higher channel and bundle powers, while retaining acceptable margin to dryout, compared to the CANDU-6. Table 4-7 shows that the combined effect of flatter power profile and larger number of fuel pins results in about 10 to 15% reduction in the maximum fuel element rating in the SEU elements of the ACR CANFLEX bundle compared to the NU elements in the 37-element bundle design, for the same bundle power. The reduced maximum element rating results in additional margins to increase thermal power output and/or facilitate higher fuel burnup, or some combination of the two. The

thicker pressure tube in the ACR increases the thermal/electric conversion efficiency by enabling the heat-transport system to operate at higher temperature and pressure.

4.4.2 Voided Lattice

Since the coolant voiding during a large LOCA occurs in a time frame of seconds, an isotopic-depletion calculation was not necessary to be performed for the duration of the LOCA event; instead, the nuclide densities used to specify the fuel isotopic compositions were as generated in the cooled-lattice simulation, over the full range of burnup calculation. The fuel isotopic compositions were read in via the input-data stream, so as to ensure that, at each burnup step, the fission-product information associated with the specific fuel mixtures was consistent between the cooled-lattice case and the voided-lattice case. The change in the lattice-cell properties resulting from coolant voiding was calculated using a coolant-density perturbation to 0.001 g/cm^3. Also, at each burnup step, the multi-group transport equation was solved using a conventional critical-buckling search option, for both the cooled-cell case and voided-cell case. The change in the element ratings for each fuel ring for a typical 900 kW bundle upon voiding of the coolant is presented in Table 4-8. It can be seen that the flux level (normalized to 900 kW constant bundle power) at the central poisoned pin increases by about 21% upon LOCA. The increased neutron absorption by the dysprosium generates a negative reactivity component, resulting in a slightly negative coolant-void reactivity in the whole lattice cell.

4.4.3 Fuel-Channel Irradiation

The fuel channel is the pressure boundary in CANDU reactors. The ACR pressure tube is made of a Zr-2.5% Nb alloy, 116 mm in outer diameter and 6.5 mm thick. Zirconium components subjected to neutron irradiation undergo dimensional changes due to irradiation-induced growth. Creep is the dimensional change that occurs in stressed components, while growth is the dimensional change that occurs due to exposure to fast-neutron flux whether or not a component is stressed. Creep and growth are caused by high-energy neutrons of energy 1 MeV or higher, and contribute to the elongation of the pressure tubes and to their diametral expansion.

The maximum radial PT creep predicted in ACR is 4.7% over a period of 30 years of full power operation. The value of pressure-tube creep to be used in safety analyses is yet to be decided.

The variation of the fast flux at the pressure tube as a function of the bundle position in the channel is given in Table 4-9. The calculations were performed for a typical channel producing 7.3 MW(th) power for a 0 % crept pressure tube. Bundle position 1 in the channel is at the coolant inlet. For this configuration, the maximum fast-neutron-flux level in the pressure tube is about 0.4 x 10^{14} n/cm^2.s.

4.4.4 Bundle End-Region Flux Peaking

There are twelve fuel bundles in each ACR fuel channel. Thermal neutron flux peaks locally at the gap between adjacent fuel bundles because the zircaloy material at the bundle ends and the H_2O coolant between bundles absorb fewer thermal neutrons than does the UO_2 fuel. The thermal-neutron flux also peaks at the ends of the fuel channel (bundle-coolant contact) where there is no adjacent bundle, only coolant. This thermal-neutron flux peak results in an increase in fission power at the ends of the bundles relative to the centre of the bundles.

A physics assessment of the ACR bundle end-region flux-peaking effect showed that, for bundle-bundle contact configuration, the power-peaking factors vary in the range of 1.4 to 1.7 during irradiation. These factors are the peak linear pin powers relative to the linear pin power averaged over the whole bundle, and account for changes with burnup in both the axial- and radial-power distributions within the bundle. For the bundle-coolant contact configuration, the power-peaking factors are typically around 2.0 for both fresh and slightly irradiated fuel. Fuel-irradiation experiments are being scheduled at the NRU reactor to demonstrate that the ACR fuel will perform satisfactorily in the presence this power-peaking phenomenon.

5. REACTIVITY FEEDBACK AND COEFFICIENTS

"Reactivity coefficients" are defined as derivatives of the reactivity with various parameters about the nominal operating conditions. "Reactivity changes" are calculated as differences between given initial and final operating states. In the accident analysis e.g., large LOCA, the combined effect of various reactivity effects calculated for an instantaneous fuel-burnup distribution in the reactor is used to determine the system reactivity. The important parameters that influence the dynamic system reactivity (i.e., including the effect of delayed neutrons) are: i) coolant temperature (including density effect), ii) fuel temperature (based on the current bundle power and the coolant temperature), and iii) moderator poison concentration.

The reactivity coefficients of these parameters govern the core behaviour in terms of reactivity feedback when a steady state is perturbed. Therefore, these coefficients are the key factors in understanding the core response to:

- Routine operational manoeuvres, such as shutdown and restart, and other power-level changes
- Changes in the primary-heat-transfer-system conditions
- Reactor control and regulation, such as reactivity hold-down or compensation by soluble moderator poison
- Locations and movements of reactivity devices in the core
- Various postulated accident scenarios.

Table 5-1 compares the reactivity effects and kinetics parameters of the ACR to those of a conventional CANDU-6. All the reactivity coefficients presented in this table are based on WIMS-IST lattice-cell calculations with the 89-group ENDF/B-VI version 1a1 library at mid-burnup equilibrium-core conditions, except for coolant-void reactivity, which is calculated from full-core RFSP-IST. All the temperature reactivity feedback coefficients, including those of coolant, fuel and moderator, are negative in the ACR at all operating power levels.

The reactor kinetics and core stability are further discussed in Section 7. The results of the lattice reactivity coefficients and reactivity changes are given in the following subsections.

5.1 Fuel Temperature

The lattice parameters are affected by variations in fuel temperature due to changes in the neutron cross sections in the neutron-energy spectrum.

During operation at constant power, the fuel-temperature distribution is related to the power distribution. However, the effect of the fuel-temperature distribution on the overall neutron balance can be reproduced by using a spatially constant value, which is a typical effective average fuel temperature from a neutronic point of view. The effective fuel temperature is the single uniform fuel-temperature value, which, when used in a 3-D RFSP-IST time-average calculation, results in the same core reactivity as would be obtained using the distributed fuel-temperature calculation. This has been determined to be 687°C for NU fuel in a CANDU-6 reactor. This value is also used in the ACR pending on future revisions based on a detailed thermalhydraulics model.

Figure 5-1 shows the WIMS-based fuel-temperature reactivity coefficient as a function of fuel temperature for the reference ACR fuel lattice at mid-burnup. The fuel-temperature coefficient as

a function of fuel burnup is shown in Figure 5-2. This is negative for the entire burnup range of the reference ACR fuel. The fuel-temperature coefficient is –0.013 mk/°C for the ACR equilibrium fuel lattice.

5.2 Moderator Temperature (Including Density Effects)

The moderator-temperature coefficient (including density effect) for the ACR equilibrium fuel lattice is –0.024 mk/°C for moderator temperatures between 70°C and 90°C. Since the moderator temperature is controlled independently of the coolant temperature and the time constant for any significant change in the moderator temperature is very long compared to the duration of most reactivity transients, the moderator-temperature reactivity effect is not important in reactor dynamics. However, the negative moderator temperature feedback in the ACR does enhance reactor stability in the medium-term time frame.

5.3 Coolant Temperature (Including Density Effects)

A change in the coolant temperature affects the coolant density and the neutron spectrum. As the coolant temperature increases, the coolant density decreases and the neutron spectrum hardens. This causes an increase in the resonance absorption in the fuel, resulting in a negative-reactivity feedback in the ACR. Lattice reactivity effects due to changes in coolant temperature are calculated over the range of 290°C to 310°C using the WIMS-IST code for mid-burnup fuel. The density change accompanying a change in coolant temperature at constant pressure is included in these calculations. The coolant-temperature coefficient (including density effect) for the ACR equilibrium core is -0.010 mk/°C. This negative coolant-temperature feedback tends to stabilize the spatial power distribution following a global power perturbation.

5.4 Loss-of-Coolant Reactivity Effects

Coolant-void reactivity is calculated as the total reactivity change due to the complete loss of coolant from all the fuel channels. The ACR-700 is designed to operate with a slightly negative full-core coolant-void reactivity. Full-core coolant-void reactivity calculated with the RFSP-IST time-average model using the WIMS-IST-generated cross sections is –5.0 mk. This is based on nominal reference values for component dimensions and operating parameters, and does not include any allowance for code uncertainty or bias. A more rigorous treatment of coolant-void reactivity, including bias, uncertainty, and the range of operating parameters, will be included in the next stage of the core-design work.

The ACR lattice is nominally undermoderated in the core region. Voiding of coolant in the core region further reduces the moderation effect in the core and increases the migration of fast neutrons towards the reflector region. Figure 5-3 shows the change in the radial thermal-neutron flux shape as a function of time after a hypothetical voiding of all the coolant from the core. The increase in thermal-neutron flux in the reflector region relative to that in the core region during a LOCA reflects the increase in the reactor leakage which will further reduce the coolant-void reactivity. Because of the large change in global thermal-flux distribution upon LOCA, the lattice code WIMS-IST alone cannot predict the full-core coolant-void reactivity accurately. Hence, the full-core coolant-void reactivity for the ACR should always be obtained from full-core RFSP-IST simulations using lattice parameters generated by WIMS-IST.

Figure 5-4 shows the power transient in the ACR-700 calculated with CERBERUS for a postulated full-core LOCA scenario where 99% of the coolant in the core is voided within two seconds. It can be seen that the reactor power drops spontaneously after LOCA before the actuation of the safety systems. The shift in the thermal-neutron flux shape towards the reflector region is also shown. Figure 5-5 shows the effects of the trip time on the reactor power transient for the same LOCA scenario in ACR-700. The naturally-declining LOCA power transient allows the shutdown systems to be actuated by process signals instead of neutronic signals. The speed requirement of the safety systems can be relaxed so that the shutdown rods can be gravity-driven only, resulting in significant cost reduction and improvement in reliability.

Large and fast downgrading of the moderator purity from the reference 99.90 wt% to 90.0 wt% in the reference ACR lattice, such as would occur following an in-core LOCA, will introduce a reactivity change of –53 mk, almost equivalent to the insertion of all the shutoff rods, as illustrated in Figure 5-6. Hence, in-core LOCA in the ACR will cause a rapid and automatic shutdown of the reactor.

5.5 Effect of Coolant-Purity Downgrading

In traditional CANDU reactors which use D_2O coolant, the coolant-void reactivity is significantly affected by the presence of additional absorbers in the coolant, such as a downgrading of the coolant. The effect of coolant purity on void reactivity is irrelevant in the ACR because it uses H_2O coolant.

5.6 Effect of Moderator Poison

The above discussion of coolant-void reactivity applies to the nominal lattice, which has no boron or gadolinium in the D_2O moderator. Voiding of the coolant causes an increase of the thermal flux inside the fuel channel and a decrease of the thermal flux in the moderator. If poison (natural boron or gadolinium) were present in the moderator, the neutron absorption in the moderator would decrease upon coolant voiding. The resulting increase in the lattice reactivity would make the coolant-void reactivity less negative than the nominal value.

Each ppm of natural boron in the moderator is worth –2.1 mk in the ACR-700. Gadolinium is also used as a moderator poison. The reactivity effect of 1 ppm of gadolinium is equivalent to that of 3.5 ppm of natural boron. Each ppm of natural boron in the moderator increases the full-core coolant-void reactivity by about 0.5 mk.

Because the presence of neutronic poison in the moderator increases the coolant-void reactivity, the usage of moderator poison in the ACR will be kept to the minimum in order to keep the full-core coolant-void reactivity at a slightly negative value. The possible range of poison concentration in the ACR-700 is 0 to 1 ppm of natural boron for normal reactor operating conditions, and up to 5 ppm of Gd for reactor start-up after long shutdown. The reference design does not have any neutron-absorbing poison in the moderator during normal operation.

5.7 Moderator Purity

The nominal moderator D_2O purity is 99.90 weight % with the remaining 0.10 weight % made up of H_2O. A decrease in moderator D_2O purity implies an increase in H_2O concentration. The small amount of H_2O in the moderator increases the absorption effect of the moderator, resulting in a

decrease in the overall lattice reactivity. Figure 5-6 shows the change in lattice reactivity due to downgrading of the moderator purity from the nominal value of 99.90 wt%.

Figure 5-7 shows the relationship between full-core coolant-void reactivity and the D_2O purity over the range of 99.95 to 98.90 wt% based on WIMS-IST calculation for mid-burnup ACR fuel lattice. The coefficient is almost linear and depicts an increase in full-core coolant-void reactivity of 0.8 mk per 0.1% reduction in D_2O purity. Full-core calculations of the effect of moderator purity on the CVR will be performed at a later stage of the design work. Downgraded moderator purity affects the core radial reflector effectiveness, and the radial & axial flux extrapolation lengths. The impact on CVR is, however, estimated to be small. Statistics from operating CANDU reactors show that the moderator purity is consistently maintained at a purity level higher than 99.90 wt% within ± 0.05 wt%.

5.8 Power Coefficient of Reactivity

The two major components of reactivity feedback associated with a small increase in reactor power level are the coolant-density coefficient and the fuel-temperature coefficient of reactivity. Both of these coefficients of reactivity in the ACR are negative, resulting in negative power coefficients at all operating power levels.

The reactivity change from hot 0% power to 100% full power in ACR is estimated to be about -8.0 mk. Between 95% and 105% power levels, the power coefficient is about -0.07 mk/% FP.

Note that the different power levels in different channels would, in general, cause spatially non-uniform changes in coolant and fuel temperatures. Thus, the reactivity effects and power perturbations would be non-uniform in the core. Detailed coupled neutronic-thermalhydraulic simulations, which will account for local thermal-hydraulic parameters at each bundle position in the core, will be conducted at a later stage to determine the power coefficient more accurately.

6. REACTIVITY-CONTROL MECHANISMS AND SAFETY SYSTEMS

The layout of the reactivity mechanisms in the ACR-700 reactor is shown in Figure 6-1. Reactivity-control devices include neutron-flux measuring devices (self-powered flux detector, ion chamber), mechanical zone-control units and mechanical control absorber units for the reactor regulating system (RRS), and the devices of both reactor shutdown systems, i.e., shutoff rods for Shutdown System 1 (SDS1), and liquid-gadolinium injection nozzles for Shutdown System 2 (SDS2). The reactor shutdown systems are independent of each other and of the reactor regulating system. The reactivity mechanisms for SDS2 are installed horizontally through the sidewall of the shield tank. The safety and reactivity control mechanisms in ACR-700 are summarized in Table 6-1, along with those in existing CANDU-6 reactors. The detailed design of the reactivity-control mechanisms has not yet been finalized.

During normal operation, the zone-control units and control absorber units are used to control the reactivity in the reactor core. Under accident conditions, the reactor is shut down rapidly either by inserting the shutoff rods into the reactor core, or by injecting liquid poison into the heavy-water moderator in the calandria.

6.1 Control Requirements and Reactivity Worth

Day-to-day reactivity control is accomplished by on-power refuelling and zone-control action. The total reactivity worth of the zone controllers is sufficient for control of refuelling perturbations and suppression of xenon oscillations.

During off-normal operations, especially those that involve large changes in power, large feedback reactivity due to changes in temperature, density, and level of saturating fission products appears and is controlled by the use of control absorbers units (CAUs), and addition of soluble boron to the moderator, when necessary.

The reactivity load at 100% power due to xenon-135 is –26 mk. When this load disappears after a long shutdown (>40 h), soluble poison in the moderator is used to suppress the excess reactivity. The poison-concentration range in the ACR-700 is 0 to 1 ppm of natural boron for normal operating conditions, and up to 5 ppm of Gd for reactor start-up after a long shutdown.

The static reactivity worths of zone-control units, mechanical control absorbers and shutoff units given in the following sections correspond to a time-average equilibrium core.

6.2 Mechanical Zone-Control Units

The zone-control system provides fine regulation of reactor power. It consists of 9 zone-control units (ZCUs) or assemblies. Each assembly contains two independently-moveable mechanical absorbers, giving a total of 18 absorbers in the zone-control system. Nine of these absorbers enter the reactor from the top and the remaining nine absorbers enter the reactor from the bottom. An insertion level of 0% corresponds to a configuration where all zone-control absorbers are completely out of the reactor, and 100% insertion corresponds to a configuration where the top and bottom absorbers meet in the centerline of the core. The in-core portion of the absorber guide assembly is heavily perforated to allow free flow of moderator. Control of local and bulk power is accomplished by adjusting the position of each zone-control absorber under the control of the reactor regulating system computer. The locations of the mechanical zone-control units are shown in Figures 6-1 and 6-2.

The zone-control system is designed to perform two main functions:

- Bulk control, i.e., control of reactor reactivity and power output
- Spatial control, i.e., control of local flux and power shapes

The zone-control system maintains the desired global flux and power distributions by counteracting any power distortion or oscillation brought on by a space-dependent reactivity perturbation. In practice, the perturbations can be caused by:

a) fuel burnup between refuelling, and refuelling of channels,
b) power-level changes,
c) changes in the heat-transport-system conditions,
d) xenon oscillations,
e) movement of absorber rods, and
f) small variations in moderator-poison concentration.

The total reactivity worth of all ZCUs is -9 mk from 0% to 100% insertion. With all 18 zone controllers acting together, the maximum reactivity insertion rate is less than 0.2 mk/s.

The zone-control system is designed so that, during normal operation, the average zone-control absorber remains in the range 20% to 80% of full insertion. Assuming that the zone controllers operate nominally at 50% insertion, approximately ± 3 to ± 4 mk is available for the following operations:

- perform bulk- and spatial-control functions,
- provide about 12 minutes of xenon override time,
- reduce power from 100% to 75% and hold indefinitely, and
- provide reactivity for about 7 full-power days without refuelling.

6.3 Mechanical Control Absorber Units

Four mechanical control absorbers units (CAU) are provided as part of the reactor regulating system. They are inserted into the reactor core to adjust the flux level only at times when greater reactivity rate or depth is required than that provided by the zone control system. They are also used to compensate for the fuel-temperature reactivity effect after a reactor long shutdown. The design is essentially the same as that of the shutoff units (see Section 6.4). Under normal operation, these control absorbers are parked outside the core. They are inserted into the core under the automatic control of the RRS when rapid controlled reductions of the reactor power are required. Their arrangement is shown in Figure 6-1.

The maximum total reactivity worth of the CAUs is about -12 mk. This control reactivity should be available at an average reactivity-change rate of no less than 0.05 mk/s, and no more than 0.2 mk/s, when all rods are moved by their drive mechanism at full speed at the same time. When the rods are dropped, they should be fully inserted from their initial position in approximately three seconds. The maximum reactivity-insertion rate in this case is about -4 mk/s, which is considered fast enough to provide a fast shutdown by the control system but slow enough to allow a controlled partial rod drop.

Since the reactivity increase following a power reduction is significant and usually rapid, the zone controllers alone are incapable of counteracting the increase in all cases. In particular, the reactivity increase is the highest following a hot shutdown (when fuel temperature drops to coolant temperature). In this case, CAUs are used to compensate for the reactivity increase.

The control absorbers are normally inserted in banks (of two rods each) but can also be inserted individually. The percentage insertion depends on the degree of reactor power reduction. The optimum speed of insertion is determined primarily from control considerations.

6.4 Shutoff Units

The ACR-700 reactor is equipped with two physically independent shutdown systems. These systems are designed to be both functionally different and spatially separate. The functional difference is achieved by the use of shutoff units for SDS1 and liquid-poison injection for SDS2. Both systems are equally effective in quickly shutting the reactor down in an accident.

Twenty vertical shutoff units are provided as part of SDS1 for the rapid termination of reactor operation under emergency conditions. Shutdown is achieved by rapidly inserting neutron-absorbing elements into the reactor core. This action is initiated by the control logic of the SDS1. The absorber withdrawal is initiated by the control logic of the reactor regulating system.

The design of the shutoff units has not been finalized. Each shutoff unit comprises an absorber element, a vertical guide assembly, and a drive mechanism. The absorber in each shutoff unit can be either a thin cadmium sheet sandwiched between two oval-shaped steel tubes, or a rectangular tube filled with boron carbide. The in-core portion of the absorber guide assembly is heavily perforated to allow free flow of moderator. The absorber elements are inserted vertically into the reactor core by gravity drop. Their locations are shown in Figure 6-1. A proposed shutoff unit is illustrated in Figure 6-3. Most aspects of the proposed shutoff-unit design have been demonstrated in existing CANDU reactors.

6.4.1 SDS1 Static Reactivity Worth

Static reactivity calculations are valid on the assumption that the delayed-neutron precursor distribution is in equilibrium with the neutron flux. Static reactivity worths are used to calculate safety margins of the shutdown systems.

The static worth of 20 shutoff units fully inserted is about –60 mk in an equilibrium core. In accident analysis, two units are often postulated to be unavailable: one for maintenance and another assumed to have failed at the time of the accident. With the two most effective units out of service, the reactivity worth of the remaining 18 units is about –50 mk. The 20 shutoff units may be withdrawn in banks after a reactor trip. Withdrawal of shutoff units normally occurs when the reactor is subcritical.

For assessment of the performance of the shutdown systems during transient accident conditions, appropriate three-dimensional space-time calculations are performed. Such calculations yield a dynamic reactivity worth, which is, in general, greater (i.e., more negative) than the static reactivity worth.

6.5 Liquid Injection Shutdown Units

Six liquid-injection (LI) nozzles are provided as part of the second shutdown system (SDS2), to quickly terminate reactor operation under accident conditions. This is accomplished by injecting under pressure a concentrated gadolinium-nitrate solution directly into the heavy-water moderator in the calandria.

The liquid-injection nozzles are positioned horizontally in the reflector region, above the top row and below the bottom row of the fuel channels, as shown in Figure 6-2 (indicated in the figure as LI1 through LI6).

6.5.1 SDS2 Static Reactivity Worth

The concentration of the gadolinium-nitrate solution is initially about 8000 mg of Gd/kg D_2O. During the initial injection transient, there is considerable neutron self-shielding within the poison jets, and hence the initial reactivity is not very sensitive to the initial poison concentration. SDS2 contains sufficient amount of gadolinium to achieve a reactivity depth greater than –150 mk when the injected gadolinium is mixed uniformly in the moderator system. This is sufficient to keep the reactor at the guaranteed shutdown state under any normal operating conditions.

It is to be noted that the effectiveness of SDS2 in shutting the reactor down is not reliant on uniform mixing of the poison in the moderator, since that takes some time. The location of the liquid-injection nozzles in the reflector region, where there is a peak in the thermal-neutron flux (which increases even further in a LOCA, relative to the flux in the center of the core), is chosen to be in the region of high neutron worth. Consequently, while the total reactivity depth of SDS2 does depend on mixing of the poison in the moderator, the initial shutdown does not. Also, the design of the moderator circulation (number, location and orientation of inlet and outlet nozzles) ensures good moderator mixing, which is confirmed through testing in the Moderator Test Facility at Chalk River Laboratories (CRL) [10].

6.6 Shutdown Margin

Owing to its large negative reactivity worth, SDS2 provides more than adequate shutdown margin for any conceivable core condition. Both shutdown systems are available at all times under nominal operating conditions and the shutdown margin provided by SDS1 is further augmented by the availability of SDS2. The systems are, nevertheless, designed to be independently capable of providing adequate shutdown margin.

The normal operation of the RRS would insert all 18 zone controllers and drop the mechanical control absorbers on a reactor trip, and automatically add moderator poison, if required.

6.7 In-Core Flux Detector Units

Vertical and horizontal in-core flux detector units are installed in the reactor as part of the system provided for reactivity control of the reactor and for the shutdown systems. They use self-powered Hilborn-type detectors to produce a current proportional to the neutron flux within the reactor. This current signal is relayed to the reactor control or safety amplifiers, then to reactor control computers or shutdown-system trip units. The exact number of vertical and horizontal flux-detector assemblies for the ACR-700 core design has not yet been determined.

7. REACTOR KINETICS AND CORE STABILITY

The use of SEU fuel, H_2O coolant, and D_2O moderator in the ACR results in a harder spectrum in the fuel than that in the existing CANDU reactors. Fast neutrons born in fission in the core region may have to travel a long distance (in terms of lattice pitches) before they are adequately thermalized to initiate another fission cycle. However, fast neutrons born in fission in the peripheral channels can be thoroughly thermalized by the reflector, creating a large pool of thermal neutrons. Many of these thermal neutrons are reflected back into the core region. Consequently, the flux and power distributions in the ACR core are naturally flat and stable.

The ACR is spatially stable for all power levels up to the 105% full power under nominal operating conditions. It is not susceptible to xenon-induced spatial power oscillations because of the negative power feedback and strong neutronic coupling in a compact-core design.

7.1 Delayed Neutrons

The dynamic characteristics of CANDU reactors are strongly influenced by the presence of delayed neutrons. The rate at which the neutron population (and, implicitly, the reactor power) will change depends on the mean generation time (the average time interval between successive neutron generations). The great majority of the neutrons produced in fission are prompt, emitted essentially instantaneously. A very small fraction (less than 1%) of the neutrons from fission, however, appear much later. These delayed neutrons are produced both by direct neutron decay of some of the fission products and by photodisintegration of the deuterons in heavy water. Without the delayed neutrons, the mean neutron generation time would be essentially the same as the prompt-neutron lifetime (average time interval between birth of a neutron and its absorption in a subsequent fission reaction).

In reactor kinetics calculations, delayed-neutron precursors from any fissionable nuclide are collapsed, for practical purposes, into six distinct groups, with half-lives ranging from 0.2 sec to 50 sec. In CANDU there are additional delayed neutrons, produced by the photodisintegration of the deuterium in heavy water. These photo-neutrons appear from another eleven distinct precursor groups, with even longer time constants, ranging from tens to hundreds of thousands of seconds. These delayed-neutron and photo-neutron time constants are such that, in spite of the small delayed fraction, the "effective" (weighted-average) mean generation time is much longer than the prompt-neutron lifetime. The contribution from the photodisintegration of the deuterons constitutes only a small percentage (about 5%) of the total delayed-neutron yield.

Table 7-1 presents the delayed-neutron fractions and decay constants for the ACR-700 equilibrium core, along with the 11-group photo-neutron data (relative group yields and half-lives). Relevant data used in kinetics calculations are also given.

7.2 Prompt-Neutron Lifetime and Reactor Period

The prompt-neutron lifetime in an ACR lattice is 0.33 millisecond (ms), due to the relatively long diffusion time of the thermal neutrons in D_2O. This is shorter than the prompt-neutron lifetime value of 0.92 ms in the CANDU 6, but it is still a factor of 10 longer than that in the light-water reactors (LWRs).

This relatively long prompt-neutron lifetime, in combination with a negative power coefficient of reactivity, makes it relatively easy to control the total power and the power distribution in the

reactor core. Furthermore, the delayed-neutron fraction is enhanced due to the presence of delayed photoneutrons. These two factors considerably slow down a potential power excursion and hence relax the performance requirements on the shutdown systems. Figure 7-1, which is a generic family of curves based on ^{235}U fissions, shows the reactor period (time needed for an e-fold increase in neutron population) versus reactivity for various prompt-neutron lifetimes. For reactivity insertions at or near prompt critical, the CANDU lattice with the long neutron lifetime between 0.3 and 1.0 millisecond does not experience a drastic reduction in reactor period and hence does not experience a sudden increase in power excursion rate, such as that experienced by reactors with much shorter neutron lifetimes. In this context, whether the coolant-void reactivity during a LOCA is slightly positive or slightly negative has no consequences on reactor safety. Figure 7-2 shows that the effect of reducing the prompt-neutron lifetime from a typical NU CANDU value of 0.92 ms to a typical ACR value of 0.33 ms is negligible for a step increase in reactivity less than 1 mk. The maximum positive reactivity insertion rate in ACR during normal operation is less than 0.5 mk/s, which can be easily compensated by the reactor regulating system.

7.3 Flux Harmonics and Core Stability

Fifteen harmonics have been calculated for the ACR-700 flux mapping system using the *MONIC module of RFSP-IST for the reference time-average equilibrium core. These 15 modes, which include the fundamental mode and the first 14 natural harmonics, constitute the standard mode basis.

This mode basis is used for flux mapping (see Section 9.1.4) when the reactor is operating under nominal conditions, i.e. all mechanical control absorbers are fully withdrawn and xenon is at the equilibrium level. It is expected that this mode basis is sufficient to account for small perturbations due to zone-control actions and on-power refuelling. However, additional perturbation modes will have to be added to the standard mode basis in order to account for a fresh-core configuration or for strong perturbations, such as start-up transients and mechanical control absorber insertions.

Table 7-2 presents the eigenvalue and subcriticality of the flux harmonics in the ACR-700. The subcriticality of corresponding harmonics in a CANDU-6 reactor, where available (Reference [16]), is also given for comparison purposes. The degree of coupling in the core (i.e., between the positive and negative regions in pictorial images of the modes in Table 7-2) is measured by the mode subcriticality for each flux harmonic. The mode subcriticality indicates the amount of reactivity that must be added in each isolated region to make it critical independently of the other regions. It reflects the probability that a fission neutron appearing in one region escapes across the internal surfaces (surface on which the flux is zero) and is absorbed in another region. The coupling between regions is therefore a function of the neutron current across the internal surfaces. The higher the leakage, the larger the core geometric buckling and the stronger the coupling.

The subcriticalities of the first three modes decrease as the degree of flux flattening increases. Table 7-2 shows that an ACR-700 reactor has larger subcriticalities of the first two azimuthal modes compared to those of a CANDU-6 reactor, but a smaller subcriticality of the first axial mode. The smaller subcriticality of the first axial mode is due to the natural flux flattening in the axial direction because of the use of the 2-bundle-shift refuelling scheme with SEU fuel. Overall, the ACR-700 core is considered to be more tightly coupled and more stable than the CANDU-6 core, mainly because of the negative power feedback.

8. CORE DESIGN AND FUEL MANAGEMENT

The reference ACR-700 core model has 284 channels producing 1982 MW(th) in a calandria shell of 5.2 m inside diameter, which includes a 51-cm thick D_2O reflector on the average. The reactor characteristics for the ACR-700 design were previously documented in an earlier version of this report [17]. The radial power form factor (core average to peak channel power ratio) for the core configuration in Reference [17] is 0.93, giving a maximum time-average channel power of 7.5 MW(th) and a maximum time-average bundle power of 887 kW(th).

An optimization of the ACR-700 time-average channel-power profile has been carried out since in order to give a better match between the channel-power profile and the channel-flow distribution based on an optimized PHT design. The maximum time-average channel power is now reduced from 7.5 MW(th) to 7.3 MW(th) by increasing the power form factor from 0.93 to 0.956. This results in an improvement in the overall Critical Power Ratio (CPR) in the ACR-700. The maximum channel and bundle powers are 7.3 MW(th) and 874 kW(th), respectively for the time-average core.

The ACR-700 is expected to operate with a maximum instantaneous channel power of 7.7 MW(th) and a maximum bundle power of 910 kW(th), while retaining acceptable margin to dryout. The CANFLEX fuel design allows ACR to operate at these power levels with fuel element ratings about 10 to 15% lower than those in current CANDU designs.

Table 8-1 summarizes the major characteristics of the optimised ACR-700 core. The next subsections detail the time-average and instantaneous channel-power (CP) and bundle-power (BP) distributions in the ACR-700 core.

8.1 Axial Power Profile and Radial Power Form Factor

Axial flux and power distributions along a fuel channel depend mainly on the refuelling scheme. They are affected by the fuelling history of that particular channel and can vary as a result of the normal manoeuvring of the reactivity-control devices, power change, or due to spatial xenon transients. Proximity of a channel to one or more mechanical zone controllers also affects the axial power profile.

The radial and axial thermal-neutron-flux distributions across central channels in the ACR-700 core are compared with those in the CANDU-6 in Figures 8-1 and 8-2, respectively. The flux flattening effect due to the adjuster rods is clearly seen in the CANDU-6. There are no adjuster rods in the ACR, because the thermal-neutron flux distributions in the ACR are naturally flat. The ACR is capable of producing 15% higher power output than a conventional CANDU reactor with the same number of fuel channels based on the improvement in the radial power form factor alone. The axial power distribution also allows higher channel power because the inlet-skewed distribution has higher thermalhydraulic margins than a cosine or outlet-skewed cosine. Further increase in the ACR power output by about 10% can be achieved by increasing the limits on maximum channel power and maximum bundle powers (due to the lower element ratings and higher thermalhydraulic margin with CANFLEX bundle compared to the 37-element bundle). Hence, the ACR produces about 28% more power than a conventional CANDU reactor on a per-channel basis.

The stability of the flat radial thermal flux distribution in the ACR can be attributed to the peak in the reflector region, where a large fraction of the fast neutrons leaking out from the core region

are slowed down to become thermal neutrons. The reflector region becomes a large reservoir of thermal neutrons and many of these thermal neutrons are reflected back into the core region, resulting in a naturally flat thermal flux distribution across the whole core. This inherently flat and stable radial-flux shape enables the ACR-700 to operate with a very high radial power form factor of 0.956, requiring only small adjustments in the fuelling rates between the inner- and outer-core regions. In contrast, the radial power form factor is about 0.83 in a conventional CANDU-6. The time-average bundle-power profiles for a 7.3 MW high-power channel in the ACR and in a conventional CANDU-6 are shown in Figure 8-3, while Figure 8-4 shows the radial channel-power distributions in ACR and CANDU-6. The linear element ratings for an ACR fuel bundle in a high-power channel operating at the maximum time-average power of 7.3 MW, as a function of the bundle position, are shown in Figure 8-5.

8.2 Equilibrium-Core Characteristics

The average exit burnup obtainable from a reactor represents the fuel economy of that reactor. It has a direct bearing on the cost of the total power generated, since the total cost of the fuel required over the life of the reactor is very significant. Accurate power distributions and discharge burnups can only be obtained through detailed core simulations, treating explicitly not only the distribution of parasitic absorbers in the core but also the refuelling frequency.

Refuelling is the reactor long-term control system for maintaining satisfactory steady-state operating conditions. The rate of refuelling is adjusted to compensate for the reduction in core reactivity due to burnup. Fuel management deals with the choice of the best refuelling scheme — one which will give satisfactory power shape, low maximum channel and bundle powers and low refuelling frequency.

Power distributions, fuelling rate and core-averaged discharge fuel burnup for the ACR-700 core design are calculated by the RFSP-IST code. This code is also used for the fuel-management design study. Details of the flux and power distributions throughout the core obtained from time-average and instantaneous full-core calculations are given in the following sub-sections. Further discussion on the flux- and power-distribution control is provided in Section 9.

8.2.1 RFSP-IST Core Model

The RFSP-IST core model used for full-core simulations is represented as a grid of lattice cells over the core. In these cells, the nuclear properties are assumed homogeneous; the reactivity devices are represented by the corresponding incremental cross sections. The core model for ACR-700 consists of 284 horizontal channels arranged in an 18×18×12 lattice array with a lattice pitch of 22 cm in the x and y directions, and 49.53 cm (1 bundle length) in the z direction. A reflector region of 51-cm average thickness surrounds this fuel-channel array. The RFSP-IST input deck for ACR-700 full-core calculations is presented in Appendix C.

The dimension of the core mesh array is 50×50×26 (thus consisting of 48×48×24 regions) in the x, y and z directions respectively. A quarter of this production core model in the x-y plane is shown in Figure 8-6. An alternate RFSP core model with a refined mesh structure in the peripheral radial region of the core is also currently being assessed. The core modelling data applicable to the RFSP-IST model used in the present report are presented in Table 8-2. The start of the lattice array marks the start of the channels and bundles relative to the absolute origin of

coordinates of the model. Table 8-3 gives the position of the mesh planes in the RFSP-IST model, with the following spatial discretization:

- The mesh structure is identical in the *x* and *y* directions. There are two meshes for each lattice cell, each one covering an 11-cm interval.
- In the *z* direction, there are 24 mesh intervals, each one covering half a bundle length.
- In the reflector region, there is a total of 6 mesh intervals: 4 mesh intervals of 11 cm each in the region near the core/reflector interface, and 2 mesh intervals of 9 cm each further outward.

The model incorporates all major reactivity and control devices, including guide tubes, but not other associated components that reside outside the calandria shell. Explicitly, these are:

- Nine zone-controller assemblies with two absorber elements each, arranged in three symmetrical rows of three assemblies each.
- Twenty shutoff assemblies with the rods out-of-core and including guide tubes traversing the core vertically.
- Four control absorber units with the rods out-of-core and including guide tubes traversing the core vertically.

The model does not include any of the flux-detector guide-tube assemblies, liquid-poison injection nozzles assemblies, or the moderator inlet nozzles.

In RFSP core simulation models, the devices are not explicitly modelled. They are represented by incremental properties which are smeared over certain mesh regions in the immediate neighbourhood of the device. The actual flux depression in the device is not intended to be reproduced in the global-flux-shape calculation; rather, the correct representation of the total reaction rates and of the device reactivity worth are considered to be more important. This approach is consistent with the fact that the fuel channel and moderator are not explicitly represented in the model either: each lattice cell in the core is a homogenized region with uniform lattice properties generated by WIMS-IST. However, the detailed flux distribution within the device is captured in the calculation of the incremental cross sections of reactivity devices.

In the RFSP-IST model, the device incremental cross sections are applied in the core over a region of 1 lattice pitch × device length × 1 bundle length. The modelled device length in the RFSP-IST core model is presented in Table 8-4. For a given uniform device, a single set of incremental cross sections is applied to all lattice cells perturbed by the modelled device volume. The 2-group incremental cross sections used to represent the reactivity devices in the full-core model were generated with the DRAGON code. They are given in Table 8-5.

The reference core configuration used in RFSP-IST simulations refers to a critical core condition at equilibrium refuelling, where all the shutoff rods and control absorbers are fully withdrawn. All the zone-control absorbers are set at 50% insertion. This nominal state also implies a moderator D_2O purity of 99.90 wt% with no soluble poison. The reactor power level is 100% full power (FP).

8.2.2 Fuelling and Burnup Regions

For design calculations the core is divided into several regions radially, with a different average irradiation in each region. The fuel-burnup distribution is adjusted to obtain the desired power

shape. These burnup values are maintained by adjustment of the refuelling rate in each burnup zone. The grouping of fuel channels into irradiation zones for the 284-channel core is shown in Figure 8-7. The refuelling scheme, along with the flow direction in each channel in the core is shown in Figure 8-8. All refuelling is performed in the direction of coolant flow. A typical time-average exit burnup per each irradiation zone is shown in Figure 8-9.

8.2.3 Time-Average Flux / Power Distributions

A time-average core calculation is used to predict the average power distribution in an equilibrium core. It is an essential step in core design to establish suitable refuelling schemes and to predict the overall core-performance parameters, such as average discharge burnup, channel visit rate, and reactivity-decay rate. In a time-average calculation, each fuel-bundle position in the core is represented by averaged properties based on the irradiation cycle of the fuel at that position in the core. For each channel or groups of channels, a refuelling scheme is specified, together with an average exit-burnup value of the discharged bundles. The selection of these variables will determine the core k-effective value, the power distribution, the channel visit rate and channel dwell time, and the reactivity decay rate per full-power day.

The *TIME-AVER module of RFSP-IST with a nominal device configuration and distributed-xenon option was used to generate the time-average flux and power distributions for the ACR-700 equilibrium core.

The core-average equilibrium exit burnup in the ACR-700 was calculated as 20.0 MW.d/kgU, about three times the current NU CANDU discharge burnup. The corresponding refuelling rate is 5.6 bundles per full-power day (2.8 channel-visits per full-power day) using a bi-directional 2-bundle-shift fuelling scheme, with an average channel dwell time (average time between refuelling of the same channel) of 100 full power days (FPD). The fuel-handling system designed for ACR can readily meet this requirement.

The distribution of time-average exit fuel burnup in the ACR-700 equilibrium core in shown in Figure 8-9, while the average dwell time for each channel in the core is shown in Figure 8-10. The time-average channel-power distribution corresponding to this fuel management scheme is shown in Figure 8-11. Figure 8-12 shows the channel-power distribution with coolant voided in all the fuel channels in the ACR-700 core, normalized to the nominal reactor power. A map showing the channel-power ratios from normal-coolant to voided-coolant conditions, for the same reactor power level, is given in Figure 8-13. It shows that there is a significant power increase in the peripheral channels relative to that in the central channels due to LOCA. However, the absolute power in all channels, including the peripheral channels, will decline automatically upon LOCA before the actuation of the safety systems, because of the negative coolant-void reactivity. Therefore, there is no increase in the absolute power in any channel, including the peripheral channels, during the LOCA transient.

The RFSP-IST full-core coolant voided reactivity is –5.0 mk. This is about 3 mk more negative than the value predicted by WIMS-IST for the mid-burnup fuel lattice. This additional negative reactivity is due to the increase in the neutron leakage from the reactor upon LOCA.

Table 8-1 summarizes the characteristics of the ACR-700 core with the typical average channel-power distribution shown in Figure 8-11. The linear element ratings for the fuel bundles in a high-power channel operating at the maximum time-average power of 7.3 MW, as a function of the bundle position and burnup, are given in Table 8-6, and presented graphically in Figure 8-5.

Detailed results of the time-average calculation are given in Table 8-7. The peak time-average channel and bundle powers are 7.3 MW and 874 kW, respectively. All calculations were performed assuming a 50% insertion level of mechanical zone controllers. The power "pinching" effect of the zone-controllers, as they approach full insertion, on the channel and bundle powers near the horizontal reactor centreline will be investigated at a later stage of the core-design work.

The time-average bundle power distributions, calculated using lattice cross sections that are averaged over the residence time of the fuel bundle at a given position, are shown in Figures 8-14 to 8-25. It should be noted that the neutron flux levels prevalent in the fuel are high enough to saturate the xenon and samarium concentrations, and their effect on flux distribution is negligible. The average end-of-cycle burnup distributions at each bundle plane in the core are presented in Appendix D, in Figures D-1 to D-12. These burnup distributions were derived from the time-average core model using the *TAVEQUIV module to produce a snapshot power shape neutronically equivalent to the time-average power distribution.

8.2.4 Instantaneous Channel Power / Bundle Power Distributions

The core of a CANDU reactor, which has been operating sufficiently long for all channels to be fuelled more than once, will contain fuel bundles with irradiations varying from fresh to discharge. This distribution of irradiation in the core will change with time as the fuel burns up and channels are refuelled, producing time-varying flux and power distributions. At any given moment in the reactor operating history, the instantaneous power distribution would reflect the variation of the power about the time-average power distribution due to refuelling. This results in a power distribution which is not as smooth as the one calculated with time-averaged cross sections. The channel power for an individual channel would be higher or lower than the time-average value depending on the fraction of fuelling cycle that the channel is at. Each instantaneous distribution (snapshot) is a sample from an infinite number of possible distributions. To assess the refuelling ripple of a given fuelling scheme, and the resultant maximum channel and bundle powers, reasonable snapshot power distributions are generated and compared to the time-average powers.

The *INSTANTAN module of RFSP-IST, based on the "patterned-channel-age" model, was used to model the instantaneous flux and power distribution at equilibrium refuelling, and to assess the resultant channel power ripple. The irradiation cycle for each fuel bundle in the core, as derived from the time-average flux distribution, was used to derive an instantaneous irradiation at that bundle position. The "patterned-channel-age" model assumes that irradiation varies linearly with time during the cycle between refuelling of a specific channel, so that the current value of irradiation is simply a function of the "age" of the channel. Every channel in the core is assigned an age between 0 and 1: 0 denotes a recently-fuelled channel, and 1 denotes a channel that is about to be fuelled. The age is "patterned" for an array of 7x7 channels, which emulate the fuelling sequence and history for a group of 49 channels. The "patterned" ages are generated with certain constraints: the most matured channel within the array is randomly chosen; the average age and the minimum age difference between adjacent channels are also specified. Thus, there is certain degree of randomness and refuelling strategy built in the "patterned" age array. The 7x7 age map is applied to cover the whole core, with the ages transposed in alternate block to create additional randomness. Based on this resultant age map, the instantaneous flux and power distribution is then obtained through a single diffusion

calculation. This instantaneous distribution can then be compared to the time-average power distribution, yielding the channel power peaking factors (CPPF) expected to occur during actual refuelling operation.

The refuelling ripple in each channel is defined as the ratio of the instantaneous channel power to the time-average channel power. The CPPF for any given snapshot is defined as the largest channel overpower (or the maximum ripple), i.e., the maximum ratio of instantaneous to time-average channel power:

$$CPPF = \max\left(\frac{P_j(t)}{\overline{P_j}}\right) \quad (1)$$

where $P_j(t)$ and $\overline{P_j}$ are the instantaneous power and the time-average power in the channel j.

To estimate the instantaneous powers with refuelling ripples, five "patterned channel age" maps were generated for the time-average model presented in Section 8.2.3. These five age maps correspond to five different selections of the most-matured channel in the 7x7 array of patterned-age distribution in the core. For a given "patterned age map", together with the irradiation cycle established in a time-average calculation, the instantaneous irradiation at each bundle position was established, and the instantaneous-power distribution was calculated. A typical age map is presented in Figure 8-26.

Based on these snapshot calculations, it is expected that the maximum instantaneous channel and bundle powers in the ACR-700 core will be 7.7 MW(th) and 910 kW(th), respectively. Figure 8-27 shows an instantaneous channel power map where the maximum channel power is 7.67 MW(th) and the maximum bundle power is 908 kW(th). The channel power ripples, which give the ratios between instantaneous and time-average channel powers (based on the age map in Figure 8-26), are shown in Figure 8-28.

The sensitivity of channel overpower to the selection of the random-age distribution is presented in Table 8-8. A typical snapshot power distribution for the ACR-700 with channel-to-channel burnup variations shows channel power "ripple" effects of the order of 6 to 7% about the time-average values. Recently refuelled channels have highest powers and channels near maximum burnup have lowest powers.

8.2.5 Uncertainties in Power Distribution

The accuracy of power-distribution calculations will be confirmed through neutron-flux measurements during commissioning of the ACR-700, and through comparisons of measured and calculated channel powers and neutron fluxes during the operation of the plant. Assessment of the accuracy of the calculation methods for the ACR reactivity and power distributions is part of the R&D program.

8.3 On-Power Refuelling and Fuel Management Strategy

The global power distribution is shaped by differential fuelling in the long term and by differential deployments of the mechanical zone controllers in the short term.

The power distribution in a channel is time-dependent. In the ACR, ^{239}Pu is continuously created from ^{238}U and burned in situ to produce power. The reactivity gained from the net production of

fissile plutonium is insufficient to compensate for the continuous depletion of ^{235}U and build-up of fission products. Hence, channel power increases immediately as a channel is refuelled, then decreases slowly until the minimum power is reached just before refuelling. Neighbouring channels are also affected, with their power increasing slightly when the channel is refuelled, and decreasing as the local neutron source decreases. Neighbours farther removed see smaller changes.

Over larger areas of the core, these local effects average out and the mean power distribution remains steady, provided the fuelling rates are adjusted correctly in each region. Without refuelling, power would decrease in the high-power region but increase in the low-power region (as the total reactor power is constant), since burnup proceeds more rapidly in the high-power region as time progresses.

The fuelling engineer chooses the channel to be refuelled by selecting one of the high-burnup channels in the region selected for refuelling. The burnup of each channel is obtained from a numerical simulation of reactor operation which produces flux, power and burnup distributions as a function of reactor history. The information from this simulation identifies the maximum bundle power and maximum channel power in the reactor. The channel burnups are printed out at regular intervals, showing the fuelling engineer at a glance which channels have high burnup, and are therefore possible choices for refuelling. Additional information to aid the fuelling engineer in selecting channels for refuelling is provided by the on-line flux mapping system.

From the fuel-management point of view, the operating life of an ACR can be separated into three periods:

- From first operation at power to onset of refuelling,
- From first refuelling to equilibrium refuelling,
- Equilibrium refuelling.

Fuel-loading patterns for the ACR-700 start-up core and the fuelling strategy for the transitional period between start-up core and equilibrium core will be addressed in a separate study. Reactor core design is mainly based on the operating characteristics during the equilibrium core period, which covers about 95% of reactor life. Fuel management during this period is straightforward. All fuel bundles in an ACR are nearly identical, and refuelling is normally performed daily and on an essentially continuous basis. By adjusting the fuelling rate of different regions of the core, the power distribution in the core can be continuously controlled and modified over a period of several weeks if desired.

For the ACR reference 2-bundle-shift refuelling scheme, 2 fresh fuel bundles from the upstream fuelling machine are pushed into the fuel channel and 2 irradiated bundles are discharged to the downstream fuelling machine. Adjacent channels are fuelled from opposite ends of the core. This gives symmetric axial flux distributions in the core. A typical sequence of a 2-bundle-shift refuelling scheme is shown in Figure 8-29. The power transient during the refuelling operation is currently under investigation.

Another important feature of refuelling is that defects can be removed when identified, by normal refuelling on-power. Thus, fuel defects need not have any significant effect on the station capacity factor, and the heat-transport system can be maintained at minimal levels of fission-product activity.

8.3.1 Fuelling-Machine Unavailability

If refuelling were to stop, the core reactivity would continuously decrease. The rate of reactivity decay is about –0.56 mk/FPD in the ACR-700 core.

The reactor regulating system would act to maintain reactor criticality by withdrawing the mechanical zone controllers from the core. Assuming that the zone controllers are operating normally at 50% insertion, and since the total reactivity worth provided by the zone-control system is about 9 mk, about 3 to 4 mk of reactivity will be, therefore, available to compensate for the lack of refuelling. The number of days which can be "survived" without refuelling is typically about 4 mk / (0.56 mk/FPD), i.e, about 7 FPD.

8.4 Initial Core Loading and Transient to Onset of Refuelling

The ACR-700 initial core loading has not yet been established. A comprehensive study is planned to determine the fuel enrichment and dysprosium content of various types of fuel bundles to be used for the ACR fresh start-up core. The loading pattern in the fresh fuel core and the estimated boron concentration in the moderator at start-up would also be estimated. The fuel designs and loading pattern will be optimized to allow the reactor to operate at full power with adequate thermal margins and with the targeted negative coolant-void reactivity.

The initial core loading study will simulate the operation of the ACR from fresh start-up to equilibrium fuelling, when the fuel in the ACR start-up core will be gradually replaced by the reference ACR fuel, i.e. 2% SEU with a central pin with NU and Dy poison. It will take about 700 to 1000 full power days of operation to replace all the fuel in the fresh start-up core with the nominal reference fuel.

The design of the initial core loading of ACR-700 and the detailed transition study are scheduled at a later stage in the overall design process.

9. REACTOR DYNAMICS AND CONTROL

9.1 Flux and Power Distribution Control

The power distribution is controlled to prevent any violation of channel- and bundle-power limits while maintaining the rated power output, and to maintain adequate margin to satisfy the design bases for critical power ratio. Several methods of control are used and each is related to a different time scale:

1. In the short-term, the primary control of the neutron flux distribution is carried out by the RRS;
   - Four mechanical-control absorbers (physically the same as the shutoff rods) are used to provide rapid controlled reductions of reactor power.
   - The zone control system provides bulk (overall) reactor-power level control and spatial control.
2. In the long-term, the power distribution is controlled by on-power refuelling by the reactor operators. The neutron-flux is shaped by distributing the reactivity available for fuel burnup judiciously over the core. This is achieved by controlling the rate of refuelling at different locations in the core.

On-line monitoring of the neutron-flux shape, together with off-line calculations, is used in support of the fuel management.

9.1.1 Channel- and Bundle-Power Limits

The maximum channel-and bundle-power limits in the ACR are still under evaluation. These values will be based on safety analysis using the results obtained from a detailed fuel-management study for the ACR core. This fuel management study, which covers the period from fresh start-up until the equilibrium-fuelling condition is established, will be performed at a later stage of the design process. However, several snapshot calculations using randomly generated channel-age patterns indicated that the maximum instantaneous channel and bundle power in the ACR equilibrium core would be 7.7 MW and 910 kW, respectively. Also, some neutron flux peaking occurs at the ends of all fuel bundles where the Zircaloy materials and H_2O coolant absorb fewer thermal neutrons than UO_2. The bundle power limits must be set such that the fuel bundle withstands these effects, including the transient powers during refuelling.

The bundle and channel powers in the reactor core will be constantly tracked, both by the reactor regulating program in the station computers and off-line by the RFSP-IST code. The on-line flux-mapping program (see Section 9.1.4) produces an approximate channel power map every 2 minutes. The more accurate RFSP-IST power-mapping calculations will be executed several times a week, and will be used to demonstrate compliance with the channel and bundle power limits.

9.1.2 Power Distribution within the Fuel Bundle

In addition to monitoring channel and bundle powers that are inferred from a combination of measurement and calculation, the distribution of power amongst the fuel elements of the bundle is taken into account in setting the limit on bundle power. The flux-peaking factors and the

effect on local fuel temperature are also taken into account when assessing the bundle-power limit. This is carried out with computer codes that have been validated over the range of conditions that exist during the life of the fuel.

9.1.3 Regional Overpower Protection

The ACR-700 will be equipped with a Regional Overpower Protection (ROP) system to protect the reactor against overpower in the fuel, whether due to a localized peak or as a result of an uncontrolled power excursion due to a loss of reactivity control (such as inadvertent removal of mechanical zone controllers).

A large number (around 1000) of global power distributions that represent various modes of reactor operation, both normal and off-normal, will be used in the design analysis of the ROP systems. Three-dimensional core calculations will be performed to obtain the power distributions for these possible reactor states and reactivity device configurations. Specifically, these power distributions are used in the calculations of the critical channel powers and subsequently in shutdown-system instrumentation settings for protection against dryout. These large numbers of analysed power shapes represent the bounds of power distribution, so that compliance with the specified acceptable fuel-design limits is ensured.

The design of the ACR-700 ROP system is scheduled at a later stage in the overall design process.

9.1.4 On-Line Flux Mapping

The ACR-700 will be equipped with an on-line flux-mapping system. This system produces detailed flux- and channel-power distributions based on self-powered in-core vanadium flux detectors. This information is used to provide a calibrated average zone-flux signal for use by the spatial-control system, a power setback parameter for the setback routine, and on-line data for operator information. A flux map is calculated automatically at approximately two-minute intervals in the current CANDU-6 reactors.

The technique of flux mapping consists essentially of synthesizing the flux distribution from a pre-selected set of flux modes. The amplitudes for the various modes are calculated using a least-squares fit to the relative fluxes measured by an array of in-core flux detectors.

The flux mode basis consists of the fundamental mode flux, the higher flux harmonics, and a set of perturbation modes. These flux modes are pre-calculated once, off-line. A set of coupling coefficients is obtained from these simulations and stored in the on-line digital computer. The least-squares algorithm involves essentially one matrix-vector multiplication to obtain the mode amplitudes, and a second matrix-vector multiplication to obtain the extended flux map.

The input to the flux-mapping system is provided by flux measurements made with a large number of vanadium detectors. These detectors are located in the vertical flux-detector assemblies. The required number of vanadium flux detectors and their locations in the ACR-700 core have not yet been established.

9.2 Spatial Control

The ACR-700 is expected to be stable at all operating power levels up to 100 % full power, because of the tight neutronic coupling in the compact core and the moderate negative power

feedback coefficient. However, the ACR-700 will be equipped with a powerful spatial-control system, which is designed to provide effective control of all spatial disturbances so that oscillatory behaviour of the flux distribution does not occur.

The maximum magnitudes of various flux tilts to be used in ACR safety analyses have yet to be determined.

9.3 Flux Detectors

The 18 zone controllers are used both for bulk reactivity and for spatial flux control. Bulk reactivity is controlled by varying the average insertion of all 18 absorbers. Spatial flux control is achieved by varying the insertion length of individual absorbers.

A prompt measurement of zone flux is made with self-powered platinum-clad inconel straight individually replaceable (SIR) in-core detectors. The number of required flux detectors has not been yet established. A slightly delayed calibrated zone-power flux is obtained from an on-line flux mapping system. These signals are processed in the on-line digital control computers. Individual zone controllers respond to zone power differences between the measured values and their respective nominal setpoints.

9.4 Shutdown Margins

Sufficient negative reactivity margin under all reactor conditions, including the condition of maximum excess reactivity, is provided independently, by each of the two Shutdown Systems (SDS). In the case of SDS1, negative reactivity margin is calculated with the least effective set of 18 of the 20 shutoff units, i.e., with 2 SOR assumed not available. The assumption is that one SOR is disabled for maintenance and the second does not fall, because of malfunction. For SDS2, negative reactivity margin is provided with one out of 6 poison tanks not available. The availability of each shutdown system is always required to be greater than 99.9%. Furthermore, the speed of detection of the onset of postulated accidents such as loss-of-coolant accidents and the speed of negative reactivity insertion by each of the two SDS is such that the power transient is terminated and the reactor brought to a shutdown state.

In each reactor unit there are two Shutdown Systems that are physically and functionally independent of the RRS and of one another. The reactivity depth of each SDS should be sufficient to maintain the reactor subcritical in the absence of:

- All fission products in the fuel.
- All negative reactivity feedback components.
- All RRS devices.

The above criteria apply at any time during reactor life and encompass all situations at operating power, the hot stand-by shutdown condition, and the cold shutdown condition. If the depth of any one shutdown system is insufficient to keep the reactor at the guaranteed shutdown state indefinitely, it must have enough depth to keep the reactor shutdown long enough to allow other measures to be taken, such as manual addition of boron or gadolinium into the moderator system, to keep the reactor in the guaranteed shutdown state indefinitely.

In addition to providing sufficient reactivity depth in each of the two shutdown systems, there is provision to add soluble neutron poison (either boron or gadolinium) to ensure a guaranteed

shutdown state following rearming of the SDS. The poison addition can compensate for the most reactive fuel condition and for accidental removal of all reactivity devices.

9.5 Trip Recovery

When the reactor trips or the power is reduced in a controlled manner, a temporary increase in the xenon-135 concentration occurs. The magnitude of the increase depends on the length of time that the reactor is shut down or is operated at a reduced power level. It also depends on the magnitude by which the power level has been reduced and the rate at which it is reduced in the case of a controlled change in power level.

In the event of a reactor trip, power must be raised again within about 12 minutes or the xenon concentration will rise beyond the capacity of the reactor regulating system to compensate. At this point, all of the mechanical zone controllers will be almost completely withdrawn to compensate for the xenon buildup. This results in peaking of the power distribution relative to the normal steady-state full-power condition. Consequently, reactor power cannot be increased immediately to 100%. However, the power can be raised sufficiently high to "burn out" the excess Xe-135 and as this happens the zone controllers can be reinserted, which in turn permits increasing power.

10. REACTIVITY PERTURBATIONS AT EQUILIBRIUM OPERATION

The major reactivity perturbations during reactor operation are as follows:

- The change in zone-controller insertion in the core to compensate for reactivity insertion during on-power refuelling.
- The change in zone-controller insertion to maintain the neutron-flux shape during on-power refuelling.
- The change in zone controller insertion during xenon override following a reactor shutdown, during operation in the absence of refuelling capability, or during various power manoeuvres.
- The change in zone-controller insertion and mechanical-absorber-rod movement during a power setback or following a power stepback or during an approach to rated power following a xenon poison-out.
- The addition or removal of moderator poison during periods of operation without refuelling.

All zone-controller movements are carried out to maintain criticality or to provide sufficient reactivity imbalance to produce the desired power-manoeuvring rate, under normal operating conditions. However, during a malfunction of the RRS, it can be postulated that reactivity devices may move to insert positive reactivity into the reactor core at the rate corresponding to their mechanical design limit. The maximum possible positive insertion rate in ACR is no higher than 0.5 mk/s. Such a transient is terminated by either one of the two shutdown systems before any damage to the fuel or the internals of the reactor can occur.

10.1 Reactivity Variations due to On-Power Refuelling

Since the reactor is fuelled continuously and on-power at a rate which keeps the reactor critical, the reactivity perturbation due to refuelling is modest, and well within the range of the zone controller response. Soluble-poison concentration is near zero and variation of the mechanical zone controllers is within ± 4.5 mk at most.

For a standard 2-bundle-shift refuelling scheme, the reactivity increase due to refuelling in an average channel is less than 0.2 mk. This reactivity change is readily controlled by the zone controllers.

10.2 Maximum Controlled Reactivity-Insertion Rate

The RRS device mechanisms are designed to limit the reactivity insertion rate to a level required for control of reactivity perturbations and for power manoeuvring. Due to the low-pressure environment of the reactivity devices, high-speed rod ejection is impossible. The maximum possible rate of positive reactivity insertion in the ACR-700 is less than 0.5 mk/s.

10.3 Xenon Override Following a Reactor Long Shutdown

Xenon load refers to the reactivity hold-up due to neutron absorption in the fission product ^{135}Xe. At equilibrium operation, the concentration of ^{135}Xe in the core is maintained at the equilibrium level, where the formation of ^{135}Xe from the β decay of ^{135}I exactly balances the removal of ^{135}Xe by β decay and burnout by neutron absorption. A change in reactor power from equilibrium will change the burnout rate, and thus the ^{135}Xe concentration. In the case of a

reactor shutdown (burnup rate practically zero), xenon will build up quite rapidly because the equilibrium level of ^{135}I is about 14 times that of ^{135}Xe.

During steady-state full-power operation of the ACR equilibrium core the xenon load is about 26 mk. The xenon load it is estimated to build up to a peak of about 120 mk in about 10 hours after shutdown from full power, and to drop back to the full-power equilibrium level of 26 mk after 45 hours due to the decay of ^{135}Xe as well as the depletion of ^{135}I. Although the amplitude of the xenon transient is dependent on the reactor power level before shutdown, it is clear that excess reactivity must be added to the reactor core to compensate for the excess xenon load if the reactor is to be restarted shortly after shutdown.

In the ACR equilibrium core, a nominal reactivity of about 3 to 4 mk can be obtained by withdrawing the mechanical zone controllers from the core. This provides enough reactivity to override the xenon for up to about 12 minutes after shutdown from full power; clearly not enough time for a reactor restart. If the reactor is not restarted within this period, it will "poison out" until the ^{135}Xe has decayed to a sufficiently low level after about 40 h.

10.4 Moderator Poison Removal

Reactivity insertion rate due to moderator-boron removal by manual operator action is dependent on the current poison concentration. The half-time of the poison concentration removal is approximately 6-10 hours, and each ppm of boron removed will increase the system reactivity by approximately 2.1 mk. Inadvertent removal of moderator poison when the reactor is at guaranteed shutdown state is prevented by disabling the moderator-purification function.

11. SUMMARY

The ACR-700 achieves substantial reduction in D_2O inventory and core size by using H_2O coolant, SEU fuel, and a tight D_2O-moderated lattice. The use of the CANFLEX fuel-bundle design and the flat flux and power distributions enable the ACR to operate at higher channel and bundle powers than those in existing CANDU reactors. The tight neutronic coupling in a small core results in excellent stability, which is further enhanced by the negative power coefficient. The discharge fuel burnup in ACR-700 is 20 MW.d/kgU, resulting in a significant reduction in spent-fuel volume per unit of energy produced.

12. REFERENCES

1. S.R. Douglas, "WIMS-AECL Release 2-5d Users Manual," COG Report, COG-94-052, Rev. 4, July 2000.
2. ENDF/B-VI library, Version u2x.1-0d.hpux10, July 1998.
3. E. Varin, A. Hébert, R. Roy and J. Koclas, "A User's Guide for DRAGON Version DRAGON_980911 Release 3.03," IGE-174 Rev. 4, École Polytechnique de Montréal, Institut de génie nucléaire, 1998 September.
4. W. Shen and D.A. Jenkins, "RFSP-IST User's Manual," AECL Report, TTR-734, Rev. 0, 2001.
5. M. Ovanes, B. Arsenault and J.V. Donnelly, "Validation of Supercell Methodologies Using Phase B Commissioning Tests In Pickering Unit 4", AECL Report, COG-98-297, Rev. 0, 1998 December.
6. M. Ovanes, "Validation of Supercell Methodologies Against Darlington NGS-A Unit 4 Commissioning Tests", AECL Report, TTR-679, Rev. 0, 1999 March.
7. H.C. Chow, B. Arsenault and M. Ovanes, "Overall Summary Report on the Evaluation of Supercell Methodologies", AECL Report, FFC-RCP-026, Rev.0, 1999 March.
8. M. Soulard, "NUCIRC-MOD2.000 Program Description", TTR-357, Volume 1, 1995.
9. G. Kugler and A.R. Dastur, "Accuracy of the Improved Quasi-Static Space-Time Method Checked with Experiment," AECL-5553, 1976.
10. L.N. Carlucci, V. Agranat, G.M. Waddington, H.F. Khartabil and J. Zhang, "Predicted and Measured Flow and Temperature Distributions in a Facility for Simulating in Reactor Moderator Circulation", 8th Annual Conference of the CFD Society of Canada, Montreal, 2000 June.
11. J.F. Briesmeister, "MCNP- A General Monte Carlo N-Particle Transport Code", LA-12625-M, Version 4B, 1997 March
12. D.V. Altiparmakov, "Physics of an ACR: Validation of WIMS-AECL and DRAGON — The "Best" WIMS-AECL Model for ACR Lattice Calculations", AECL Technical Note 108-119190-440-001, FFC-RRP-414, 2002 September.
13. D.V. Altiparmakov, "Physics of an ACR: Validation of WIMS-AECL and DRAGON — Recommended Practical WIMS-AECL Model for Routine Calculations of ACR-Type Lattices "," AECL 108-119190-440-003, FFC-RRP-460, Rev D1, 2002 October.
14. D.V. Altiparmakov, "An Addition to the WIMS-AECl ENDF/B-VI-based Library to Include Dysprosium Burnup Chain", AECL Report FFC-RRP-365, 2001 June.
15. D.V. Altiparmakov, "Modifications to Burnup Data Section of WIMS-IST Library", AECL Report FFC-RRP-420, COG-01-226, 2002 March.
16. D. B. Buss, "Pt. Lepreau- 2-Group WIMS-IST Based Harmonic Mode Calculation Using RFSP-IST version: RFSP-IST.REL_3-01HP", 87-03312-400, 2002 September.
17. M. Ovanes, "ACR-700 Reactor Physics Design" AECL Report 10810-03300-ASD-001, Rev 1, 2002 September.

TAppendix T

Table 4-1
Fuel-Channel Characteristics for ACR-700

Lattice Pitch	22 cm square		
Fuelling Scheme	Bi-directional 2-bundle-shift		
Fuel	43-element CANFLEX bundle design		
	Uniform 2.0% SEU in 42 elements; Central pin replaced by a mixture of NU (0.7 wt% U-235 in total U) with 4.6 wt% dysprosium		
	Temperature		687.0 °C
	Effective Density	Central Pin & Inner Ring	10.298 g × cm^{-3}
		Intermediate and Outer Ring	9.820 g × cm^{-3}
Fuel Channel	12 bundles / channel		
	Pressure Tube	ID = 5.1689 cm	OD = 5.8169 cm
	Calandria Tube	ID = 7.55 cm	OD = 7.80 cm
Coolant H_2O	Temperature (core-average)		300 °C
	Density		0.71273* g × cm^{-3}
Moderator D_2O	Temperature (core-average)		80 °C
	Isotopic Purity		99.90 wt %
	Density		1.07801* g × cm^{-3}
	Gadolinium Concentration		0.0 ppm
	Boron Concentration		0.0 ppm

* internally computed by WIMS-IST

Table 4-2
Description of CANFLEX Fuel Bundles for WIMS-IST Calculations

Description	Unit	Value
Bundle length	cm	49.53
Lattice pitch	cm	22.0
Bundle Total Uranium Mass	kg	17.98
Bundle Zr Mass	kg	2.3
Fuel stack length	cm	48.11
Fuel cluster - number of fuel pins in the bundle	-	43
Radius of the UO_2 pellets – inner elements	cm	0.631
Fuel-sheathing outside radius* – inner elements	cm	0.675
Radius of the UO_2 pellets – outer elements	cm	0.536
Fuel-sheathing outside radius* – outer elements	cm	0.575
Sheath material	-	Zircaloy-4
Sheath density	$g \times cm^{-3}$	7.48
Number of pins in the innermost ring	-	1
Number of pins in the inner ring	-	7
Radius of the inner pins' pitch circle	cm	1.730
Angle of the first pin in the inner ring	radians	0.000
Number of pins in the middle ring	-	14
Radius of the central pins' pitch circle	cm	3.075
Angle of the first pin in the central circle	radians	0.2244
Number of pins in the outer ring		21
Radius of the outer pins' pitch circle	cm	4.384
Angle of the first pin in the outer circle	radians	0.000
Pressure tube inner radius	cm	5.1689
Pressure tube outer radius	cm	5.8169**
Pressure tube material	-	Zr-2.5%Nb
Pressure tube temperature	K	573.16
Pressure tube density	$g \times cm^{-3}$	6.57
Gap material	-	CO_2
Gap density	$g \times cm^{-3}$	0.0016987
Gap temperature	K	353.16
Calandria tube inner radius	cm	7.550
Calandria tube outer radius	cm	7.800
Calandria tube material	-	Zircaloy-2
Calandria tube density	$g \times cm^{-3}$	6.44
Calandria tube temperature	K	353.16

* based on nominal cold dimensions
** PT dimensions correspond to an uncrept channel

Table 4-3
Fuel Isotopic Composition

Fuel Composition	Central Pin	Ring 2	Ring3	Ring 4
Effective Density* (g/cm^3) in WIMS-IST Models	10.298	10.298	9.820	9.820
Nuclide Weight Fractions** (wt%)				
O16	13.4529	13.4529	13.4529	13.4529
Dy160	0.1061	-	-	-
Dy161	0.8623	-	-	-
Dy162	1.1708	-	-	-
Dy163	1.1502	-	-	-
Dy164	1.3106	-	-	-
U235	0.710971	2.00	2.00	2.00
U238	99.290	98.00	98.00	98.00

* The effective densities of the UO2 in each fuel ring in the WIMS-IST calculations were defined so as to preserve the total mass of UO_2 in the bundle. The total mass of uranium in the fuel bundle is 17.98 kg.

** Normalized to Uranium 100%

Table 4-4
Densities and Weight Fractions of Zirconium and Its Alloys

Quantity	Zirconium Metal	Zircaloy-2 (CT)	Zircaloy-4 (Clad)	Zr-2.5%Nb (PT)
Physical Density (g/cm^3)	6.5060	6.5257	6.5167	6.5083
Effective Density* (g/cm^3) in WIMS-IST Models	6.5060	6.4003	7.48*	6.5041
Isotopic Composition (wt%)				
Zr	100	98.2083	98.1813	97.3126
Nb93	-	-	-	2.58
Fe	-	0.135	0.21	0.04678
Cr	-	0.1	0.1	0.008088
Ni	-	0.055	0.007	0.0035
B10	-	0.00005962	0.00005962	0.00002431

* The effective density of the fuel sheath in the WIMS-IST calculations was defined so as to preserve the total mass of zirconium in the bundle. The total mass of Zr in the bundle is 2.3 kg.

Table 4-5
Standard ACR Fuel Lattice — K-infinity vs. Bundle Average Burnup

Time (days)	Average Bundle Burnup (MWd/TeU)	K-infinity (Cooled)
0	0.0000	1.24848
1	0.0323	1.21004
2	0.0646	1.20446
3	0.0970	1.20250
4	0.1293	1.20093
5	0.1616	1.19955
6	0.1940	1.19832
7	0.2263	1.19724
8	0.2586	1.19629
9	0.2910	1.19546
10	0.3233	1.19473
11	0.3557	1.19407
21	0.6792	1.18967
31	1.0028	1.18607
41	1.3262	1.18226
51	1.6495	1.17818
71	2.2954	1.16937
91	2.9407	1.16003
111	3.5855	1.15039
131	4.2299	1.14060
151	4.8739	1.13076
171	5.5175	1.12092
191	6.1608	1.11112
211	6.8038	1.10136
231	7.4467	1.09166
251	8.0894	1.08203
271	8.7316	1.07244
291	9.3737	1.06291
311	10.0154	1.05343
331	10.6573	1.04400

Time (days)	Average Bundle Burnup (MWd/TeU)	K-infinity (Cooled)
		(cont.)
351	11.2995	1.03465
371	11.9410	1.02533
391	12.5823	1.01605
411	13.2235	1.00686
431	13.8650	0.99774
451	14.5061	0.98870
471	15.1472	0.97974
491	15.7882	0.97080
511	16.4295	0.96194
531	17.0708	0.95318
551	17.7121	0.94452
571	18.3534	0.93596
591	18.9943	0.92752
611	19.6357	0.91919
631	20.2767	0.91099
651	20.9177	0.90292
671	21.5590	0.89499
691	22.2002	0.88720
711	22.8417	0.87958
731	23.4832	0.87211
751	24.1250	0.86480
771	24.7665	0.85766
791	25.4087	0.85070
811	26.0504	0.84391
831	26.6926	0.83731
851	27.3347	0.83088
871	27.9771	0.82465
891	28.6194	0.81860
911	29.2618	0.81275

Table 4-6
Standard ACR Fuel Lattice — Burnup and Power Distribution

Step	Time (days)	Irradiat. (n/kb)	Bundle Average Burnup (MWd/kgU)	Burnup (MWd/kgU) Ring 1	Burnup (MWd/kgU) Ring 2	Burnup (MWd/kgU) Ring 3	Burnup (MWd/kgU) Ring 4	Relative Power Density Ring 1	Relative Power Density Ring 2	Relative Power Density Ring 3	Relative Power Density Ring 4	LER (kW/m) Ring 1	LER (kW/m) Ring 2	LER (kW/m) Ring 3	LER (kW/m) Ring 4
1	0	0.000	0.0000	0.0000	0.0000	0.0000	0.0000	0.1727	0.7023	0.8846	1.2691	9.74	39.60	35.99	51.63
2	1	0.005	0.0323	0.0056	0.0219	0.0289	0.0414	0.1739	0.6985	0.8819	1.2726	9.80	39.38	35.88	51.77
3	2	0.010	0.0646	0.0112	0.0436	0.0577	0.0830	0.1743	0.6982	0.8817	1.2727	9.83	39.37	35.87	51.78
4	3	0.014	0.0970	0.0169	0.0654	0.0865	0.1246	0.1748	0.6984	0.8819	1.2725	9.86	39.38	35.88	51.77
5	4	0.019	0.1293	0.0225	0.0871	0.1153	0.1661	0.1753	0.6987	0.8820	1.2723	9.88	39.39	35.88	51.76
6	5	0.024	0.1616	0.0282	0.1089	0.1441	0.2077	0.1758	0.6988	0.8821	1.2721	9.91	39.40	35.89	51.75
7	6	0.029	0.1940	0.0339	0.1307	0.1729	0.2493	0.1763	0.6989	0.8822	1.2720	9.94	39.41	35.89	51.75
8	7	0.034	0.2263	0.0396	0.1524	0.2018	0.2908	0.1769	0.6990	0.8822	1.2719	9.97	39.41	35.89	51.75
9	8	0.038	0.2586	0.0454	0.1742	0.2306	0.3324	0.1774	0.6991	0.8823	1.2718	10.00	39.42	35.89	51.74
10	9	0.043	0.2910	0.0511	0.1960	0.2594	0.3740	0.1780	0.6992	0.8824	1.2716	10.04	39.42	35.90	51.73
11	10	0.048	0.3233	0.0569	0.2178	0.2883	0.4155	0.1786	0.6993	0.8824	1.2715	10.07	39.43	35.90	51.73
12	11	0.053	0.3557	0.0627	0.2396	0.3171	0.4571	0.1791	0.6994	0.8825	1.2714	10.10	39.43	35.90	51.72
13	21	0.101	0.6792	0.1208	0.4577	0.6057	0.8728	0.1849	0.7006	0.8833	1.2699	10.43	39.50	35.94	51.66
14	31	0.149	1.0028	0.1808	0.6761	0.8944	1.2879	0.1903	0.7019	0.8843	1.2683	10.73	39.58	35.98	51.60
15	41	0.197	1.3262	0.2425	0.8948	1.1834	1.7024	0.1958	0.7037	0.8855	1.2663	11.04	39.68	36.03	51.52
16	51	0.245	1.6495	0.3060	1.1140	1.4727	2.1161	0.2013	0.7056	0.8867	1.2642	11.35	39.78	36.08	51.43
17	71	0.340	2.2954	0.4363	1.5532	2.0514	2.9413	0.2120	0.7098	0.8895	1.2598	11.95	40.02	36.19	51.25
18	91	0.436	2.9407	0.5735	1.9945	2.6314	3.7627	0.2225	0.7144	0.8924	1.2549	12.55	40.28	36.31	51.06
19	111	0.532	3.5855	0.7173	2.4384	3.2129	4.5804	0.2329	0.7195	0.8956	1.2498	13.13	40.57	36.44	50.85
20	131	0.629	4.2299	0.8678	2.8851	3.7961	5.3942	0.2433	0.7248	0.8989	1.2445	13.72	40.87	36.57	50.63
21	151	0.726	4.8739	1.0249	3.3349	4.3811	6.2041	0.2536	0.7303	0.9023	1.2390	14.30	41.18	36.71	50.41
22	171	0.825	5.5175	1.1885	3.7879	4.9679	7.0099	0.2639	0.7362	0.9057	1.2333	14.88	41.51	36.85	50.18
23	191	0.924	6.1608	1.3588	4.2442	5.5566	7.8115	0.2742	0.7422	0.9092	1.2276	15.46	41.85	36.99	49.94
24	211	1.024	6.8038	1.5355	4.7040	6.1473	8.6091	0.2845	0.7484	0.9127	1.2217	16.04	42.20	37.13	49.70
25	231	1.126	7.4467	1.7189	5.1676	6.7403	9.4027	0.2948	0.7547	0.9163	1.2157	16.62	42.55	37.28	49.46
26	251	1.229	8.0894	1.9089	5.6350	7.3354	10.1922	0.3053	0.7612	0.9198	1.2096	17.21	42.92	37.42	49.21
27	271	1.333	8.7316	2.1055	6.1061	7.9322	10.9772	0.3157	0.7677	0.9234	1.2035	17.80	43.29	37.57	48.96
28	291	1.439	9.3737	2.3088	6.5810	8.5314	11.7580	0.3262	0.7743	0.9266	1.1977	18.39	43.66	37.70	48.73
29	311														

Step	Time (days)	Irradiat. (n/kb)	Bundle Average Burnup (MWd/kgU)	Burnup (MWd/kgU) Ring 1	Burnup (MWd/kgU) Ring 2	Burnup (MWd/kgU) Ring 3	Burnup (MWd/kgU) Ring 4	Relative Power Density Ring 1	Relative Power Density Ring 2	Relative Power Density Ring 3	Relative Power Density Ring 4	LER (kW/m) Ring 1	LER (kW/m) Ring 2	LER (kW/m) Ring 3	LER (kW/m) Ring 4
30	331	1.655	10.6573	2.7354	7.5429	9.7354	13.3076	0.3474	0.7879	0.9332	1.1856	19.59	44.42	37.97	48.23
31	351	1.765	11.2995	2.9590	8.0304	10.3409	14.0769	0.3581	0.7949	0.9363	1.1796	20.19	44.82	38.09	47.99
32	371	1.877	11.9410	3.1894	8.5218	10.9479	14.8417	0.3689	0.8020	0.9392	1.1737	20.80	45.22	38.21	47.75
33	391	1.991	12.5823	3.4266	9.0174	11.5565	15.6022	0.3797	0.8089	0.9421	1.1678	21.41	45.61	38.33	47.51
34	411	2.107	13.2235	3.6707	9.5171	12.1669	16.3589	0.3905	0.8157	0.9449	1.1621	22.02	45.99	38.44	47.28
35	431	2.225	13.8650	3.9218	10.0214	12.7794	17.1122	0.4014	0.8226	0.9475	1.1565	22.63	46.38	38.55	47.05
36	451	2.344	14.5061	4.1799	10.5295	13.3931	17.8613	0.4125	0.8294	0.9498	1.1510	23.26	46.77	38.64	46.83
37	471	2.466	15.1472	4.4451	11.0419	14.0085	18.6070	0.4234	0.8360	0.9519	1.1459	23.87	47.14	38.73	46.62
38	491	2.590	15.7882	4.7171	11.5583	14.6250	19.3491	0.4347	0.8427	0.9539	1.1407	24.51	47.51	38.81	46.41
39	511	2.716	16.4295	4.9967	12.0790	15.2431	20.0883	0.4457	0.8492	0.9558	1.1358	25.13	47.88	38.88	46.21
40	531	2.844	17.0708	5.2833	12.6038	15.8625	20.8244	0.4566	0.8557	0.9574	1.1310	25.74	48.25	38.95	46.01
41	551	2.974	17.7121	5.5769	13.1325	16.4829	21.5573	0.4675	0.8618	0.9588	1.1265	26.36	48.59	39.01	45.83
42	571	3.106	18.3534	5.8775	13.6650	17.1043	22.2872	0.4783	0.8677	0.9601	1.1222	26.97	48.92	39.06	45.65
43	591	3.241	18.9943	6.1848	14.2009	17.7260	23.0139	0.4891	0.8733	0.9611	1.1182	27.58	49.24	39.10	45.49
44	611	3.378	19.6357	6.4994	14.7406	18.3489	23.7387	0.4998	0.8787	0.9619	1.1145	28.18	49.54	39.13	45.34
45	631	3.517	20.2767	6.8206	15.2833	18.9720	24.4605	0.5103	0.8838	0.9624	1.1111	28.77	49.83	39.15	45.20
46	651	3.659	20.9177	7.1485	15.8292	19.5954	25.1802	0.5206	0.8886	0.9627	1.1080	29.35	50.10	39.17	45.08
47	671	3.803	21.5590	7.4832	16.3783	20.2192	25.8981	0.5309	0.8931	0.9629	1.1051	29.93	50.36	39.17	44.96
48	691	3.949	22.2002	7.8246	16.9301	20.8431	26.6142	0.5409	0.8973	0.9628	1.1026	30.50	50.59	39.17	44.86
49	711	4.098	22.8417	8.1724	17.4847	21.4672	27.3289	0.5507	0.9011	0.9626	1.1003	31.05	50.81	39.16	44.76
50	731	4.249	23.4832	8.5266	18.0418	22.0912	28.0422	0.5602	0.9046	0.9621	1.0984	31.59	51.00	39.14	44.69
51	751	4.403	24.1250	8.8871	18.6012	22.7151	28.7544	0.5695	0.9077	0.9615	1.0967	32.11	51.18	39.12	44.62
52	771	4.558	24.7665	9.2534	19.1622	23.3383	29.4653	0.5785	0.9105	0.9607	1.0953	32.62	51.34	39.09	44.56
53	791	4.717	25.4087	9.6259	19.7257	23.9618	30.1761	0.5873	0.9129	0.9598	1.0943	33.11	51.47	39.05	44.52
54	811	4.877	26.0504	0.0038	20.2902	24.5842	30.8857	0.5957	0.9149	0.9587	1.0935	33.59	51.59	39.00	44.49
55	831	5.040	26.6926	0.3874	20.8563	25.2063	31.5953	0.6038	0.9166	0.9576	1.0930	34.04	51.68	38.96	44.47
56	851	5.205	27.3347	0.7761	21.4234	25.8276	32.3044	0.6115	0.9179	0.9563	1.0927	34.48	51.75	38.91	44.46
57	871	5.372	27.9771	1.1700	21.9916	26.4484	33.0137	0.6190	0.9189	0.9549	1.0927	34.90	51.81	38.85	44.45
58	891	5.541	28.6194	1.5686	22.5603	27.0682	33.7229	0.6260	0.9195	0.9534	1.0929	35.30	51.85	38.79	44.46
59	911	5.713	29.2618	1.9718	23.1295	27.6871	34.4324	0.6327	0.9198	0.9519	1.0934	35.67	51.86	38.73	44.48

* LER (Linear Element Rating) based on constant bundle power of 900 kW.

Table 4-7
Element Ratings for a Typical 900 kW Bundle Power at Mid-Burnup

Fuel Ring	ACR (CANFLEX SEU) (kW/m)	CANDU-6 (37-element NU) (kW/m)	% Change* ACR vs. CANDU-6
1 (Central Pin)	19.0	39.7	-52.1
2	43.8	41.3	+6.1
3	37.9	46.5	-18.5
4	48.5	57.2	-15.2

* lower element rating allows higher power and higher burnup

Table 4-8
Change in Bundle Power Profile Due to LOCA
(Normalized to 900 kW Bundle Power at Mid-burnup)

Fuel Ring	ACR Cooled (kW/m)	ACR Voided (kW/m)	% Change* due to LOCA
Ring 1 (Central Pin) (NU + 4.6 wt% Dy)	19.0	23.0	+ 21.1
Ring 2 (2.0 % SEU)	43.8	50.2	+ 17.2
Ring 3 (2.0 % SEU)	37.9	39.4	+ 4.0
Ring 4 (2.0 % SEU)	48.5	45.2	- 6.8

Table 4-9
Fast Flux at the Pressure Tube

Bundle	Power (kW)	Fast Flux (>1 MeV) ($n/cm^2 \cdot s$)
1	234.06	1.10400E+13
2	577.10	2.72200E+13
3	774.83	3.65400E+13
4	843.88	3.98000E+13
5	832.07	3.92400E+13
6	796.45	3.75600E+13
7	755.92	3.56500E+13
8	716.59	3.38000E+13
9	659.65	3.11100E+13
10	560.78	2.64500E+13
11	393.47	1.85600E+13
12	155.21	7.32000E+12

Table 5-1
Reactivity Coefficients in ACR-700 for Mid-Burnup Fuel

Parameter	Unit	ACR-700	CANDU 6
Moderator Temperature (including density) Effect	mk/°C	-0.024	slightly positive
Coolant Temperature (including density) Effect	mk/°C	-0.010	positive
Fuel Temperature Effect (from 687 to 787 °C)	mk/°C	-0.013	small negative
Boron increased from 0 to 5 ppm in Moderator	mk/ppm	-2.1	-6.8
Power Coefficient (95% -105% Full Power)	mk/%power	-0.07	~ 0
Reactivity change from 0% to 100% full power	mk	-8.0	small negative
CT and PT gap filled with H_2O Coolant	mk/channel	-0.24	N/A
CT and PT gap filled with D_2O Moderator	mk/channel	+0.08	~ 0
Full-core Coolant-Void Reactivity	mk	-5.0	+10 to +15 mk

Note: Reactivity coefficients estimated from WIMS-IST calculations with ENDF/B-VI 1a1 library at mid-burnup, except for CVR which is estimated from RFSP-IST calculations with full distribution of burnup.

Table 6-1
Safety and Control Parameters in ACR-700 and CANDU-6

Parameter	ACR-700	CANDU 6
Bulk & Spatial Control	18 Zone Controllers in 9 Assemblies No Adjuster Rods	14 Controllers in 7 Assemblies 21 Adjuster Rods
Fast Power Reduction	4 Mechanical Control Absorber Units	4 Mechanical Absorber Rods
Shutdown System (SDS1)	20 Shutoff Units	28 Absorber Rods
Shutdown System (SDS2)	6 Poison Nozzles (reflector region)	6 Poison Nozzles (core region)

Table 7-1
Delayed-Neutron Parameters and Kinetics Data

Parameter	ACR-700	CANDU-6
Total Delayed Neutron Fraction (ß)	0.0056	0.0058
Prompt Neutron Lifetime (millisecond)	0.33	0.92

Delayed Neutron Data		
Group #	**BETA**	**LAMBDA**
1	2.8045E-04	5.9095E-04
2	1.1214E-03	3.1469E-02
3	9.8604E-04	1.2268E-01
4	2.2328E-03	3.1901E-01
5	7.4979E-04	1.3936E+00
6	1.8776E-04	3.7591E+00
Total ß	**5.5582E-03**	
l-star (sec)	**0.000326**	

Delayed Photo-neutron Data		
Group #	**Fractional Group Yield**	**Half Life**
1	1.100E-03	307.6 h
2	2.300E-03	53.0 h
3	7.300E-03	4.4 h
4	5.270E-02	5924.0 s
5	4.660E-02	1620
6	7.570E-02	462.1
7	1.576E-01	144.1
8	4.480E-02	55.7
9	2.239E-01	22.7
10	1.940E-01	6.22
11	1.940E-01	2.3

Table 7-2
ACR-700 Flux Harmonic Modes

Mode No.	Description	ACR-700 K-effective	ACR-700 Reactivity (mk)	CANDU-6 Reactivity (mk)*	Harmonic Mode (Pictorial)
1	Fundamental	1.00200	0.0	0.0	
2	1st Axial	0.988279	-13.85	-24.43	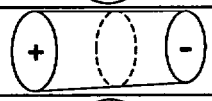
3	1st Azimuthal (A)	0.984096	-18.16	-13.93	
4	1st Azimuthal (B)	0.982883	-19.41	-14.72	
5*	1st Azimuthal, 1st Axial (A)	0.969651	-33.29	-42.54	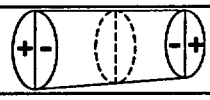
6	1st Azimuthal, 1st Axial (B)	0.968427	-35.38	-41.94	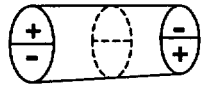
7*	2nd Axial	0.958536	-45.26	—	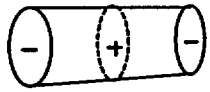
8*	2nd Azimuthal (A)	0.955945	-49.29	-40.70	
9	2nd Azimuthal (B)	0.948411	-56.39	-38.43	
10	2nd Azimuthal, 1st Axial (A)	0.941979	-63.59	-71.29	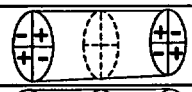
11	1st Azimuthal, 2nd Axial (A)	0.939998	-65.85	—	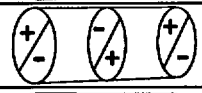
12	1st Azimuthal, 2nd Axial (B)	0.939802	-66.05	—	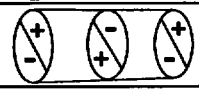
13	2nd Azimuthal, 1st Axial	0.934239	-72.39	-68.54	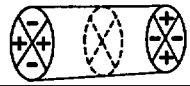
14	1st Radial	0.928638	-83.27	—	
15	3rd Axial	0.922409	-86.11	—	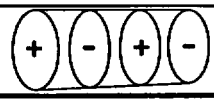

Table 8-1
Summary of Major Characteristics of ACR-700

Parameter	ACR-700 (Optimised)
Number of Fuel Channels	284
Number of Fuel Bundles per Channel	12
Reflector Average Thickness (cm)	51
Core Length (m)	5.94
Calandria Shell Inner Diameter (m)	5.20
Lattice Pitch (Square) (cm)	22
Total Fission Power (MW)	2056
Reactor Thermal Power Output (MW(th))	1982
Gross Electrical Power Output (MW(e))	731
Radial Form Factor	0.956
Core-Average Discharge Fuel Burnup (MWd/kgU)	20.0
Full-Core Coolant Void Reactivity (mk)	-5.0
Max. Fuel Element Burn-up (MW.d/kgU)	26
Fuel Bundles Required per Full Power Day	5.6
Channel Visits per Full Power Day	2.8
Core-Average Dwell Time (FPD)	100
Reactivity Decay Rate (mk/FPD)	-0.56
Max. Time-Average Channel Power (MW(th)	7.3
Max. Time-Average Bundle Power (kW(th))	874
Max. Instantaneous Channel Power (MW(th))	7.7
Max. Instantaneous Bundle Power (kWth))	910
Max. Instantaneous Element Rating (kW/m)	51

Note: Values calculated at nominal operating conditions

Table 8-2
ACR-700 Core Modelling Data

Parameter	Value
Core Length (cm)	594.0
Core Radius (cm)	260.0
Dimensions of Mesh Array	50×50×26
Max. Number of In-Core Mesh Points in a Plane	1781
Number of Channels in Lattice Array	284
Number of Bundles in Core	3408
Number of Modelled Devices	75
Origin of Coordinates of Mesh Array	$x = 0.00$ $y = 0.00$ $z = 0.00$
Origin of Coordinates of Lattice Array	$x = 62.00$ $y = 62.00$ $z = 0.00$
Lattice Spacings of Lattice Array	$x = 22.00$ $y = 22.00$ $z = 49.53$
Radial Extrapolation Factor	1.420798
Axial Extrapolation Factor	1.420798

Note: The extrapolation distance used to calculate coupling coefficients at the boundary mesh equals one half the extrapolation factor at that boundary times the transport mean free path. The standard extrapolation factor of 1.420798 gives an extrapolation distance corresponding to vacuum boundary conditions.

Table 8-3
Mesh Spacings for Core Calculations

* Coordinates in centimetres of start of the mesh array relative to absolute origin of coordinates

Mesh Interval / Mesh Plane	X Direction		Y Direction		Z Direction	
	Mesh Spacings	Mesh Plane Position	Mesh Spacings	Mesh Plane Position	Mesh Spacings	Mesh Plane Position
1	0.0	0.0	0.0	0.0	0.0	0.000
2	9.0	4.5	9.0	4.5	24.765	12.383
3	9.0	13.5	11.0	13.5	24.765	37.148
4	11.0	23.5	11.0	23.5	24.765	61.913
5	11.0	34.5	11.0	34.5	24.765	86.678
6	11.0	45.5	11.0	45.5	24.765	111.443
7	11.0	56.5	11.0	56.5	24.765	136.207
8	11.0	67.5	11.0	67.5	24.765	160.972
9	11.0	78.5	11.0	78.5	24.765	185.737
10	11.0	89.5	11.0	89.5	24.765	210.502
11	11.0	100.5	11.0	100.5	24.765	235.267
12	11.0	111.5	11.0	111.5	24.765	260.032
13	11.0	122.5	11.0	122.5	24.765	284.797
14	11.0	133.5	11.0	133.5	24.765	309.563
15	11.0	144.5	11.0	144.5	24.765	334.328
16	11.0	155.5	11.0	155.5	24.765	359.093
17	11.0	166.5	11.0	166.5	24.765	383.858
18	11.0	177.5	11.0	177.5	24.765	408.623
19	11.0	188.5	11.0	188.5	24.765	433.388
20	11.0	199.5	11.0	199.5	24.765	458.153
21	11.0	210.5	11.0	210.5	24.765	482.918
22	11.0	221.5	11.0	221.5	24.765	507.683
23	11.0	232.5	11.0	232.5	24.765	532.448
24	11.0	243.5	11.0	243.5	24.765	557.213
25	11.0	254.5	11.0	254.5	24.765	581.978
26	11.0	265.5	11.0	265.5	0.0	594.360
27	11.0	276.5	11.0	276.5		
28	11.0	287.5	11.0	287.5		
29	11.0	298.5	11.0	298.5		
30	11.0	309.5	11.0	309.5		
31	11.0	320.5	11.0	320.5		
32	11.0	331.5	11.0	331.5		
33	11.0	342.5	11.0	342.5		
34	11.0	353.5	11.0	353.5		
35	11.0	364.5	11.0	364.5		
36	11.0	375.5	11.0	375.5		
37	11.0	386.5	11.0	386.5		
38	11.0	397.5	11.0	397.5		
39	11.0	408.5	11.0	408.5		
40	11.0	419.5	11.0	419.5		
41	11.0	430.5	11.0	430.5		
42	11.0	441.5	11.0	441.5		
43	11.0	452.5	11.0	452.5		
44	11.0	463.5	11.0	463.5		
45	11.0	474.5	11.0	474.5		
46	11.0	485.5	11.0	485.5		
47	11.0	496.5	11.0	496.5		
48	9.0	506.5	9.0	506.5		
49	9.0	515.5	9.0	515.5		
50	0.0	520.0	0.0	520.0		

Table 8-4
Device Modelled Length in RFSP-IST

Device	Total Static Reactivity Worth	Device Length in RFSP-IST Model (cm)	
18 Zone Control Units	9 mk	Upper & Lower Zone Controllers ZCU Assembly	241.5 520.0
4 Mechanical Control Absorbers	12 mk	Control Absorber Guide Tube	493.0 520.0
20 Shutoff Units	60 mk	Short Shutoff Absorber (# 01, 05, 06, 10, 11, 15, 16 & 20) Long Shutoff Absorber (# 02, 03, 04, 07, 08, 09, 12, 13, 14, 17, 18 & 19) Guide Tube	451.0 493.0 520.0

Table 8-5
Reactivity-Device Incremental Cross Sections for Equilibrium Core

(2-Group 3-Dimensional Supercell Calculations with DRAGON using the ENDF/B-V library)

Incremental Cross Section	Zone Controller	Guide Tube (ZCU)	SU & CAU	Guide Tube (SU &CAU)
Fast Transport $\Delta\Sigma_{tr1}$	5.2388459E-03	1.0262430E-04	2.2888333E-03	1.0173023E-04
Thermal Transport $\Delta\Sigma_{tr2}$	5.5274665E-03	-8.7827444E-04	7.9998076E-03	-8.7037683E-04
Fast Absorption $\Delta\Sigma_{a1}$	8.8870525E-05	1.1026859E-05	5.2061680E-04	1.0877848E-05
Thermal Absorption $\Delta\Sigma_{a2}$	1.9517243E-03	5.0425529E-05	2.0300030E-02	4.9948692E-05
Down Scattering $\Delta\Sigma s_{1\rightarrow 2}$	-1.3297889E-04	-5.0528906E-05	-2.1139067E-04	-5.0115399E-05
Up Scattering $\Delta\Sigma s_{2\rightarrow 1}$	2.9888324E-05	1.1664088E-06	9.9993384E-05	1.1548691E-06
Fast Production $\Delta\nu\Sigma_{f1}$	-4.5860652E-06	-1.7260900E-06	-6.8685040E-06	-1.7117709E-06
Thermal Production $\Delta\nu\Sigma_{f2}$	4.9045403E-04	2.4325214E-05	2.1973327E-09	2.4086796E-05
F Factor ΔF	1.2458622E-02	6.4146519E-04	5.0170124E-02	6.3544512E-04
H Factor (Epithermal Group) ΔH_1	-1.2910637E-04	-4.9493698E-05	-1.8886664E-04	-4.9087561E-05
H Factor (Thermal Group) ΔH_2	1.4412985E-02	7.1454793E-04	6.4747274E-02	7.0756971E-04

Table 8-6
Linear Element Ratings for 7.3 MW High-Power Channel in ACR-700

Bundle Position	Burnup MWd/kgU	Bundle Power * (kW)	Bundle Power Time-Avg (kW)	Ring Burnup (MWd/kgU)				Element Rating (kW/m)			
				Ring 1 (NU/Dy)	Ring 2 (SEU)	Ring 3 (SEU)	Ring 4 (SEU)	Ring 1 (NU/Dy)	Ring 2 (SEU)	Ring 3 (SEU)	Ring 4 (SEU)
1	0.78	234.06	233.9	0.14	0.53	0.70	1.00	2.7	10.3	9.3	13.4
2	1.93	577.10	576.7	0.36	1.30	1.72	2.47	7.4	25.6	23.2	32.9
3	4.19	774.83	774.3	0.86	2.86	3.76	5.34	11.8	35.2	31.5	43.6
4	6.73	843.88	843.3	1.52	4.65	6.08	8.52	15.0	39.5	34.8	46.6
5	9.57	832.07	831.5	2.37	6.73	8.72	12.00	17.2	40.5	34.9	45.0
6	12.18	796.45	795.9	3.28	8.71	11.18	15.13	18.6	40.1	33.9	42.2
7	14.81	755.92	755.4	4.31	10.77	13.69	18.22	19.8	39.4	32.5	39.2
8	17.15	716.59	716.1	5.32	12.67	15.94	20.92	20.6	38.4	31.0	36.6
9	19.44	659.65	659.2	6.40	14.58	18.16	23.52	20.5	36.2	28.7	33.3
10	21.31	560.78	560.4	7.35	16.16	19.97	25.62	18.5	31.3	24.4	28.0
11	22.85	393.47	393.2	8.17	17.49	21.47	27.33	13.6	22.2	17.1	19.6
12	23.61	155.21	155.1	8.60	18.15	22.21	28.18	5.5	8.8	6.7	7.7
	Channel Power	7300.0	7295.0								

* normalized to the maximum time-average channel power of 7.3 MW

Table 8-7
Optimised ACR-700 Core - Summary of Time-Average Calculation

Region	No. of chn	Avg. Exit Irradiation (n/kb)	Avg. Burnup (MW·d/kgU)	Channel Power (kW)		Bundle Power (kW)		Feed Rate		Dwell Time (FPD)	Reactivity Decay Rate (milli-k/FPD)
				Avg.	Max.	Avg.	Max.	(Bdl/FPD)	(Chnl/FPD)		
REG1T	26	2.29	13.97	6726.10	7149.46	560.51	851.79	0.736	0.368	70.65	-0.03952
REG2T	20	3.57	20.61	6923.29	7165.80	576.94	846.23	0.395	0.197	101.25	-0.03718
CORNER	8	2.36	14.36	7090.06	7098.65	590.84	874.39	0.232	0.116	68.90	-0.01447
REG4T0	12	4.17	23.26	7051.01	7265.74	587.58	837.45	0.213	0.106	112.21	-0.02507
REG3T0	8	4.20	23.35	7142.41	7215.59	595.20	848.38	0.143	0.071	111.21	-0.01757
REG4T1	8	4.24	23.55	7250.39	7285.31	604.20	852.64	0.144	0.072	110.47	-0.01838
REG3T	12	4.05	22.72	6776.04	7258.01	564.67	842.52	0.210	0.105	114.07	-0.02246
REG5T0	8	4.34	23.95	7270.47	7284.29	605.87	848.76	0.142	0.071	112.07	-0.01864
REG2T0	6	3.00	17.50	6623.59	6737.01	551.97	783.44	0.133	0.066	89.86	-0.00977
REG4T	14	4.05	22.72	6870.21	7134.07	572.52	831.21	0.248	0.124	112.49	-0.02706
REG6T	12	4.39	24.18	7285.37	7295.16	607.11	846.08	0.212	0.106	112.89	-0.02820
REG5T	12	4.36	24.05	7232.57	7281.00	602.71	844.10	0.212	0.106	113.10	-0.02760
REG2B0	6	3.00	17.50	6623.19	6736.81	551.93	783.38	0.133	0.066	89.86	-0.00977
REG4B	14	4.05	22.72	6869.86	7133.90	572.49	831.04	0.248	0.124	112.50	-0.02705
REG5B	12	4.36	24.05	7232.29	7280.51	602.69	843.96	0.212	0.106	113.10	-0.02759
REG6B	12	4.39	24.18	7284.96	7295.01	607.08	845.97	0.212	0.106	112.89	-0.02820
REG3B	12	4.05	22.72	6775.13	7256.63	564.59	842.19	0.210	0.105	114.08	-0.02245
REG4B1	8	4.24	23.55	7249.44	7284.43	604.12	852.36	0.144	0.072	110.49	-0.01837
REG5B0	8	4.34	23.95	7269.57	7283.46	605.80	848.58	0.142	0.071	112.09	-0.01864
REG1B	26	2.29	13.97	6724.35	7147.21	560.36	851.50	0.735	0.367	70.67	-0.03949
REG2B	20	3.57	20.61	6921.57	7163.79	576.80	845.97	0.395	0.197	101.27	-0.03715
REG3B0	8	4.20	23.35	7140.92	7213.94	595.08	848.17	0.143	0.071	111.24	-0.01756
REG4B0	12	4.17	23.26	7049.59	7264.41	587.47	837.29	0.213	0.106	112.23	-0.02506
WHOLE CORE	**284**	**3.51**	**20.02**	**6978.87**	**7295.16**	**581.57**	**874.39**	**5.82**	**2.91**	**97.6**	**-0.55736**

Table 8-8
Optimised ACR-700 - Sensitivity of Overpower to Selection of Random Age Distribution
(2-BS Fuelling Scheme, without Spatial Control)

Parameter	Select Channel No. 1 in Array of 7x7	Select Channel No. 7 in Array of 7x7	Select Channel No. 13 in Array of 7x7	Select Channel No. 25 in Array of 7x7	Select Channel No. 37 in Array of 7x7
K-effective	1.00254	1.002051	1.00252	1.00250	1.00252
Zone Controllers (% inserted)	50	50	50	50	50
Max. Channel Power (MW)	7.67 (L-12)	7.65 (H-12)	7.66 (M-11)	7.67 (G-8)	7.67 (G-8)
Max. Bundle Power (kW)	907.86 (N-15 bundle 4)	906.09 (G-7 bundle 4)	906.25 (E-5 bundle 5)	908.60 (G-5 bundle 5)	905.89 (O-14 bundle 5)
CP Max Ripple (Whole Core)	1.055 (M-4)	1.057 (M-15)	1.059 (D-12)	1.056 (G-5)	1.059 (P-7)
Max. Bundle Overpower	1.085	1.084	1.086	1.084	1.089
Excess Reactivity (mk)	2.5265	2.5056	2.5106	2.5057	2.5106

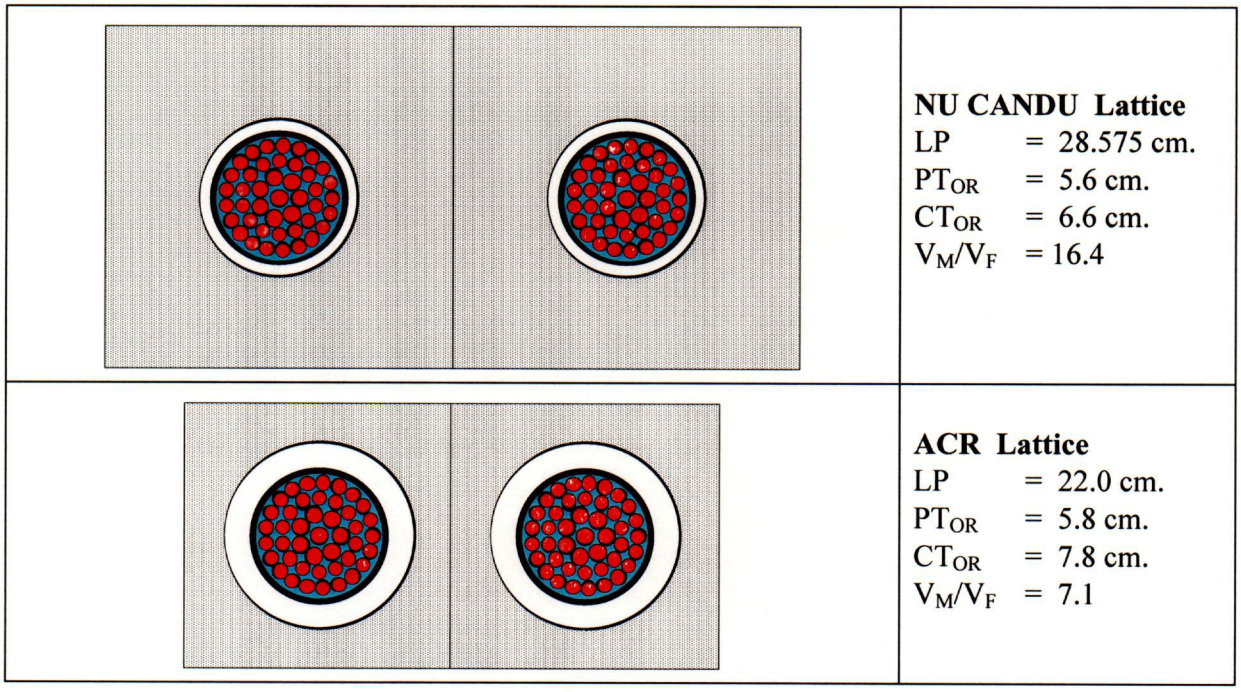

Figure 4-1 ACR and NU CANDU Lattice-Cell Configurations

C01

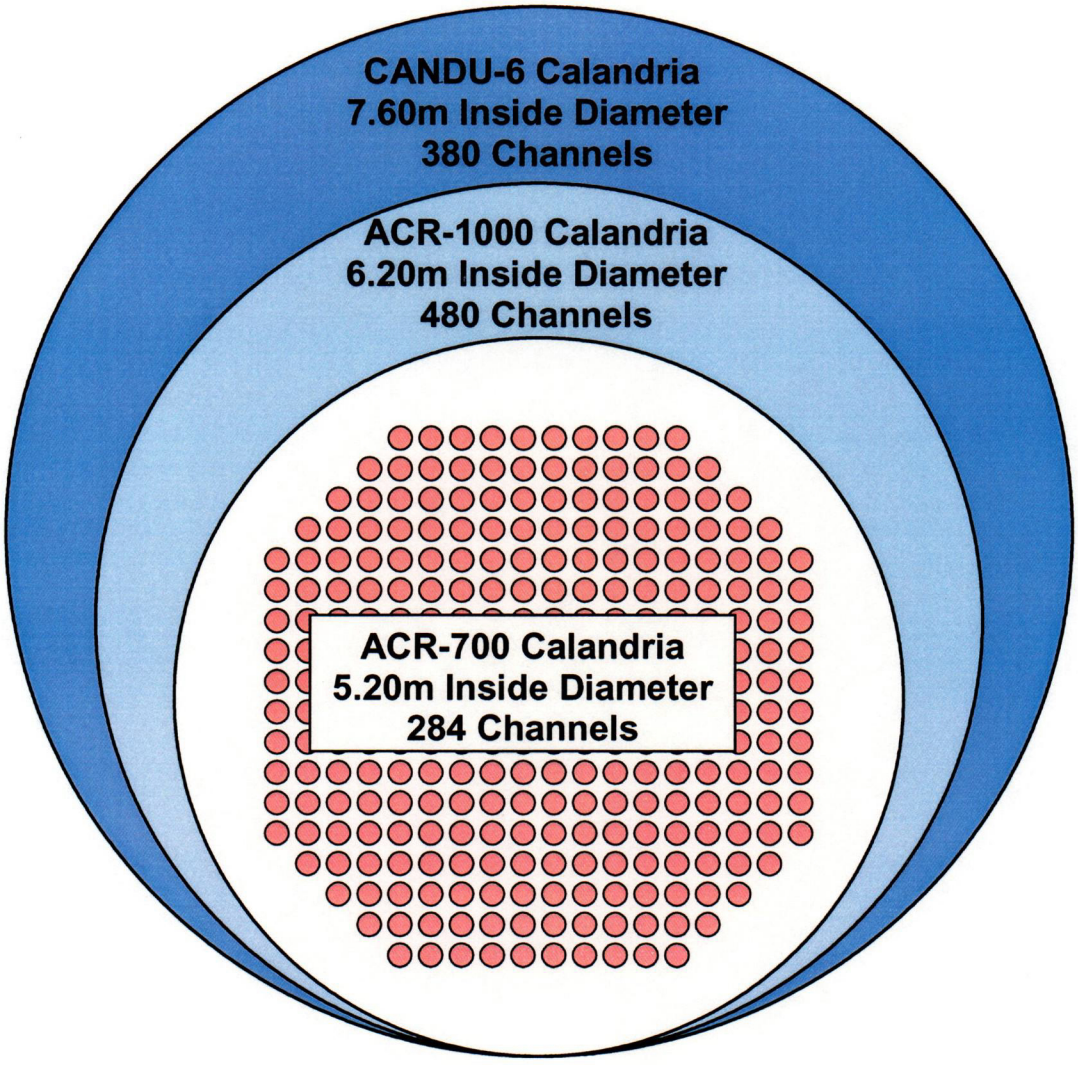

Figure 4-2 Comparison of Reactor-Core Sizes

C02

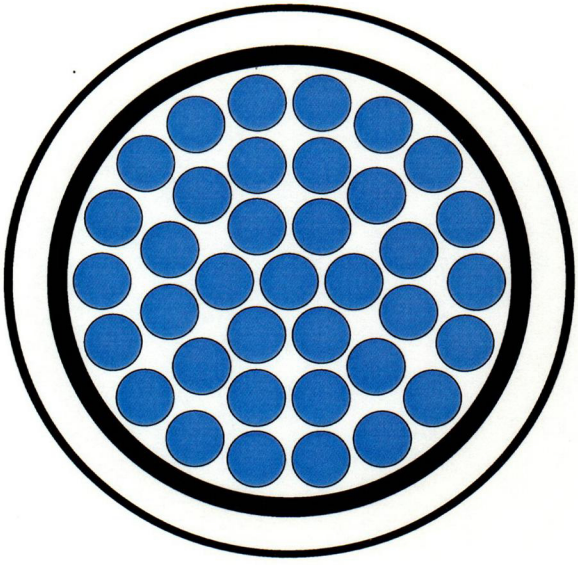

37-Element Bundle
CANDU-6 Fuel Channel

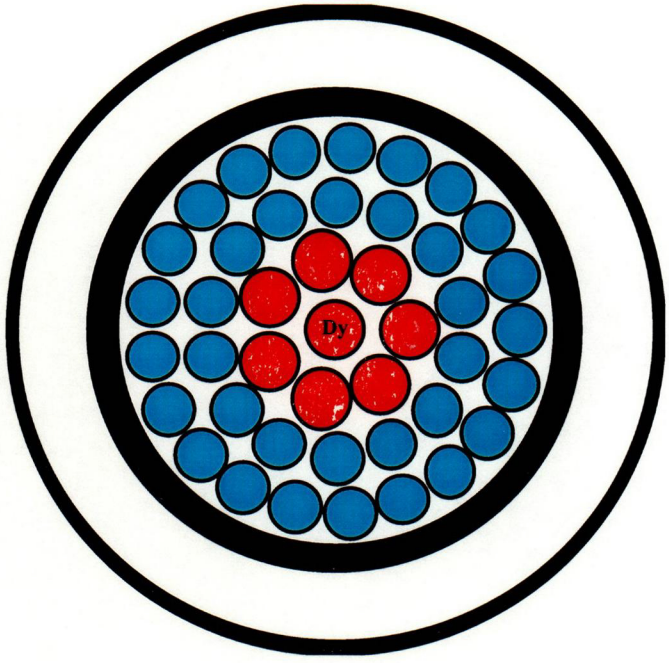

CANFLEX Bundle
(43-Elements)
ACR Fuel Channel

Figure 4-3 ACR and CANDU-6 Fuel Bundle

C03

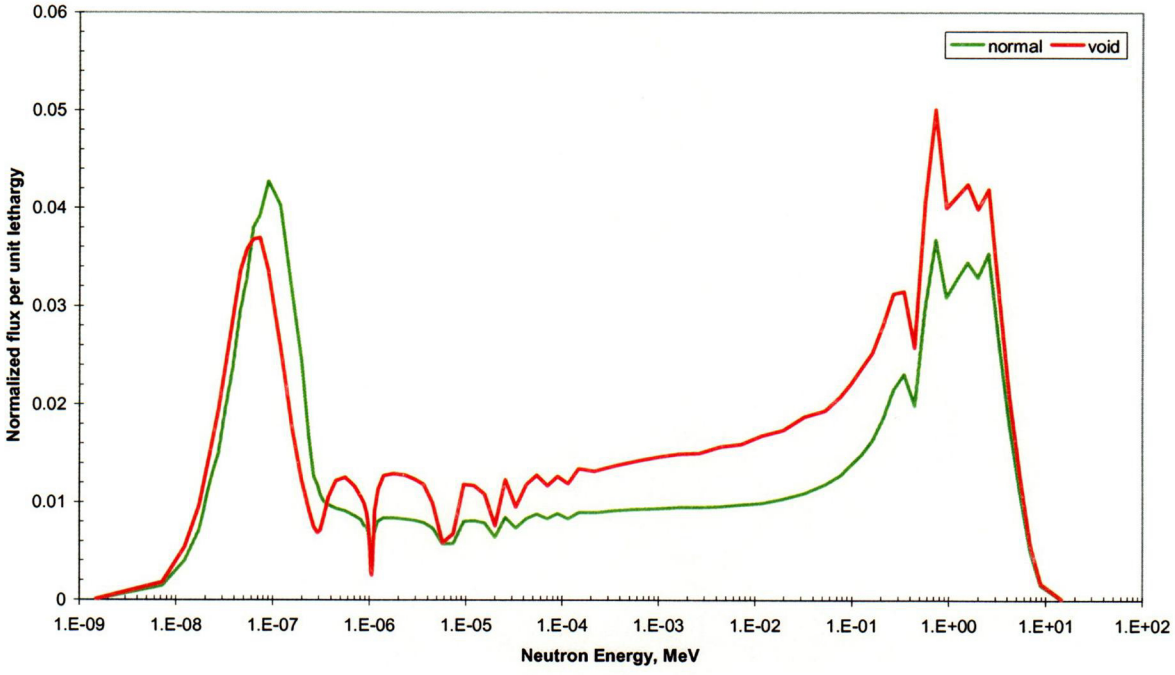

Figure 4-4 Neutron Flux Averaged Over Fuel and Coolant within the Pressure Tube (MCNP Model)

C04

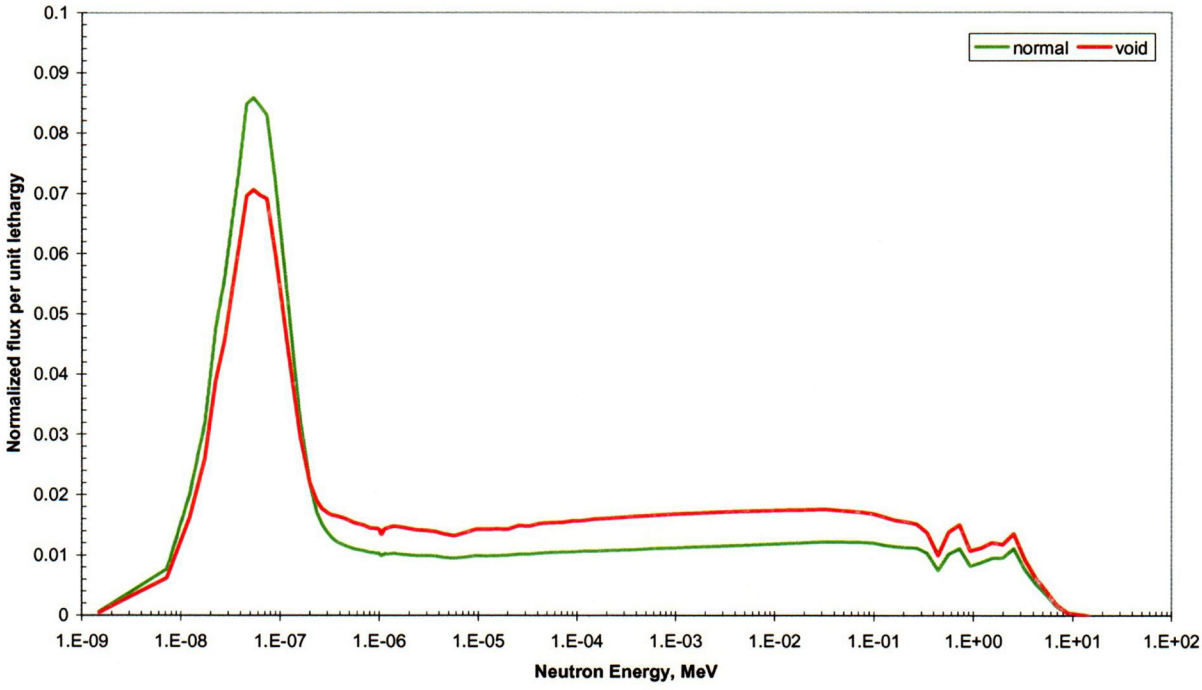

Figure 4-5 Neutron Flux Averaged over Moderator Region (MCNP Model)

C05

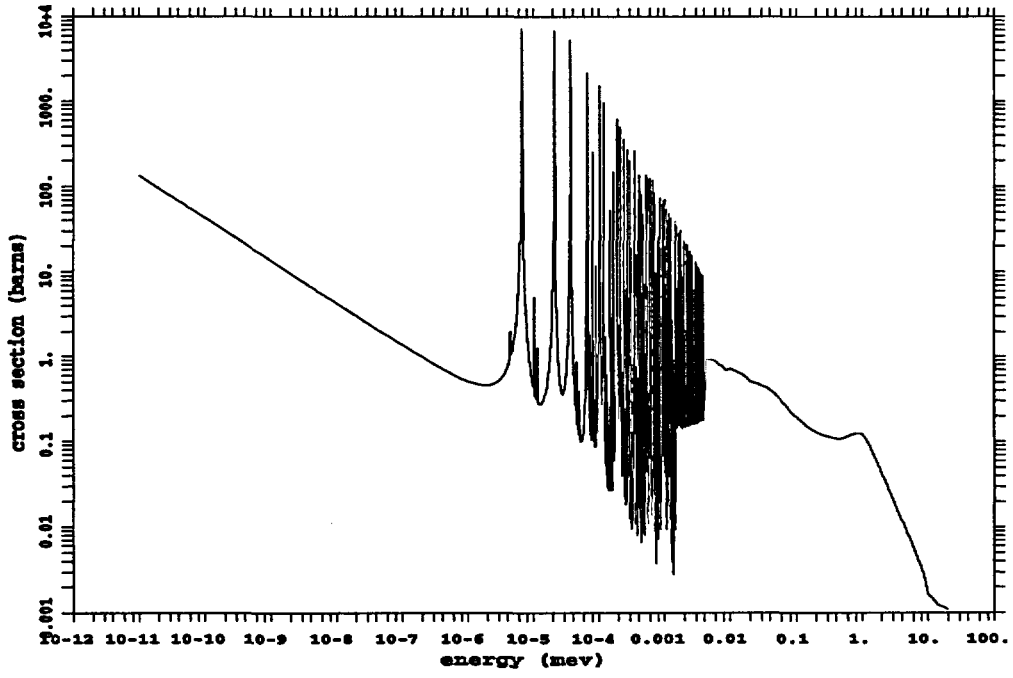

Figure 4-6 Absorption Cross Section of ^{238}U

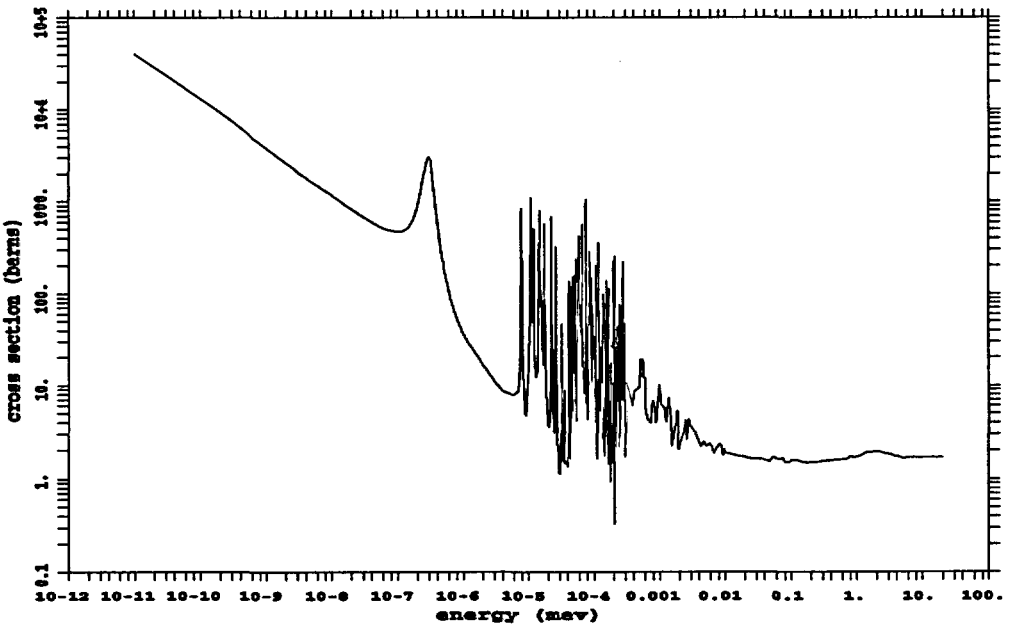

Figure 4-7 Fission Cross Section of ^{239}Pu

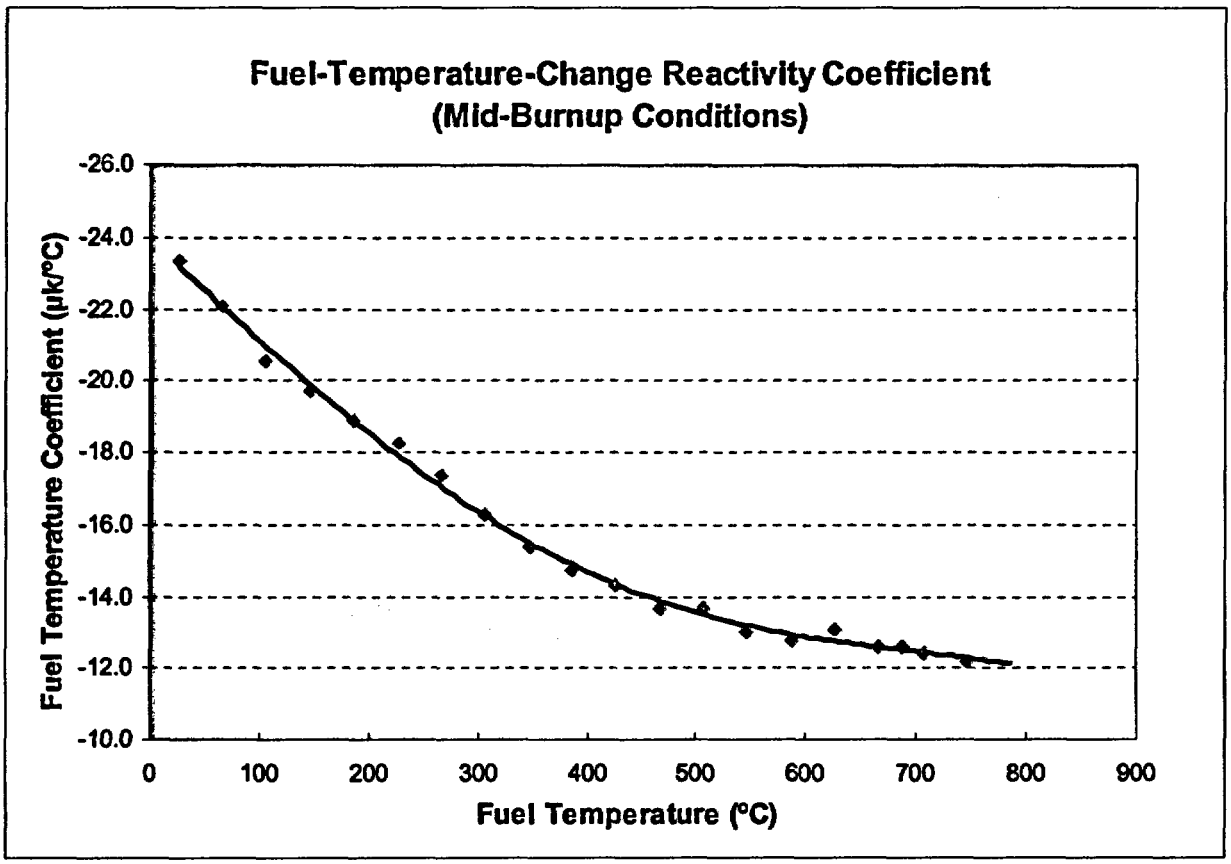

Figure 5-1 Change in Reactivity due to Instantaneous Change in Fuel Temperature (Equilibrium Fuel, WIMS-IST Calculation)

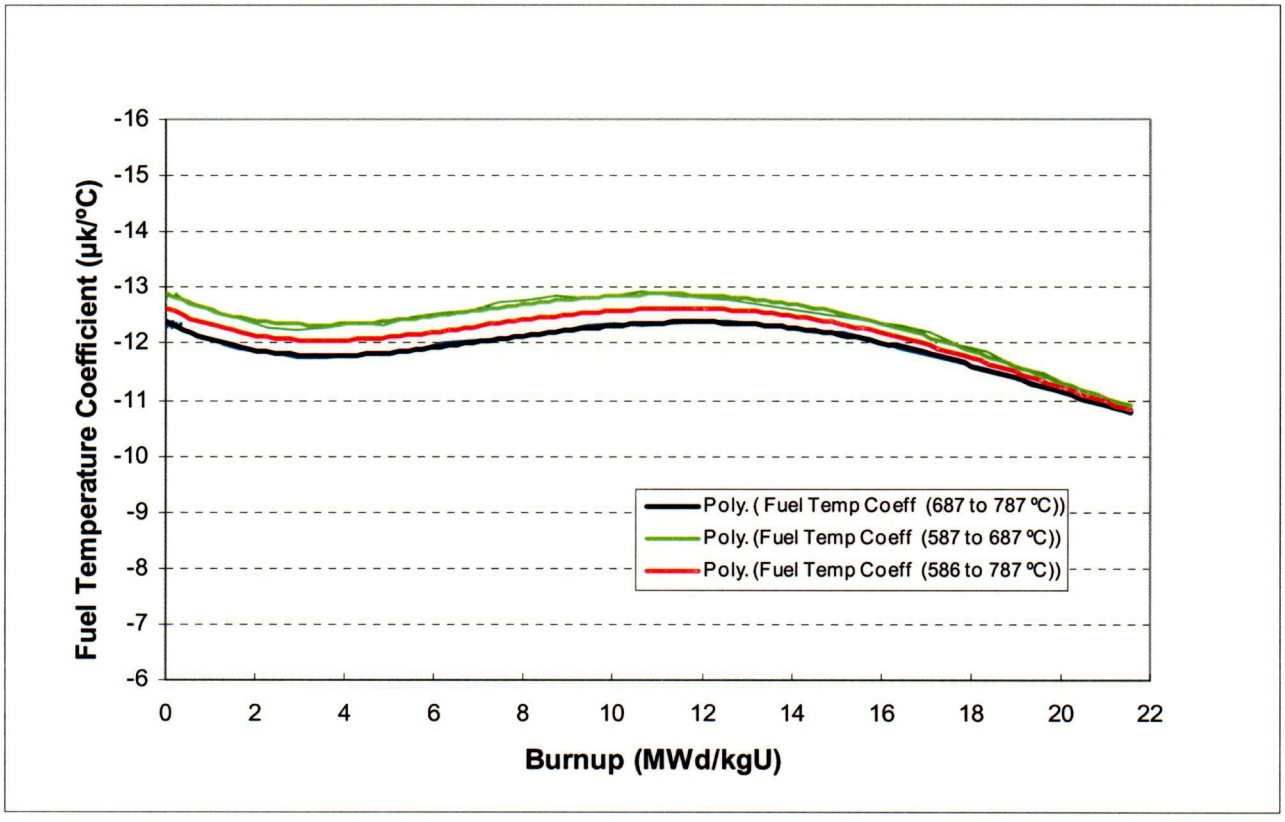

Figure 5-2 Fuel-Temperature-Change Reactivity versus Fuel Burnup (WIMS-IST Calculation)

C06

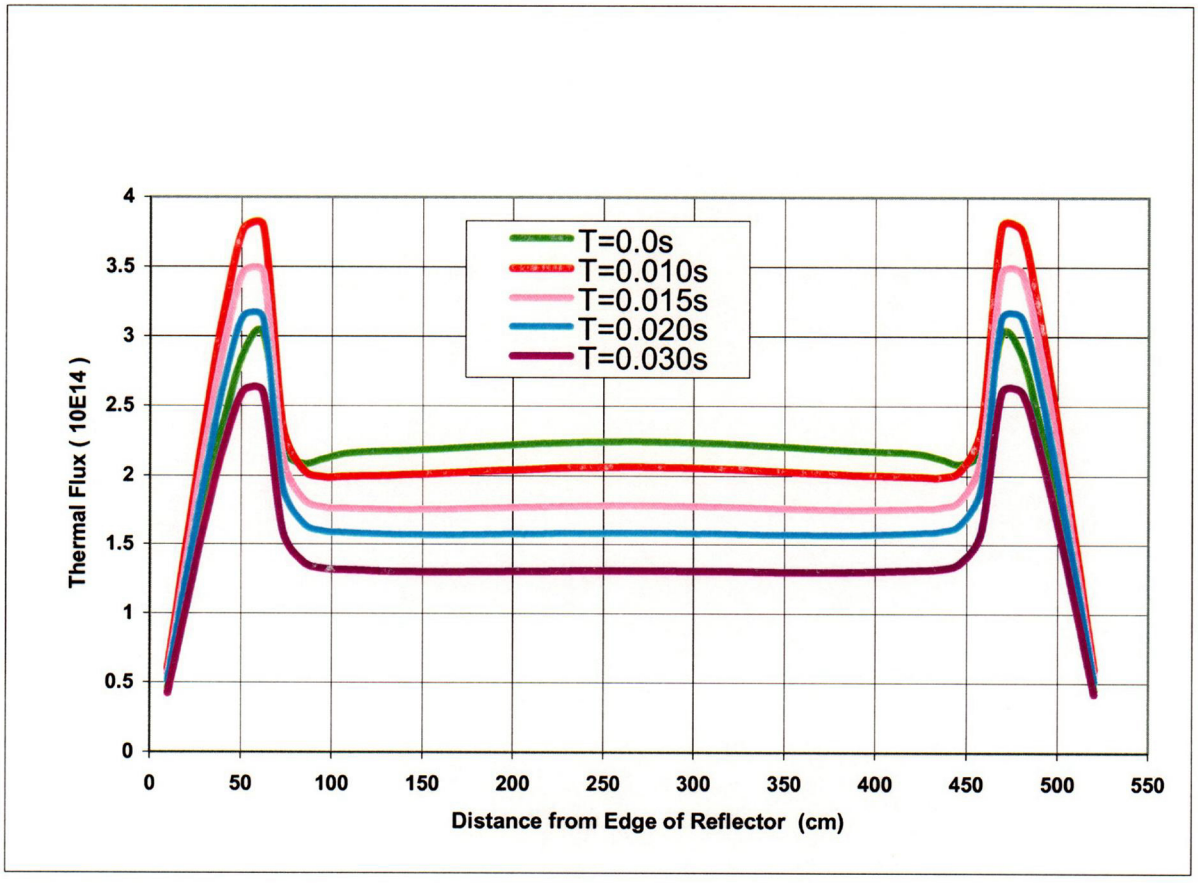

Figure 5-3 Effect of Instantaneous Coolant Voiding on Radial Neutron-Flux Distribution in ACR Core

C07

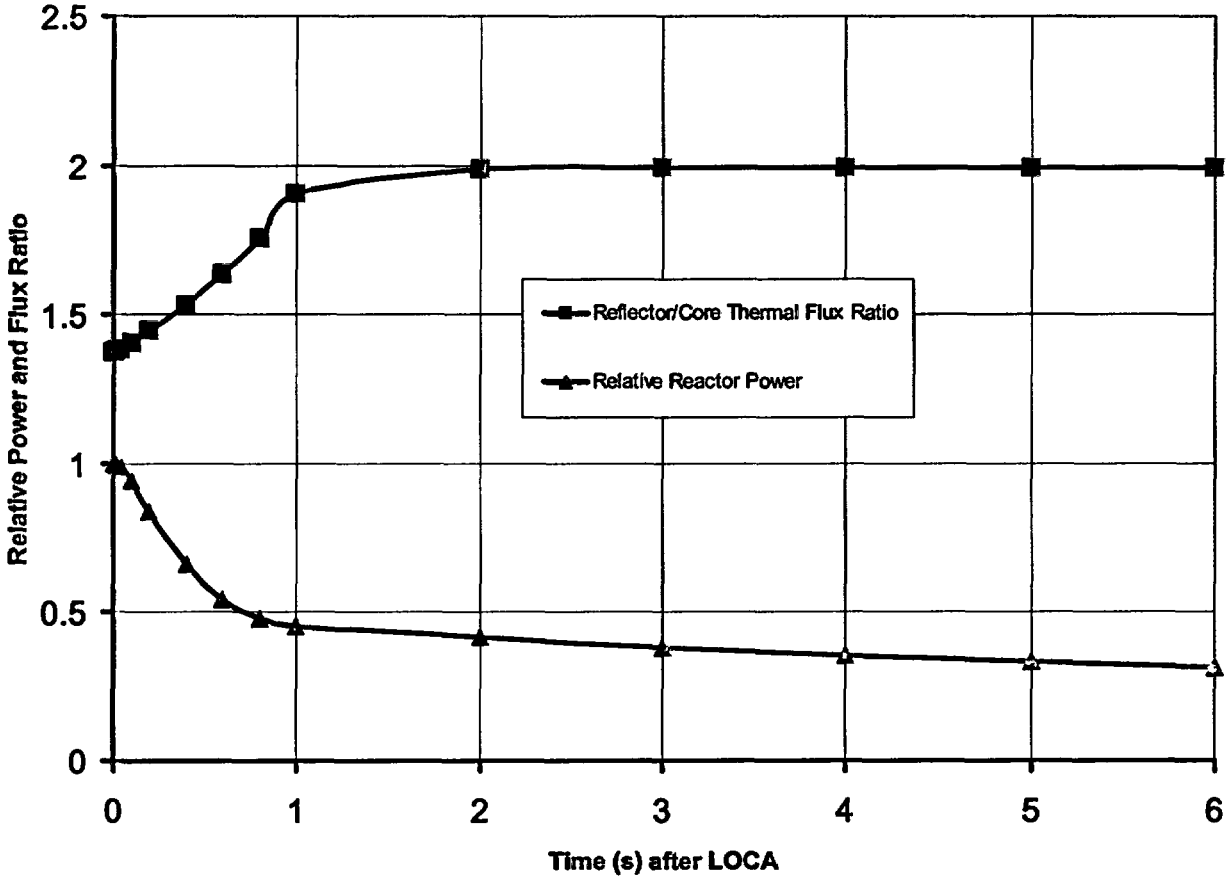

Figure 5-4 Relative Reactor Power and Thermal Fluxes after LOCA in ACR (Nominal Coolant-Voiding Rate)

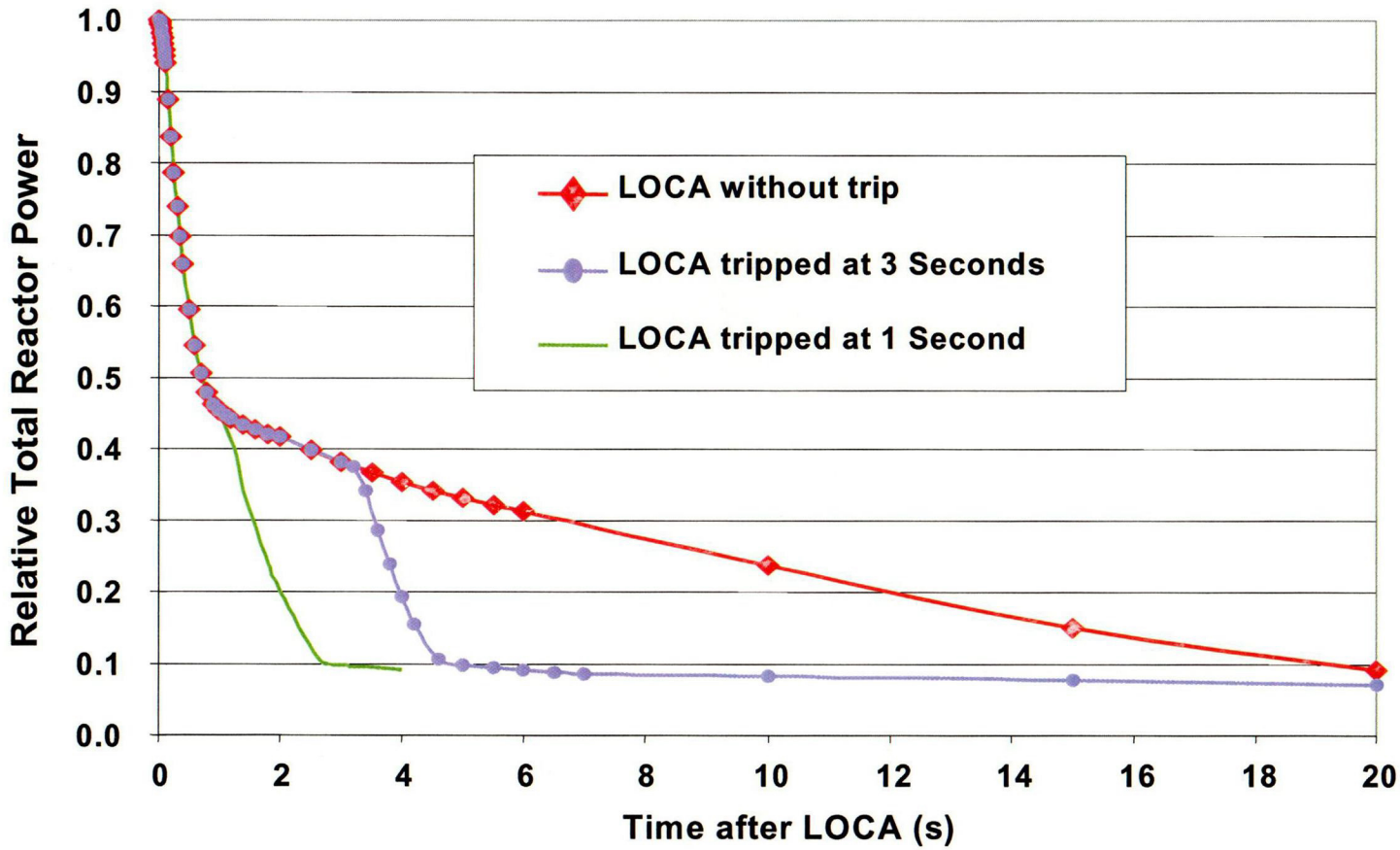

Figure 5-5 Effect of Trip Time on LOCA Transient in ACR (Nominal Coolant Voiding Rate)

C08

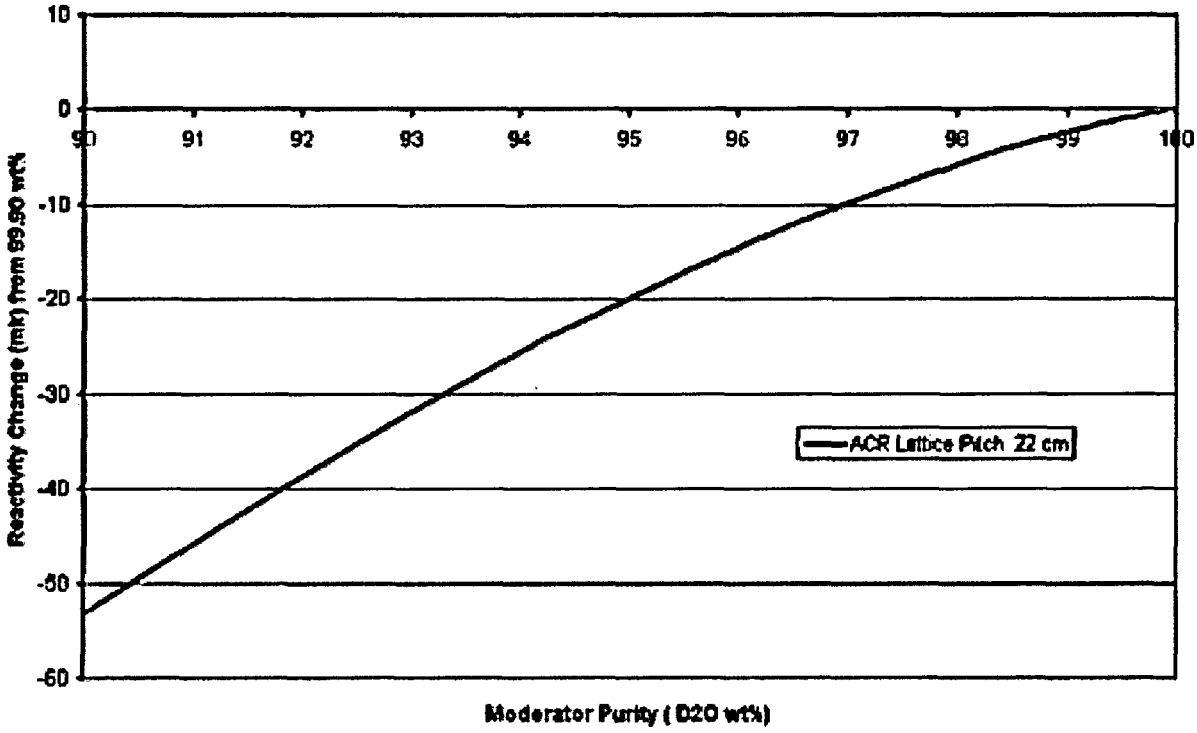

Figure 5-6 Reactivity Change Due to Moderator Purity Downgrading

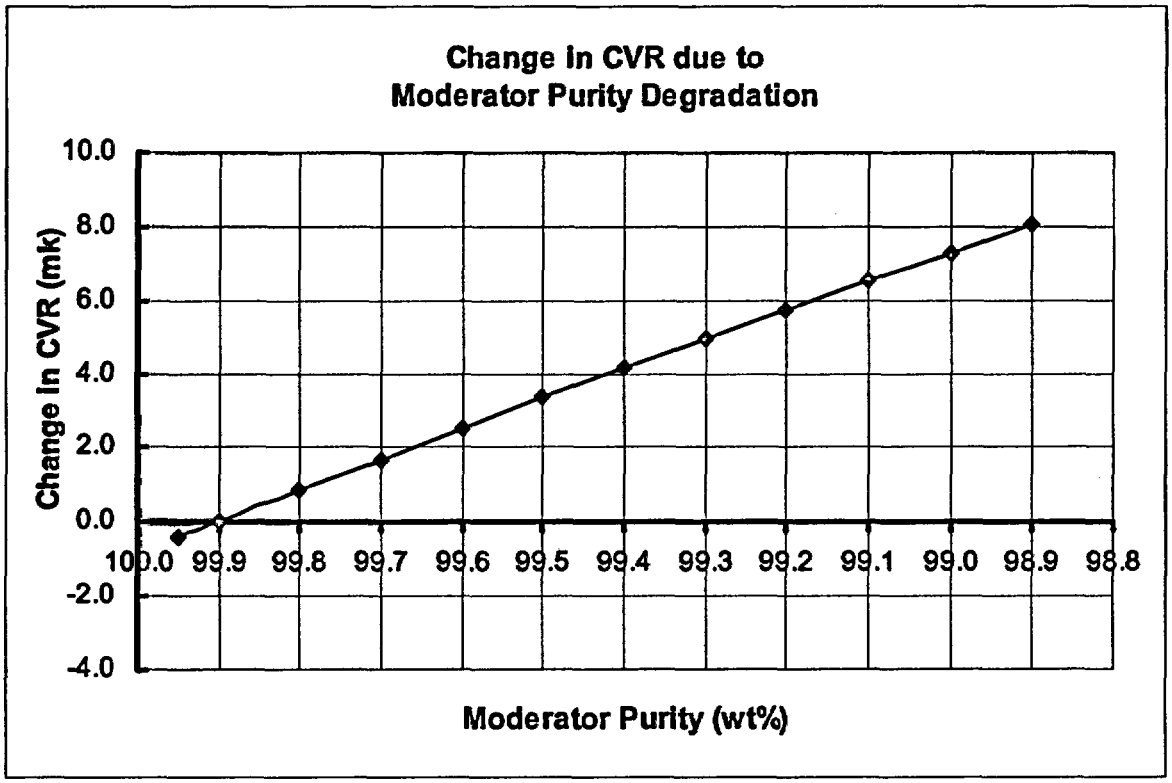

Figure 5-7 Full-Core Coolant-Void-Reactivity Change Due to Change in Moderator Purity

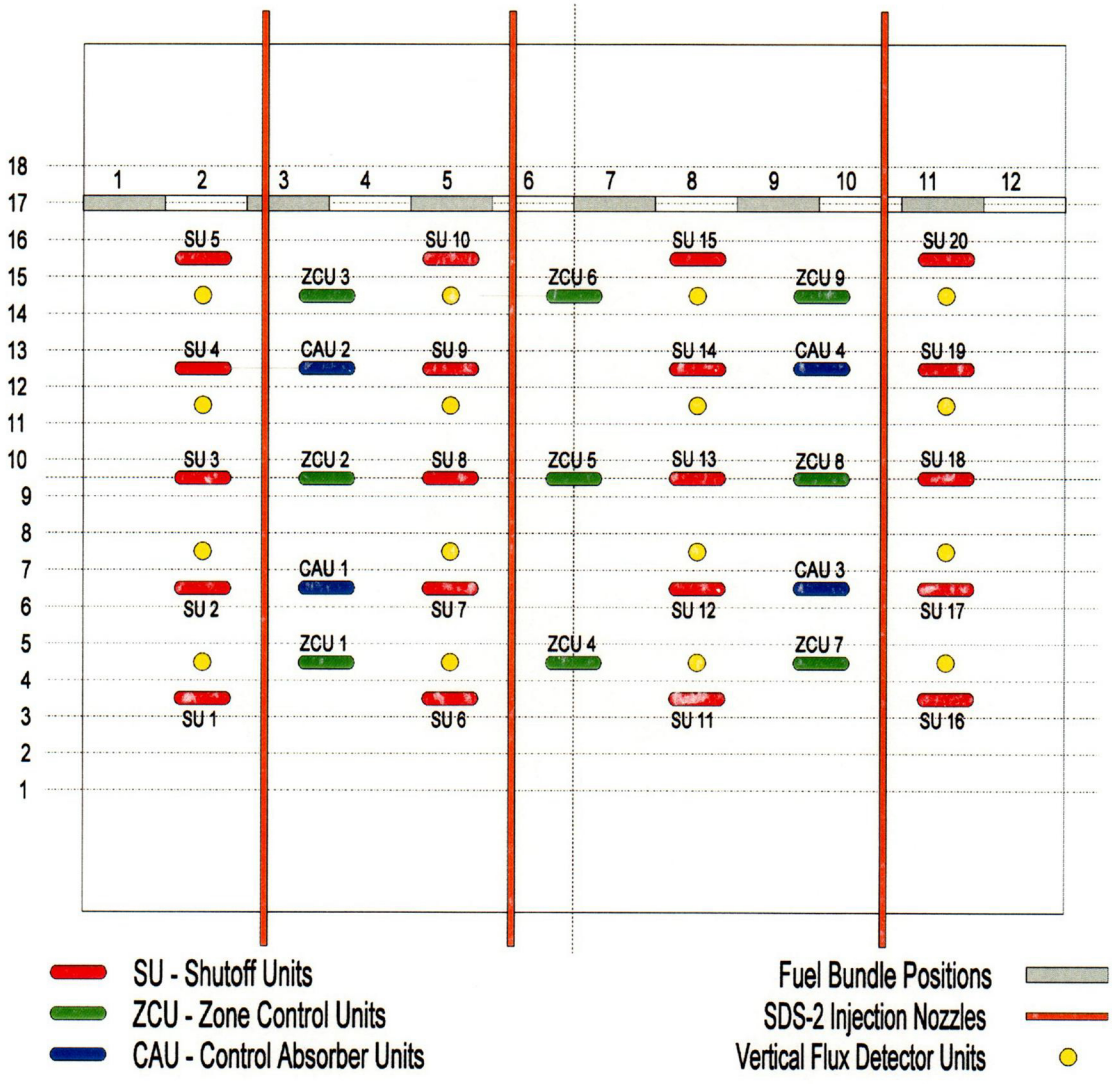

Figure 6-1 ACR-700 Reactivity-Mechanism Deck Plan View

C09

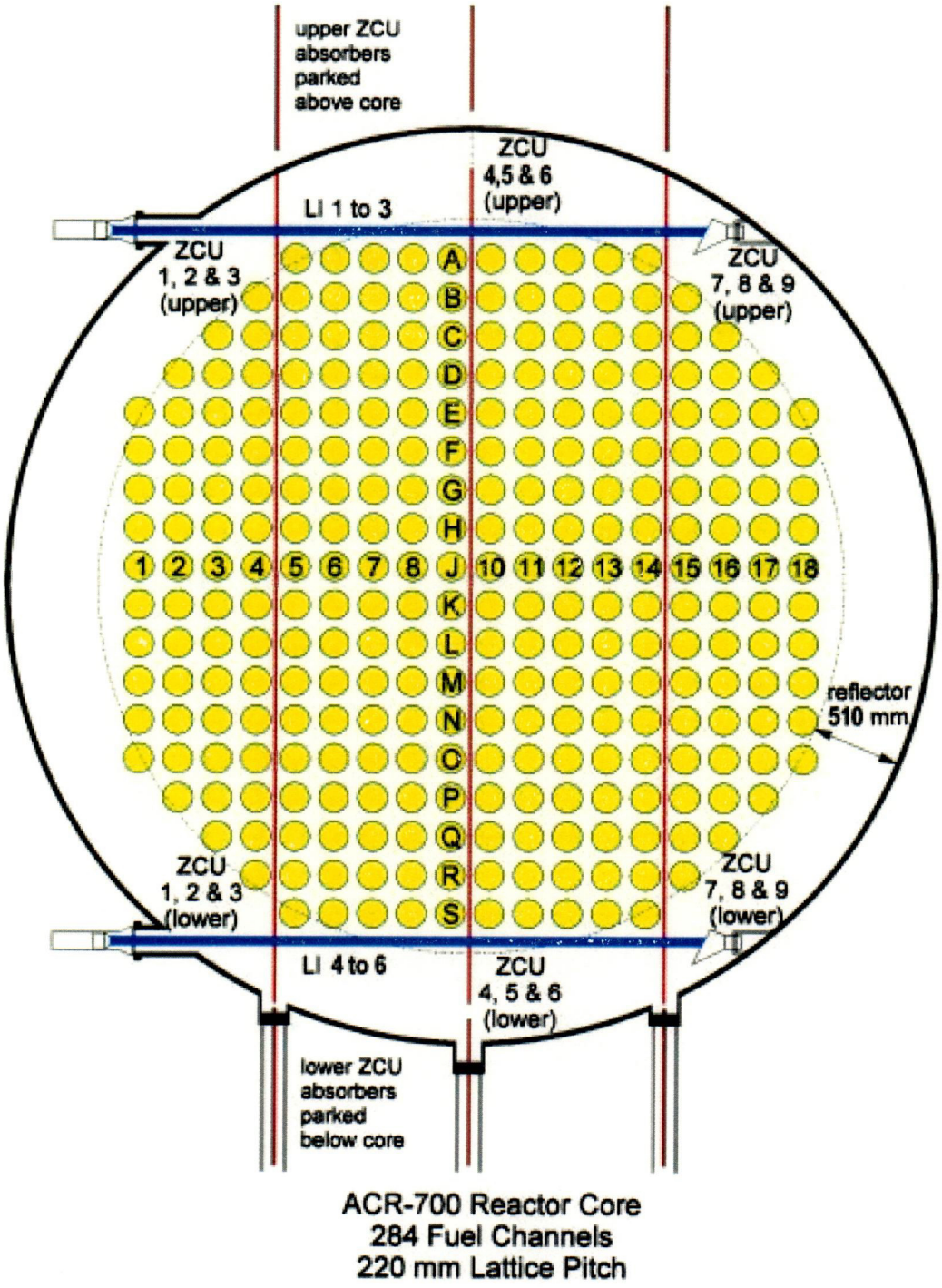

Figure 6-2 End View of ACR-700

CID

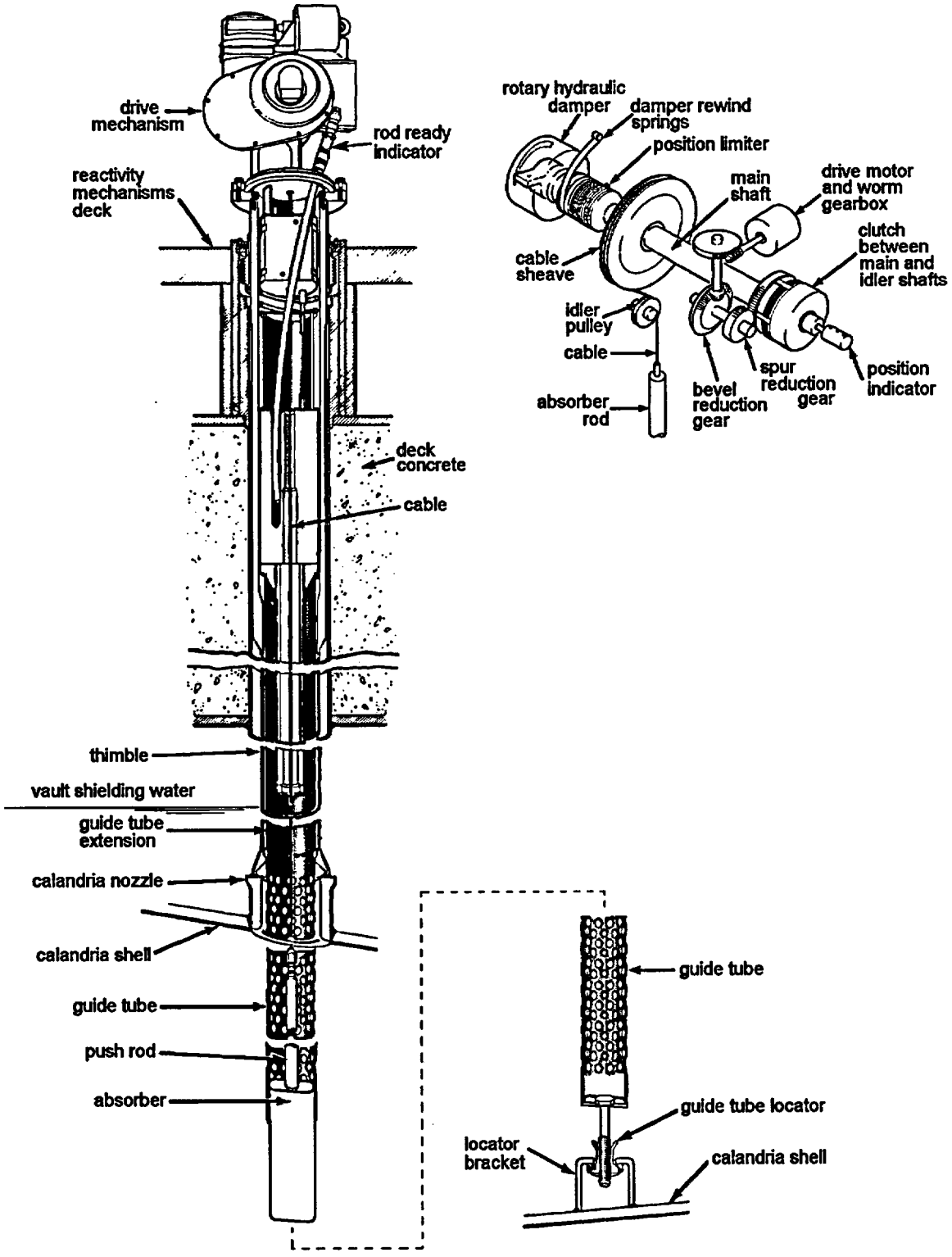

Figure 6-3 Shutdown System No. 1 Mechanical Shutoff Units

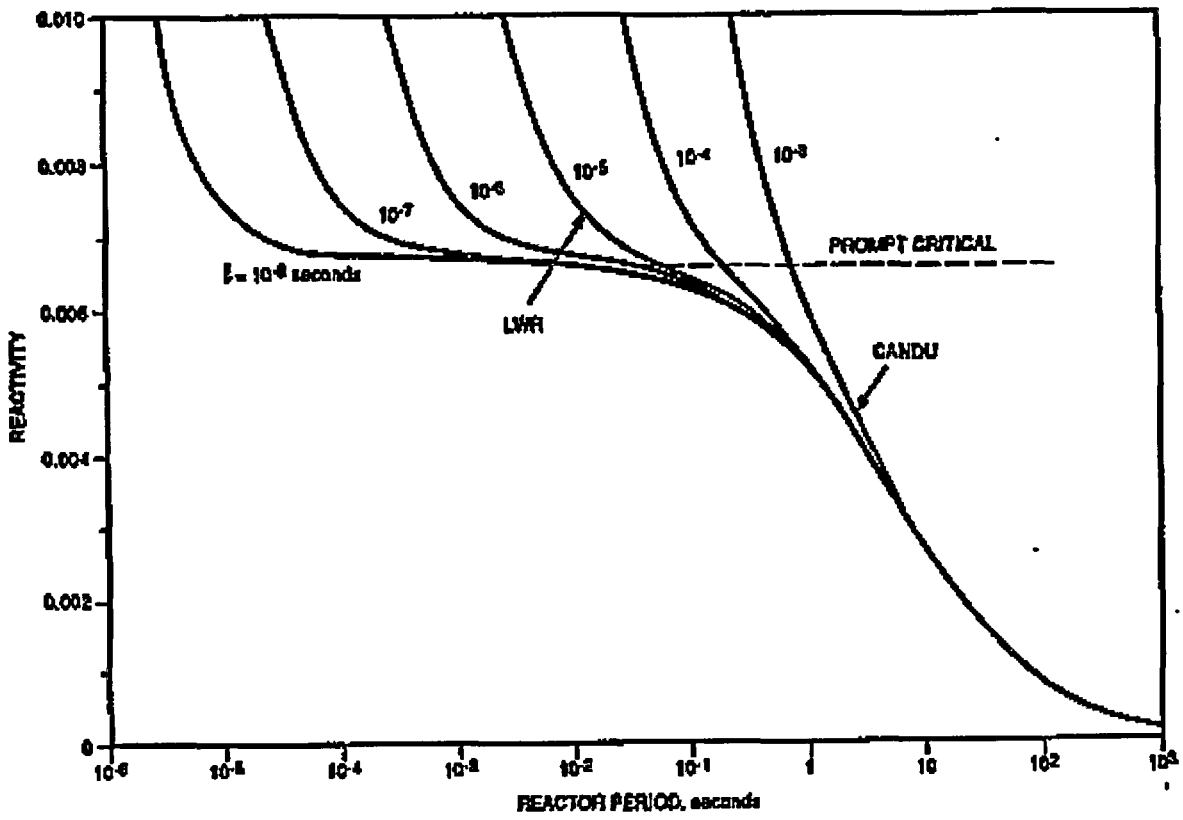

Figure 7-1 Reactor Period vs. Reactivity for Various Prompt-Neutron Lifetimes

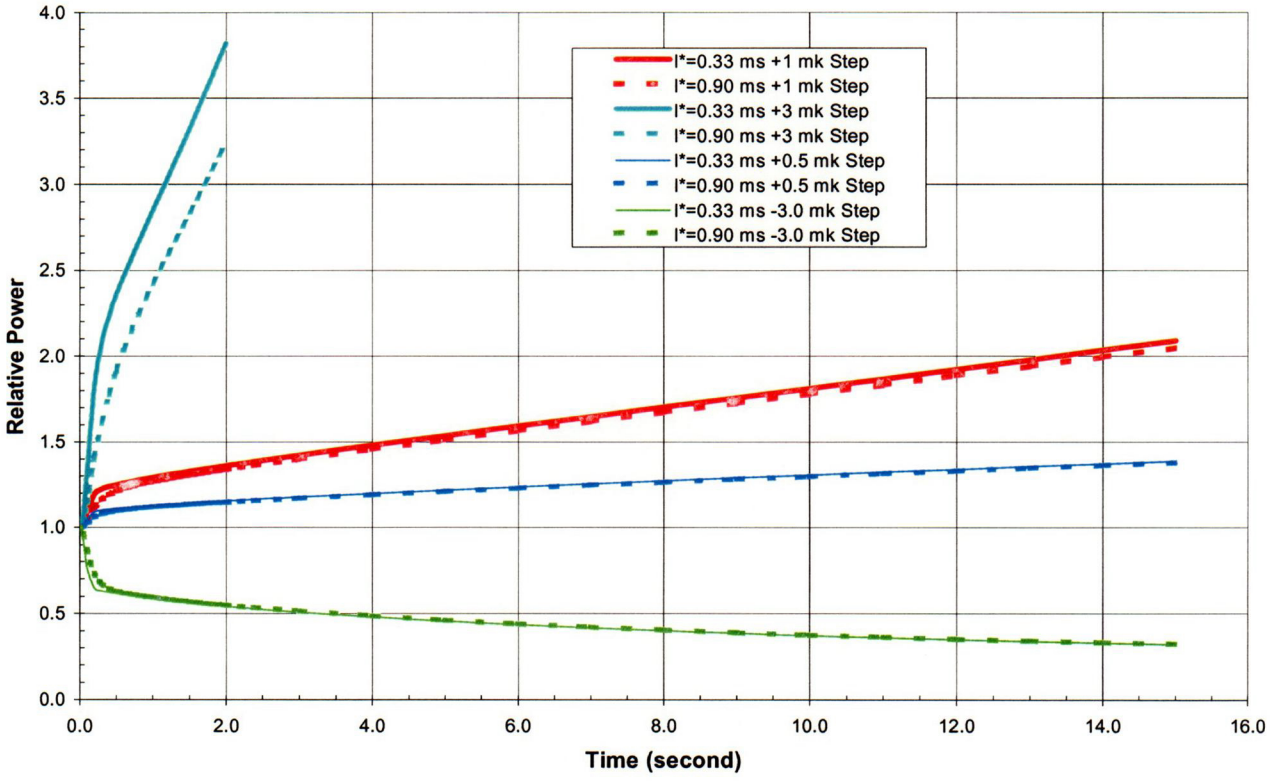

Figure 7-2 Effect of Reactivity and Prompt-Neutron Lifetime on ACR Power Transient (Reactor Initially Critical)

C11

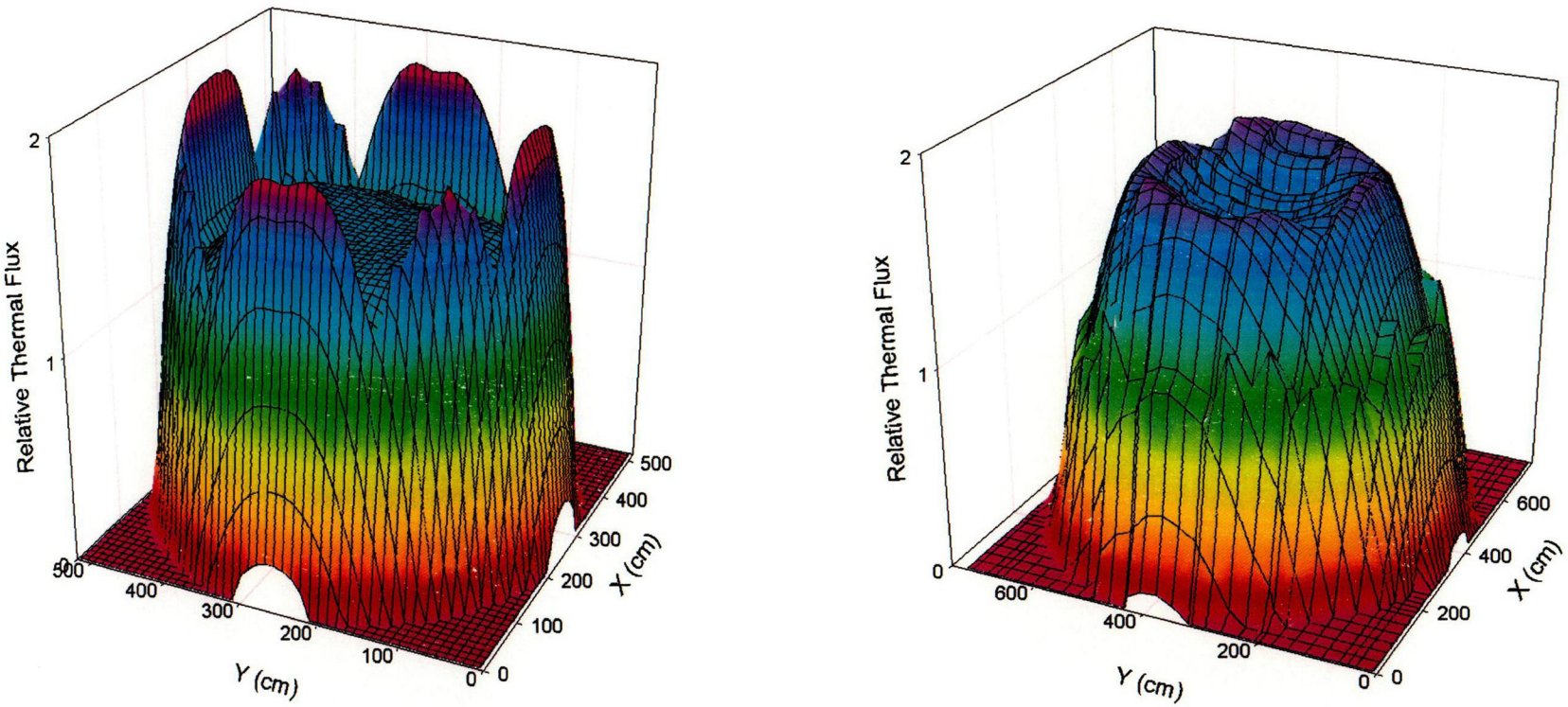

ACR **CANDU-6**

Figure 8-1 Radial Thermal-Neutron-Flux Distribution in ACR versus CANDU-6

C12

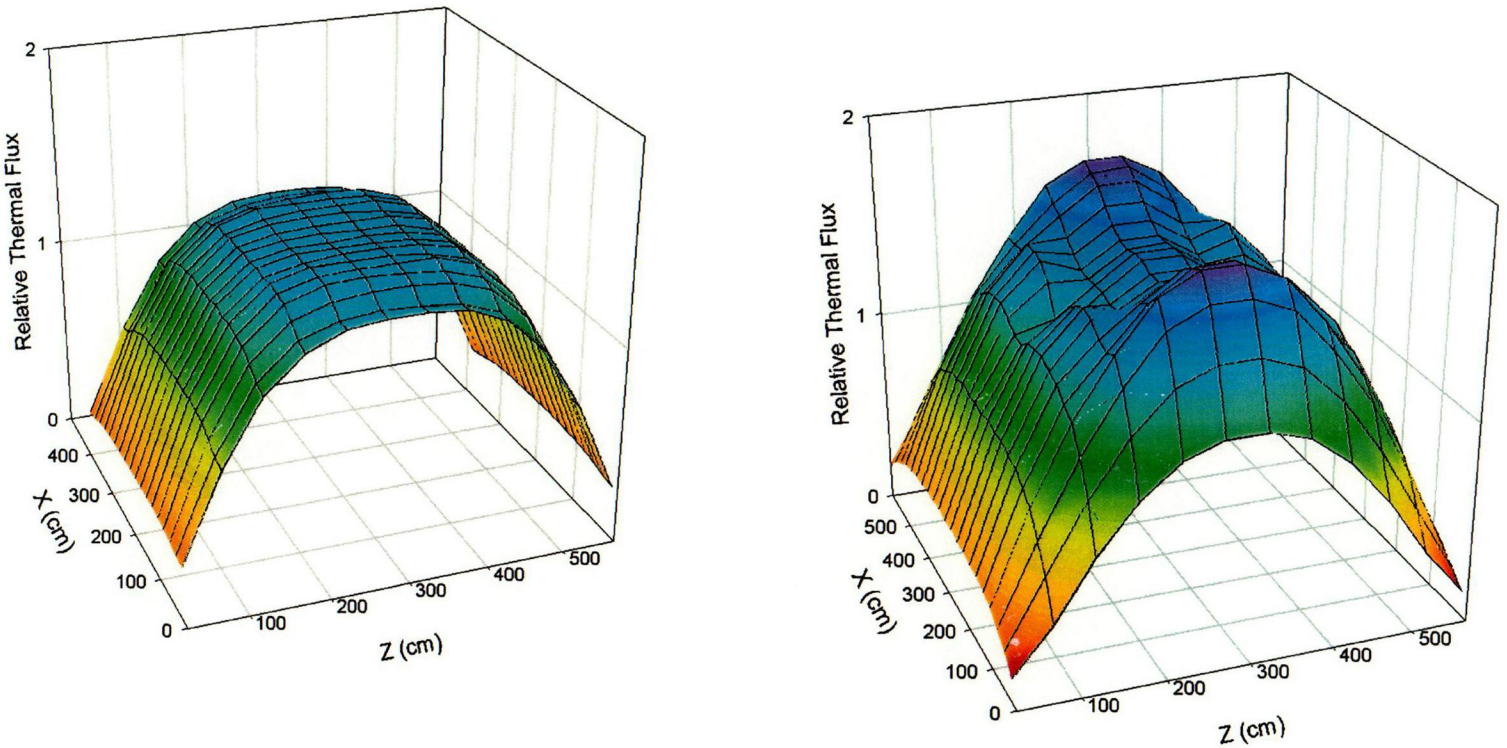

ACR **CANDU-6**

Figure 8-2 Axial Thermal-Neutron-Flux Profile in ACR vs. CANDU-6

C13

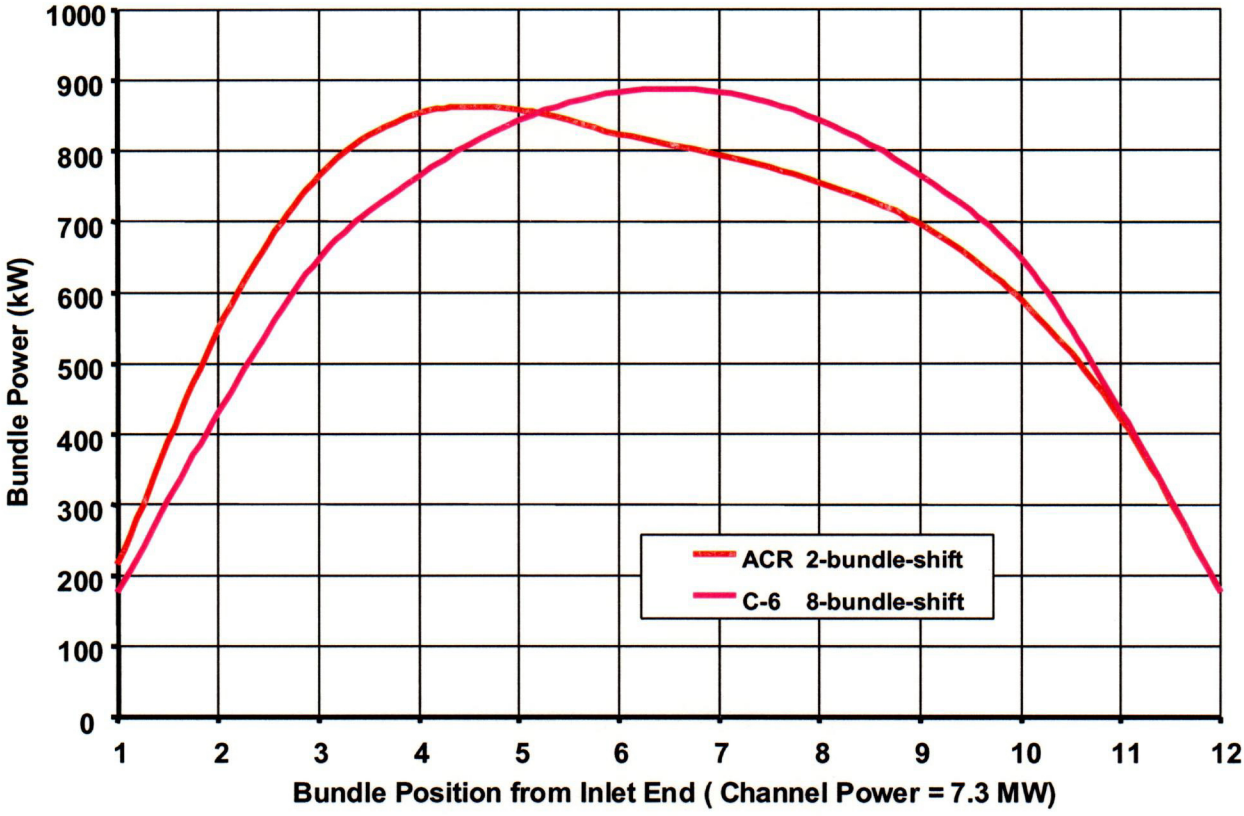

Figure 8-3 Bundle-Power Profile in ACR-700 vs. CANDU-6

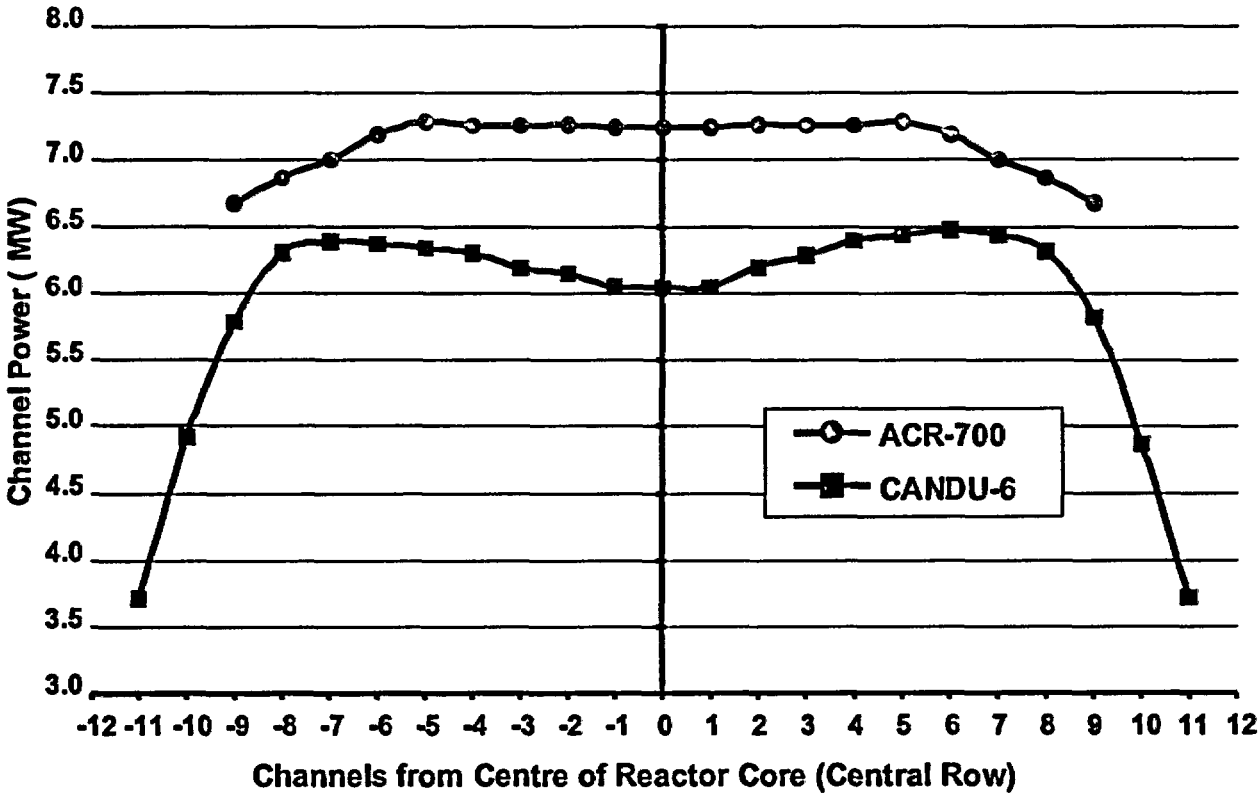

Figure 8-4 Radial Channel-Power Profile in ACR-700 vs. CANDU-6

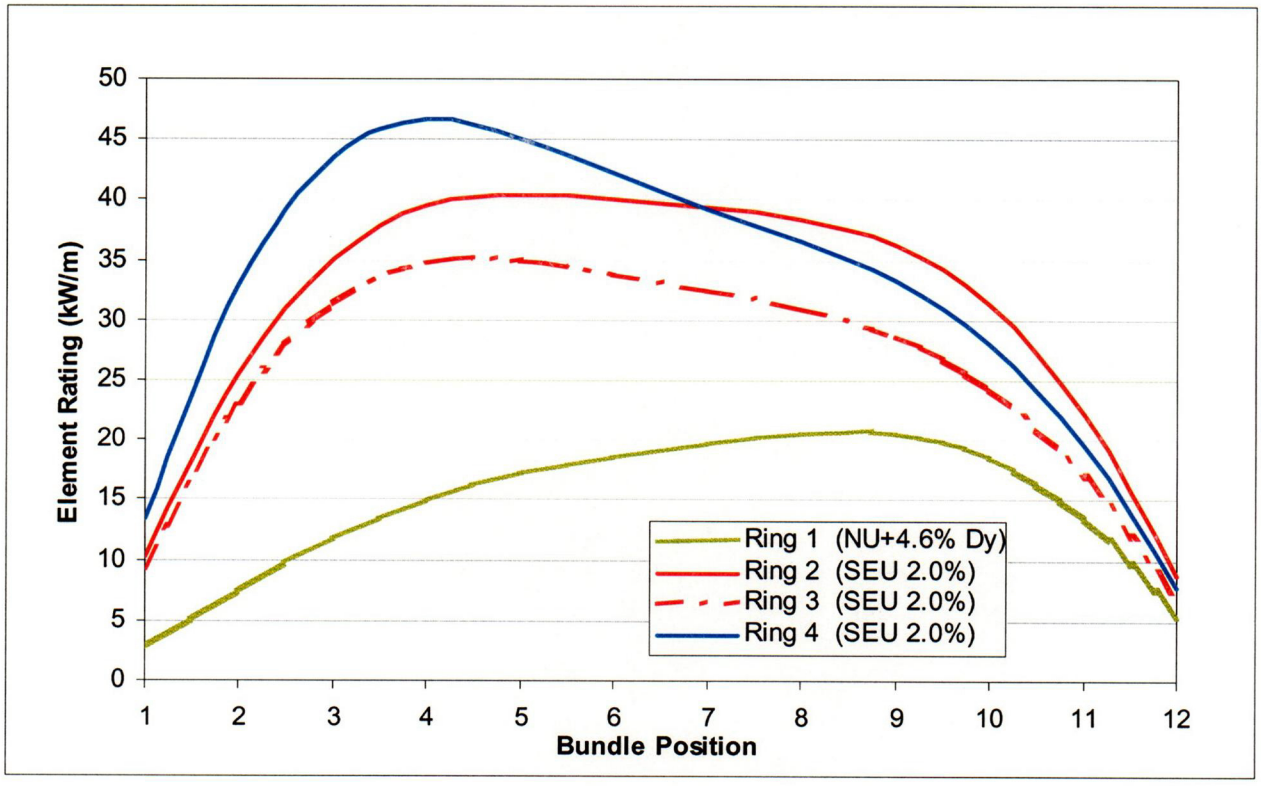

Figure 8-5 Linear Element Ratings for a 7.3 MW High-Power Channel in ACR-700

C15

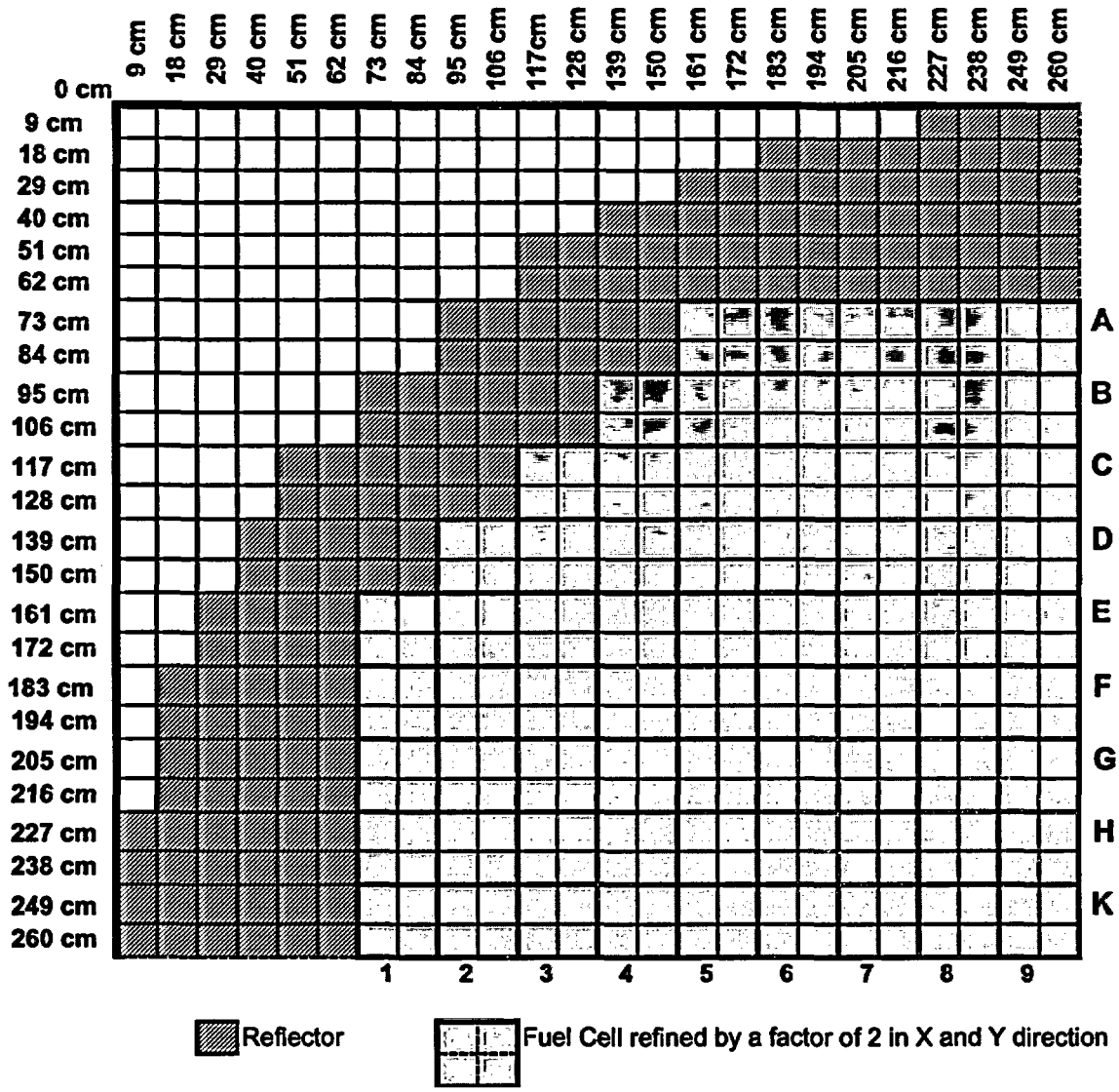

Figure 8-6 RFSP-IST Core Model - Mesh Intervals

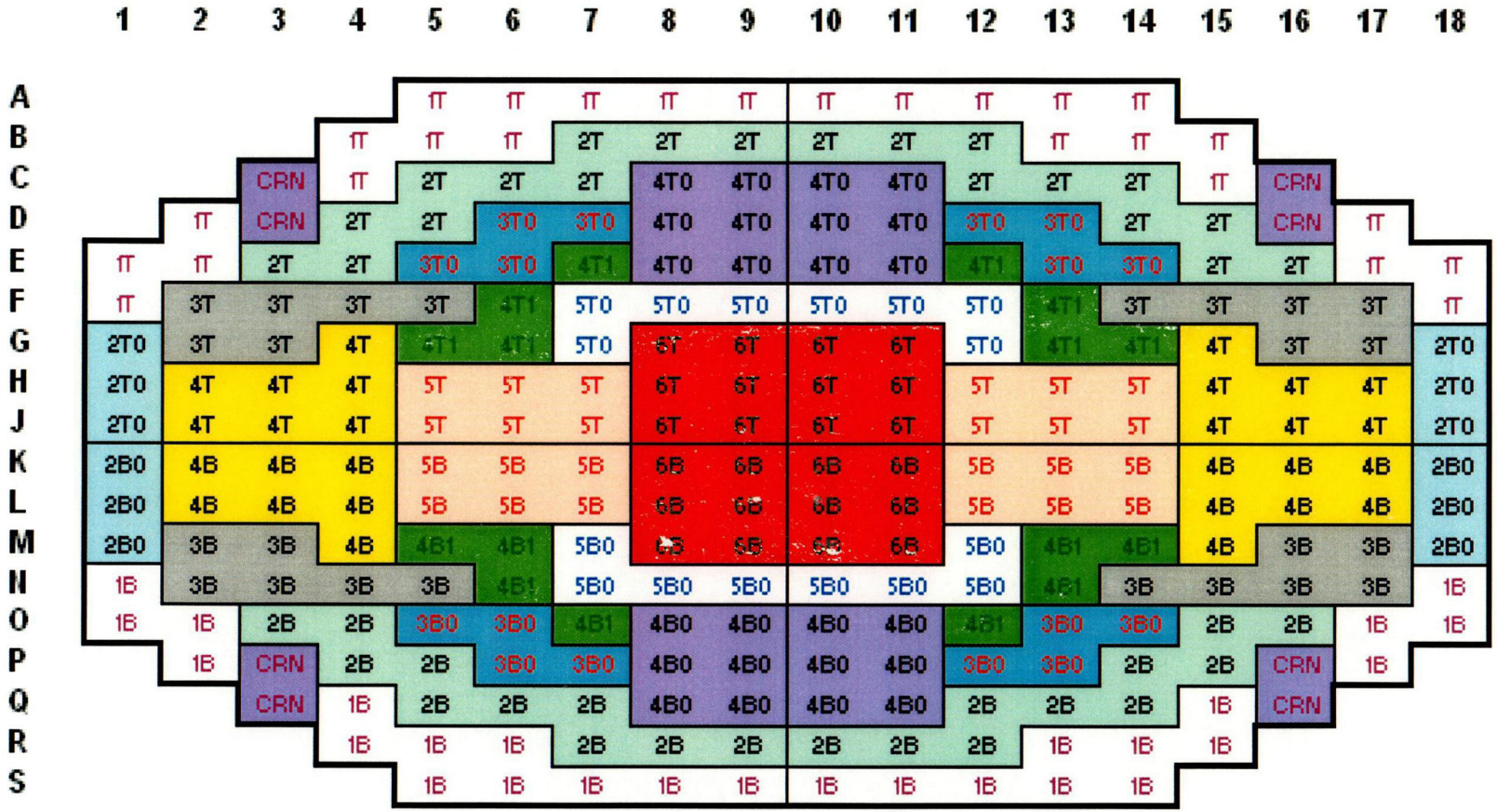

Figure 8-7 Irradiation Regions in ACR-700
(Optimised 284-Channel Core – Time-Average Model, 2-BS Fuelling Scheme)

C16

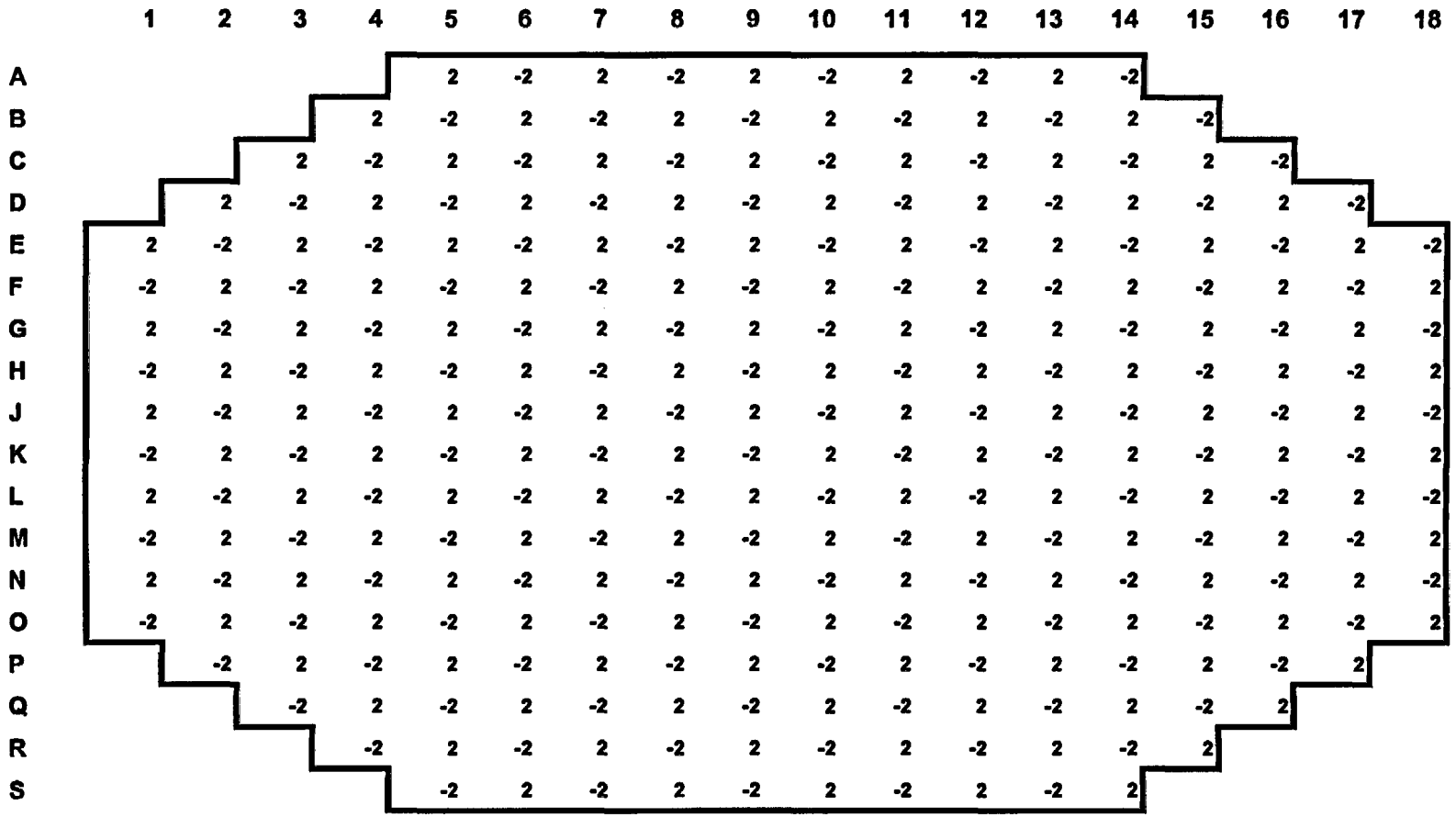

Figure 8-8 Fuelling Scheme and Channel Flow Direction in ACR-700 (Optimised 284-Channel Core – Time-Average Model, 2-BS Fuelling Scheme)

	1	2	3	4	5	6	7	8	9	10	11	12	13	14	15	16	17	18
A					13.8	13.9	13.9	13.9	14.0	14.0	13.9	13.9	13.9	13.8				
B				13.8	14.2	14.2	20.6	20.6	20.6	20.6	20.6	20.6	14.2	14.2	13.8			
C			14.2	14.2	20.7	20.6	20.6	23.2	23.3	23.3	23.2	20.6	20.6	20.7	14.2	14.2		
D		13.8	14.5	20.6	20.6	23.4	23.3	23.2	23.3	23.3	23.2	23.3	23.4	20.6	20.6	14.5	13.8	
E	13.8	14.1	20.6	20.6	23.4	23.3	23.5	23.2	23.2	23.2	23.2	23.5	23.3	23.4	20.6	20.6	14.1	13.8
F	13.9	22.7	22.7	22.7	22.7	23.5	24.0	23.9	24.0	24.0	23.9	24.0	23.5	22.7	22.7	22.7	22.7	13.9
G	17.5	22.7	22.7	22.7	23.5	23.5	24.0	24.2	24.2	24.2	24.2	24.0	23.5	23.5	22.7	22.7	22.7	17.5
H	17.5	22.7	22.7	22.7	24.0	24.0	24.0	24.2	24.2	24.2	24.2	24.0	24.0	24.0	22.7	22.7	22.7	17.5
J	17.5	22.7	22.7	22.7	24.0	24.0	24.0	24.2	24.2	24.2	24.2	24.0	24.0	24.0	22.7	22.7	22.7	17.5
K	17.5	22.7	22.7	22.7	24.0	24.0	24.0	24.2	24.2	24.2	24.2	24.0	24.0	24.0	22.7	22.7	22.7	17.5
L	17.5	22.7	22.7	22.7	24.0	24.0	24.0	24.2	24.2	24.2	24.2	24.0	24.0	24.0	22.7	22.7	22.7	17.5
M	17.5	22.7	22.7	22.7	23.5	23.5	24.0	24.2	24.2	24.2	24.2	24.0	23.5	23.5	22.7	22.7	22.7	17.5
N	13.9	22.7	22.7	22.7	22.7	23.5	24.0	23.9	24.0	24.0	23.9	24.0	23.5	22.7	22.7	22.7	22.7	13.9
O	13.8	14.1	20.6	20.6	23.4	23.3	23.5	23.2	23.2	23.2	23.2	23.5	23.3	23.4	20.6	20.6	14.1	13.8
P		13.8	14.5	20.6	20.6	23.4	23.3	23.2	23.3	23.3	23.2	23.3	23.4	20.6	20.6	14.5	13.8	
Q			14.2	14.2	20.7	20.6	20.6	23.2	23.3	23.3	23.2	20.6	20.6	20.7	14.2	14.2		
R				13.8	14.2	14.2	20.6	20.6	20.6	20.6	20.6	20.6	14.2	14.2	13.8			
S					13.8	13.9	13.9	13.9	14.0	14.0	13.9	13.9	13.9	13.8				

Figure 8-9 Channel Average Exit Burnup (MW·d/kgU) in ACR-700
(Optimised 284-Channel Core – Time-Average Model, 2-BS Fuelling Scheme)

	1	2	3	4	5	6	7	8	9	10	11	12	13	14	15	16	17	18
A					78.0	72.1	67.6	66.2	67.8	67.8	66.2	67.6	72.2	78.0				
B				70.8	73.2	68.6	102.8	102.6	105.6	105.6	102.6	102.9	68.6	73.2	70.8			
C			68.0	69.8	104.5	99.4	97.8	114.2	117.6	117.6	114.2	97.9	99.4	104.5	69.9	68.0		
D		67.3	69.8	101.7	98.7	112.2	111.2	110.9	112.9	112.9	110.9	111.2	112.2	98.7	101.8	69.9	67.3	
E	74.6	71.1	102.1	97.8	111.4	110.1	110.7	108.8	109.4	109.4	108.8	110.7	110.1	111.4	97.8	102.2	71.1	74.6
F	73.3	122.5	114.0	109.1	106.5	110.3	112.2	112.0	112.3	112.3	112.0	112.2	110.3	106.5	109.1	114.0	122.6	73.4
G	91.8	120.7	113.3	108.7	111.0	109.9	111.9	112.9	113.1	113.1	112.9	111.9	110.0	111.0	108.7	113.3	120.8	91.9
H	89.5	119.4	112.7	108.5	114.0	112.9	112.4	112.8	113.0	113.0	112.8	112.4	112.9	114.0	108.5	112.7	119.4	89.5
J	88.3	118.6	112.4	108.4	114.0	113.0	112.4	112.7	112.9	112.9	112.7	112.4	113.0	114.0	108.4	112.4	118.6	88.3
K	88.3	118.6	112.4	108.4	114.0	113.0	112.4	112.7	112.9	112.9	112.7	112.4	113.0	114.0	108.4	112.4	118.6	88.3
L	89.5	119.4	112.7	108.5	114.0	112.9	112.4	112.8	113.0	113.0	112.8	112.4	112.9	114.0	108.5	112.7	119.4	89.5
M	91.9	120.7	113.3	108.7	111.0	110.0	111.9	112.9	113.1	113.1	112.9	111.9	110.0	111.0	108.7	113.3	120.8	91.9
N	73.4	122.6	114.0	109.1	106.5	110.3	112.2	112.0	112.3	112.3	112.0	112.2	110.3	106.6	109.1	114.0	122.6	73.4
O	74.6	71.1	102.2	97.8	111.4	110.1	110.7	108.8	109.4	109.4	108.8	110.7	110.1	111.5	97.8	102.2	71.1	74.6
P		67.3	69.9	101.8	98.7	112.2	111.2	110.9	112.9	112.9	110.9	111.2	112.2	98.8	101.8	69.9	67.3	
Q			68.0	69.9	104.5	99.4	97.9	114.2	117.7	117.7	114.3	97.9	99.4	104.5	69.9	68.0		
R				70.8	73.2	68.6	102.9	102.7	105.6	105.6	102.7	102.9	68.7	73.2	70.8			
S					78.0	72.2	67.6	66.2	67.9	67.9	66.2	67.6	72.2	78.0				

Figure 8-10 Channel Dwell Times (FPD) in ACR-700
(Optimised 284-Channel Core - Time-Average Model, 2-BS Fuelling Scheme)

	1	2	3	4	5	6	7	8	9	10	11	12	13	14	15	16	17	18
A					6029	6571	7009	7149	6996	6996	7149	7008	6570	6027				
B				6653	6600	7046	6809	6817	6647	6647	6817	6808	7045	6599	6651			
C			7099	6913	6727	7051	7158	6924	6744	6744	6923	7157	7050	6726	6911	7096		
D		6979	7086	6900	7107	7083	7143	7129	7015	7015	7128	7142	7082	7104	6897	7083	6977	
E	6278	6773	6858	7166	7131	7216	7237	7266	7229	7229	7265	7236	7214	7129	7164	6856	6770	6276
F	6453	6305	6785	7091	7258	7265	7263	7276	7260	7259	7276	7262	7264	7256	7089	6783	6303	6451
G	6485	6396	6826	7116	7216	7285	7284	7284	7272	7271	7283	7283	7284	7215	7114	6825	6394	6483
H	6652	6469	6861	7128	7177	7245	7281	7292	7283	7283	7292	7280	7244	7176	7126	6859	6467	6650
J	6737	6509	6881	7134	7174	7241	7280	7295	7287	7287	7295	7280	7240	7173	7133	6879	6508	6735
K	6737	6509	6880	7134	7174	7241	7280	7295	7287	7287	7295	7280	7240	7173	7133	6879	6508	6735
L	6651	6468	6860	7127	7176	7244	7281	7292	7283	7282	7292	7280	7243	7175	7126	6859	6467	6649
M	6484	6395	6826	7115	7215	7284	7283	7283	7271	7271	7283	7283	7284	7214	7114	6824	6394	6482
N	6452	6304	6784	7089	7257	7264	7262	7275	7259	7259	7275	7261	7263	7256	7088	6783	6302	6450
O	6277	6771	6857	7164	7129	7214	7235	7264	7228	7228	7264	7235	7213	7128	7163	6855	6769	6275
P		6977	7083	6897	7104	7081	7141	7127	7014	7014	7127	7141	7080	7103	6896	7082	6975	
Q			7096	6911	6725	7049	7156	6922	6743	6743	6922	7156	7048	6724	6909	7095		
R				6651	6598	7044	6807	6815	6646	6646	6815	6806	7043	6597	6650			
S					6027	6569	7007	7147	6994	6994	7147	7006	6568	6026				

MAXIMUM CHANNEL POWER= 7295.15 kW LOCATION IS CHANNEL J- 8
MAXIMUM BUNDLE POWER= 874.39 kW LOCATION IS CHANNEL C- 3 BUNDLE 5

Figure 8-11 Channel Power Distribution (kW) - Nominal Core
(Optimised 284-Channel Core - Time-Average Model, 2-BS Fuelling Scheme)

	1	2	3	4	5	6	7	8	9	10	11	12	13	14	15	16	17	18
A					6854	7151	7599	7777	7632	7631	7774	7596	7146	6849				
B				7473	6746	6989	6753	6791	6650	6649	6790	6749	6984	6740	7467			
C			7961	7059	6624	6861	6952	6757	6608	6608	6755	6949	6855	6619	7052	7953		
D		7851	7238	6790	6914	6846	6899	6896	6801	6800	6895	6895	6842	6907	6783	7229	7842	
E	7232	6998	6784	6981	6892	6957	6963	6995	6959	6959	6992	6960	6951	6886	6973	6777	6989	7223
F	7175	6390	6690	6884	7008	6987	6979	6989	6970	6968	6987	6975	6982	7001	6877	6682	6382	7165
G	7211	6490	6722	6916	6963	7008	6993	6992	6973	6973	6989	6989	7002	6957	6908	6714	6481	7201
H	7419	6564	6764	6926	6934	6969	6991	6996	6981	6979	6994	6986	6965	6927	6919	6755	6556	7408
J	7519	6613	6783	6937	6932	6969	6989	6998	6982	6982	6995	6986	6963	6926	6929	6776	6603	7509
K	7519	6612	6783	6936	6932	6968	6989	6997	6982	6981	6995	6984	6963	6924	6929	6774	6604	7508
L	7417	6563	6762	6925	6932	6968	6989	6995	6978	6978	6991	6985	6962	6925	6917	6754	6554	7407
M	7209	6487	6720	6913	6961	7004	6990	6988	6971	6969	6986	6986	6999	6953	6906	6711	6479	7198
N	7172	6387	6686	6881	7004	6984	6974	6985	6965	6965	6982	6971	6978	6998	6873	6679	6378	7162
O	7228	6993	6780	6976	6888	6951	6958	6989	6954	6953	6988	6954	6946	6881	6969	6772	6985	7218
P		7846	7232	6785	6907	6841	6892	6891	6795	6794	6888	6889	6835	6902	6777	7224	7836	
Q			7955	7052	6618	6853	6946	6750	6602	6601	6749	6942	6849	6612	7046	7946		
R				7466	6739	6982	6745	6785	6642	6642	6782	6743	6977	6734	7459			
S					6847	7143	7591	7768	7624	7622	7766	7587	7139	6842				

Figure 8-12 Channel Power Distribution (kW) – Full-Core Voided
(Optimised 284-Channel Core - Time-Average Model, 2-BS Fuelling Scheme)

	1	2	3	4	5	6	7	8	9	10	11	12	13	14	15	16	17	18
A					1.14	1.09	1.08	1.09	1.09	1.09	1.09	1.08	1.09	1.14				
B				1.12	1.02	0.99	0.99	1.00	1.00	1.00	1.00	0.99	0.99	1.02	1.12			
C			1.12	1.02	0.98	0.97	0.97	0.98	0.98	0.98	0.98	0.97	0.97	0.98	1.02	1.12		
D		1.12	1.02	0.98	0.97	0.97	0.97	0.97	0.97	0.97	0.97	0.97	0.97	0.97	0.98	1.02	1.12	
E	1.15	1.03	0.99	0.97	0.97	0.96	0.96	0.96	0.96	0.96	0.96	0.96	0.96	0.97	0.97	0.99	1.03	1.15
F	1.11	1.01	0.99	0.97	0.97	0.96	0.96	0.96	0.96	0.96	0.96	0.96	0.96	0.96	0.97	0.98	1.01	1.11
G	1.11	1.01	0.98	0.97	0.96	0.96	0.96	0.96	0.96	0.96	0.96	0.96	0.96	0.96	0.97	0.98	1.01	1.11
H	1.12	1.01	0.99	0.97	0.97	0.96	0.96	0.96	0.96	0.96	0.96	0.96	0.96	0.97	0.97	0.98	1.01	1.11
J	1.12	1.02	0.99	0.97	0.97	0.96	0.96	0.96	0.96	0.96	0.96	0.96	0.96	0.97	0.97	0.98	1.01	1.11
K	1.12	1.02	0.99	0.97	0.97	0.96	0.96	0.96	0.96	0.96	0.96	0.96	0.96	0.97	0.97	0.98	1.01	1.11
L	1.12	1.01	0.99	0.97	0.97	0.96	0.96	0.96	0.96	0.96	0.96	0.96	0.96	0.97	0.97	0.98	1.01	1.11
M	1.11	1.01	0.98	0.97	0.96	0.96	0.96	0.96	0.96	0.96	0.96	0.96	0.96	0.96	0.97	0.98	1.01	1.11
N	1.11	1.01	0.99	0.97	0.97	0.96	0.96	0.96	0.96	0.96	0.96	0.96	0.96	0.96	0.97	0.98	1.01	1.11
O	1.15	1.03	0.99	0.97	0.97	0.96	0.96	0.96	0.96	0.96	0.96	0.96	0.96	0.97	0.97	0.99	1.03	1.15
P		1.12	1.02	0.98	0.97	0.97	0.97	0.97	0.97	0.97	0.97	0.96	0.97	0.97	0.98	1.02	1.12	
Q			1.12	1.02	0.98	0.97	0.97	0.98	0.98	0.98	0.97	0.97	0.97	0.98	1.02	1.12		
R				1.12	1.02	0.99	0.99	1.00	1.00	1.00	1.00	0.99	0.99	1.02	1.12			
S					1.14	1.09	1.08	1.09	1.09	1.09	1.09	1.08	1.09	1.14				

Figure 8-13 Channel Power Ratios from Normal-Coolant to Voided-Coolant Conditions (Optimised 284-Channel Core – Time-Average Model, 2-BS Fuelling Scheme)

	1	2	3	4	5	6	7	8	9	10	11	12	13	14	15	16	17	18
A					471.3	388.7	497.2	409.7	503.3	403.3	488.2	377.0	428.6	314.5				
B				536.5	418.4	517.2	373.4	515.7	368.8	504.3	360.3	486.1	376.1	427.9	333.0			
C			565.1	448.0	552.3	400.0	548.2	373.8	533.5	364.8	524.8	372.7	497.2	336.5	434.1	336.4		
D		546.6	447.0	567.3	417.1	570.5	389.9	560.3	381.9	547.3	374.6	533.2	355.4	496.5	334.7	430.4	328.7	
E	479.6	421.8	552.7	416.5	581.3	399.8	575.2	395.2	565.9	387.1	556.1	374.4	533.0	354.2	490.6	326.8	411.0	301.2
F	388.6	508.9	381.3	569.8	405.4	581.2	395.4	577.5	390.7	568.2	384.5	555.5	373.7	531.3	352.4	474.5	298.6	400.7
G	485.0	351.6	539.5	392.9	576.2	398.4	579.7	393.9	575.8	389.2	569.7	383.5	554.0	371.6	521.7	341.3	453.1	325.5
H	367.8	499.7	371.3	556.8	388.4	575.3	393.9	579.6	392.6	575.5	389.8	567.8	381.4	550.5	370.7	505.9	327.0	455.7
J	482.2	343.3	526.0	383.0	564.2	388.9	575.3	393.3	577.8	392.4	576.6	389.6	565.8	379.5	542.2	359.7	484.1	356.8
K	357.0	484.3	359.8	542.3	379.6	565.9	389.6	576.7	392.4	577.8	393.3	575.2	388.8	564.0	382.9	525.9	343.2	482.0
L	455.8	327.0	506.0	370.7	550.6	381.4	567.8	389.8	575.4	392.6	579.5	393.9	575.1	388.3	556.6	371.2	499.5	367.6
M	325.6	453.2	341.4	521.7	371.6	554.0	383.5	569.7	389.2	575.7	393.8	579.5	398.3	576.0	392.7	539.2	351.4	484.8
N	400.8	298.7	474.6	352.4	531.3	373.7	555.5	384.5	568.1	390.6	577.3	395.3	581.0	405.2	569.5	381.1	508.7	388.3
O	301.2	411.1	326.9	490.7	354.2	533.0	374.4	556.1	387.1	565.7	395.1	575.0	399.6	581.0	416.3	552.4	421.6	479.3
P		328.7	430.5	334.7	496.5	355.4	533.1	374.6	547.1	381.8	560.1	389.7	570.2	416.9	566.9	446.7	546.2	
Q			336.4	434.1	336.5	497.2	372.6	524.7	364.7	533.3	373.7	547.9	399.7	552.0	447.7	564.7		
R				333.0	427.9	376.1	486.0	360.2	504.1	368.7	515.5	373.2	516.9	418.1	536.1			
S					314.4	428.5	376.9	488.1	403.2	503.1	409.5	497.0	388.5	471.0				

Figure 8-15 Bundle Power Distribution (kW) at Bundle Position 2
(Optimised 284-Channel Core – Time-Average Model, 2-BS Fuelling Scheme)

	1	2	3	4	5	6	7	8	9	10	11	12	13	14	15	16	17	18
A					584.4	533.0	670.7	562.5	635.9	526.8	652.4	530.5	580.7	416.3				
B				671.2	545.0	686.9	523.8	680.2	490.0	638.5	501.0	656.1	525.4	556.5	446.5			
C			751.1	591.5	697.3	555.3	732.1	520.6	676.7	490.3	694.6	527.7	669.6	458.9	573.5	482.1		
D		744.3	624.8	737.6	570.6	754.4	550.5	742.6	525.4	712.4	527.6	718.3	505.3	661.8	470.8	603.3	482.5	
E	661.4	599.1	745.8	587.2	770.2	565.5	769.1	559.0	753.4	546.3	746.5	534.7	722.2	506.1	674.5	477.0	584.3	444.9
F	558.0	690.7	547.2	766.6	575.3	778.8	562.6	773.0	555.1	762.1	548.1	750.2	535.9	723.6	509.9	658.6	438.8	571.2
G	671.7	507.8	733.4	562.5	773.7	567.9	777.9	560.7	772.3	554.7	766.0	548.6	750.7	533.8	715.2	497.3	629.5	478.3
H	534.3	683.9	536.1	755.0	554.7	773.4	561.8	777.3	559.5	772.8	556.0	765.2	546.4	745.1	534.9	696.7	476.9	640.2
J	672.7	498.4	719.8	550.7	760.1	555.7	773.5	560.5	775.6	559.4	774.3	556.4	763.1	543.6	738.9	521.5	667.1	521.0
K	521.2	667.2	521.6	739.1	543.7	763.2	556.5	774.3	559.4	775.5	560.4	773.4	555.6	759.9	550.5	719.5	498.2	672.4
L	640.4	477.1	696.8	535.0	745.2	546.4	765.3	556.0	772.8	559.4	777.2	561.7	773.2	554.5	754.7	535.8	683.6	534.0
M	478.4	629.7	497.3	715.2	533.8	750.7	548.6	765.9	554.7	772.2	560.6	777.7	567.7	773.4	562.3	733.1	507.5	671.3
N	571.3	438.9	658.6	509.9	723.6	535.9	750.2	548.0	762.0	555.0	772.8	562.4	778.5	575.0	766.1	546.9	690.3	557.7
O	445.0	584.4	477.0	674.5	506.1	722.2	534.6	746.4	546.1	753.2	558.8	768.7	565.2	769.6	586.7	745.3	598.7	661.0
P		482.5	603.3	470.8	661.7	505.3	718.2	527.6	712.2	525.3	742.4	550.2	753.9	570.0	736.8	624.3	743.8	
Q			482.1	573.5	458.9	669.5	527.6	694.5	490.1	676.5	520.3	731.7	555.0	696.8	591.0	750.5		
R				446.5	556.4	525.3	656.0	500.9	638.3	489.8	679.9	523.5	686.5	544.6	670.7			
S					416.2	580.6	530.4	652.3	526.6	635.7	562.2	670.3	532.7	584.0				

Figure 8-16 Bundle Power Distribution (kW) at Bundle Position 3
(Optimised 284-Channel Core - Time-Average Model, 2-BS Fuelling Scheme)

	1	2	3	4	5	6	7	8	9	10	11	12	13	14	15	16	17	18
A					676.9	645.4	778.8	684.6	748.5	649.0	766.9	650.8	689.8	524.6				
B				767.3	655.8	789.7	635.4	773.8	600.3	733.7	612.8	755.1	643.6	667.5	564.6			
C			846.5	704.1	783.0	667.5	822.9	628.4	761.7	596.7	783.2	640.8	770.7	571.1	689.0	603.8		
D		836.3	736.4	820.0	681.5	834.0	657.7	823.5	630.8	795.0	634.6	806.4	614.6	763.7	583.4	717.7	600.1	
E	745.6	704.5	825.2	696.7	846.3	671.5	845.3	663.8	831.4	650.7	827.8	640.6	810.0	614.7	775.1	586.4	691.5	550.0
F	660.3	761.9	650.2	842.5	681.1	852.6	665.1	845.6	656.8	836.3	650.6	828.8	641.1	811.7	617.1	749.7	538.4	672.3
G	756.7	606.0	808.4	666.5	846.9	670.3	848.8	661.0	842.5	654.7	838.4	650.4	829.6	638.1	800.9	600.5	714.7	583.2
H	639.9	759.4	637.7	831.2	656.2	844.1	661.7	846.1	658.3	842.0	655.5	837.6	647.6	822.0	638.8	779.4	576.3	735.1
J	764.4	597.5	797.8	653.6	832.8	655.9	843.3	659.3	843.6	657.8	843.2	656.0	835.4	644.9	818.2	623.4	747.0	628.3
K	628.5	747.2	623.6	818.4	645.0	835.5	656.1	843.3	657.8	843.6	659.2	843.2	655.8	832.6	653.4	797.5	597.3	764.1
L	735.3	576.4	779.6	638.9	822.1	647.6	837.6	655.5	841.9	658.3	846.0	661.6	843.9	656.0	830.9	637.4	759.1	639.6
M	583.3	714.8	600.6	801.0	638.2	829.6	650.4	838.4	654.7	842.3	660.8	848.5	670.1	846.6	666.2	808.0	605.7	756.4
N	672.4	538.5	749.8	617.2	811.8	641.1	828.8	650.6	836.2	656.6	845.4	664.9	852.3	680.8	842.1	649.9	761.5	659.9
O	550.1	691.6	586.5	775.1	614.7	810.0	640.5	827.7	650.6	831.2	663.6	845.0	671.2	845.7	696.1	824.7	704.1	745.2
P		600.1	717.7	583.4	763.6	614.5	806.3	634.5	794.8	630.7	823.2	657.4	833.5	680.9	819.3	735.8	835.7	
Q			603.8	689.0	571.1	770.6	640.7	783.1	596.5	761.5	628.2	822.6	667.2	782.5	703.6	845.9		
R				564.6	667.4	643.5	755.0	612.7	733.5	600.1	773.5	635.1	789.2	655.4	766.7			
S					524.6	689.7	650.6	766.7	648.8	748.2	684.3	778.4	645.0	676.5				

Figure 8-17 Bundle Power Distribution (kW) at Bundle Position 4
(Optimised 284-Channel Core – Time-Average Model, 2-BS Fuelling Scheme)

	1	2	3	4	5	6	7	8	9	10	11	12	13	14	15	16	17	18
A					762.0	733.4	832.4	784.1	851.8	779.4	840.5	743.8	761.2	646.5				
B				842.5	763.8	841.2	718.4	815.3	712.1	806.4	706.0	797.3	739.2	768.7	694.3			
C			874.4	801.6	835.2	750.8	846.2	712.4	813.6	699.6	814.8	725.0	817.7	684.5	789.1	708.3		
D		848.8	798.1	845.2	768.2	842.9	729.7	836.6	716.9	826.2	713.2	825.5	698.1	822.0	683.9	783.5	690.3	
E	756.4	755.8	823.8	763.7	848.4	738.4	843.2	731.1	837.4	721.3	836.2	711.6	826.8	696.6	813.5	667.1	745.5	626.0
F	711.7	755.9	708.6	836.6	745.0	845.2	726.4	839.0	718.9	832.6	715.1	830.0	709.9	828.3	691.0	771.7	610.3	718.4
G	767.5	663.4	801.3	726.1	839.6	729.7	837.6	719.9	831.8	713.8	831.6	712.2	830.3	706.0	811.4	667.8	733.0	653.4
H	700.9	759.3	695.9	825.7	716.7	832.9	719.0	833.8	714.9	829.9	714.0	829.5	708.7	821.8	703.0	786.0	641.1	762.7
J	783.4	658.3	795.9	713.8	826.1	714.2	831.3	716.1	830.0	713.8	831.4	713.7	827.2	706.9	818.2	684.7	754.3	694.4
K	694.6	754.5	684.9	818.3	707.0	827.2	713.8	831.5	713.8	829.9	716.1	831.2	714.1	825.9	713.6	795.7	658.1	783.2
L	762.9	641.2	786.1	703.2	821.8	708.8	829.5	714.0	829.9	714.8	833.7	718.9	832.8	716.5	825.5	695.7	759.1	700.7
M	653.5	733.2	667.9	811.5	706.1	830.3	712.2	831.6	713.7	831.7	719.7	837.5	729.5	839.3	725.9	801.1	663.1	767.2
N	718.6	610.4	771.8	691.0	828.3	709.9	830.0	715.1	832.5	718.8	838.8	726.2	845.0	744.7	836.3	708.2	755.5	711.3
O	626.0	745.6	667.2	813.6	696.6	826.8	711.5	836.1	721.2	837.3	731.0	843.0	738.1	848.1	763.4	823.4	755.4	756.0
P		690.3	783.5	683.9	822.0	698.0	825.4	713.1	826.0	716.7	836.4	729.4	842.6	767.8	844.8	797.7	848.4	
Q			708.3	789.1	684.5	817.6	724.9	814.7	699.4	813.4	712.1	845.9	750.5	834.8	801.1	873.9		
R				694.3	768.6	739.1	797.2	705.9	806.2	711.9	815.0	718.1	840.9	763.4	842.1			
S					646.4	761.0	743.6	840.3	779.2	851.5	783.8	832.0	733.0	761.6				

Figure 8-18 Bundle Power Distribution (kW) at Bundle Position 5
(Optimised 284-Channel Core – Time-Average Model, 2-BS Fuelling Scheme)

	1	2	3	4	5	6	7	8	9	10	11	12	13	14	15	16	17	18
A					678.1	736.4	804.4	790.2	778.6	753.2	810.0	772.5	746.0	637.3				
B				749.2	727.3	801.3	744.4	768.5	703.2	736.1	729.7	772.3	764.7	728.6	696.7			
C			814.5	766.2	750.9	768.4	806.9	736.3	741.4	701.6	772.4	763.6	792.0	697.9	761.4	755.3		
D		805.4	799.9	775.0	769.9	792.6	763.0	791.0	732.7	771.0	747.5	796.9	741.2	788.7	718.1	794.7	749.1	
E	725.9	766.7	778.4	783.7	795.1	771.1	803.3	765.3	796.0	755.0	802.3	756.7	802.4	741.5	801.4	722.7	763.2	679.6
F	729.8	715.8	740.1	793.3	776.2	805.3	765.1	800.1	756.6	796.6	756.4	801.7	757.5	805.6	741.7	762.6	664.2	732.3
G	742.8	696.9	766.2	761.6	798.8	768.4	801.3	758.4	795.2	753.6	797.7	757.0	804.0	751.7	791.8	718.8	721.7	702.2
H	735.2	729.6	735.1	792.0	754.6	797.4	759.6	796.7	754.0	794.4	754.6	798.6	753.6	791.6	748.6	767.1	687.6	757.2
J	768.2	698.8	769.0	754.4	790.4	755.8	797.5	755.4	794.0	753.1	795.9	756.1	795.6	748.4	791.2	729.5	732.8	736.4
K	736.6	733.0	729.7	791.4	748.5	795.7	756.1	795.9	753.1	793.9	755.4	797.5	755.7	790.3	754.2	768.9	698.6	768.0
L	757.4	687.8	767.2	748.7	791.7	753.6	798.6	754.6	794.4	754.0	796.6	759.5	797.2	754.4	791.9	734.9	729.4	734.9
M	702.3	721.8	718.9	791.9	751.8	804.0	757.0	797.6	753.6	795.1	758.3	801.2	768.2	798.6	761.3	765.9	696.6	742.5
N	732.4	664.3	762.7	741.8	805.7	757.5	801.6	756.4	796.5	756.5	799.9	764.9	805.1	775.9	793.0	739.8	715.5	729.5
O	679.7	763.2	722.8	801.5	741.5	802.4	756.7	802.3	754.9	795.8	765.1	803.1	770.9	794.9	783.4	778.1	766.3	725.6
P		749.1	794.7	718.1	788.7	741.1	796.8	747.3	770.9	732.6	790.8	762.7	792.3	769.5	774.8	799.6	805.1	
Q			755.3	761.3	697.8	792.0	763.5	772.2	701.4	741.2	736.0	806.6	768.1	750.6	765.8	814.1		
R				696.6	728.5	764.5	772.2	729.5	735.9	703.0	768.3	744.1	801.0	726.9	748.8			
S					637.2	745.8	772.3	809.8	753.0	778.4	789.9	804.1	736.1	677.8				

Figure 8-19 Bundle Power Distribution (kW) at Bundle Position 6
(Optimised 284-Channel Core – Time-Average Model, 2-BS Fuelling Scheme)

	1	2	3	4	5	6	7	8	9	10	11	12	13	14	15	16	17	18
A					637.4	746.1	772.5	810.1	753.2	778.6	790.1	804.3	736.2	678.0				
B				696.8	728.7	764.7	772.4	729.7	736.1	703.1	768.5	744.2	801.1	727.1	749.0			
C			755.4	761.5	698.0	792.1	763.6	772.4	701.6	741.4	736.2	806.8	768.3	750.7	766.0	814.3		
D		749.3	794.9	718.2	788.8	741.3	797.0	747.5	771.0	732.7	791.0	762.9	792.5	769.7	774.9	799.7	805.2	
E	679.8	763.4	722.9	801.6	741.6	802.5	756.8	802.4	755.0	796.0	765.2	803.2	771.0	795.0	783.5	778.2	766.4	725.7
F	732.5	664.4	762.8	741.9	805.8	757.6	801.7	756.5	796.6	756.5	800.0	764.9	805.2	776.0	793.1	739.9	715.6	729.5
G	702.4	721.9	719.0	792.0	751.8	804.1	757.1	797.7	753.6	795.2	758.3	801.2	768.3	798.7	761.4	766.0	696.6	742.6
H	757.4	687.8	767.3	748.8	791.7	753.6	798.6	754.6	794.5	754.0	796.7	759.6	797.3	754.4	791.9	735.0	729.4	735.0
J	736.6	733.0	729.7	791.4	748.5	795.7	756.1	796.0	753.1	793.9	755.4	797.5	755.7	790.3	754.2	768.9	698.6	768.0
K	768.2	698.8	769.0	754.3	790.4	755.8	797.5	755.4	793.9	753.1	795.9	756.0	795.6	748.4	791.2	729.5	732.8	736.4
L	735.1	729.6	735.1	792.0	754.5	797.3	759.6	796.7	753.9	794.4	754.6	798.5	753.5	791.5	748.6	767.1	687.6	757.1
M	742.7	696.8	766.1	761.4	798.7	768.3	801.2	758.3	795.1	753.5	797.6	757.0	803.9	751.7	791.7	718.8	721.6	702.1
N	729.6	715.7	739.9	793.2	776.0	805.2	764.9	800.0	756.5	796.5	756.3	801.6	757.4	805.5	741.7	762.6	664.1	732.2
O	725.8	766.5	778.2	783.5	795.0	770.9	803.2	765.2	795.8	754.9	802.2	756.6	802.3	741.4	801.3	722.6	763.1	679.5
P		805.3	799.7	774.9	769.6	792.4	762.8	790.9	732.6	770.9	747.3	796.7	741.0	788.5	717.9	794.6	748.9	
Q			814.3	766.0	750.7	768.2	806.7	736.1	741.2	701.4	772.2	763.4	791.9	697.7	761.2	755.1		
R				749.0	727.0	801.0	744.1	768.3	703.0	735.9	729.5	772.1	764.5	728.4	696.5			
S					677.9	736.1	804.1	789.9	778.4	753.0	809.8	772.3	745.8	637.1				

Figure 8-20 Bundle Power Distribution (kW) at Bundle Position 7
(Optimised 284-Channel Core – Time-Average Model, 2-BS Fuelling Scheme)

	1	2	3	4	5	6	7	8	9	10	11	12	13	14	15	16	17	18
A					646.6	761.2	743.8	840.5	779.4	851.7	784.0	832.2	733.2	761.8				
B				694.4	768.8	739.2	797.4	706.0	806.4	712.0	815.2	718.3	841.0	763.5	842.2			
C			708.4	789.2	684.6	817.8	725.0	814.8	699.6	813.6	712.2	846.1	750.6	835.0	801.3	874.1		
D		690.4	783.6	684.0	822.1	698.1	825.6	713.2	826.2	716.8	836.5	729.5	842.7	767.9	844.9	797.8	848.5	
E	626.1	745.7	667.2	813.7	696.7	826.9	711.6	836.2	721.3	837.4	731.0	843.1	738.2	848.2	763.4	823.5	755.5	756.1
F	718.6	610.4	771.9	691.1	828.4	710.0	830.0	715.1	832.6	718.9	838.9	726.2	845.1	744.8	836.3	708.3	755.6	711.4
G	653.6	733.2	667.9	811.6	706.1	830.4	712.3	831.6	713.7	831.8	719.8	837.5	729.5	839.4	725.9	801.1	663.1	767.3
H	762.9	641.2	786.1	703.1	821.9	708.8	829.5	714.0	829.9	714.8	833.7	718.9	832.8	716.5	825.5	695.7	759.1	700.7
J	694.6	754.5	684.8	818.3	706.9	827.2	713.7	831.5	713.7	829.9	716.0	831.2	714.1	825.9	713.6	795.7	658.1	783.2
K	783.4	658.2	795.8	713.7	826.0	714.1	831.3	716.1	829.9	713.7	831.4	713.7	827.1	706.8	818.2	684.7	754.3	694.4
L	700.8	759.2	695.8	825.6	716.6	832.8	718.9	833.7	714.8	829.8	713.9	829.4	708.7	821.7	703.0	785.9	641.0	762.7
M	767.4	663.2	801.2	726.0	839.4	729.6	837.5	719.7	831.7	713.7	831.5	712.1	830.2	705.9	811.4	667.7	733.0	653.3
N	711.5	755.7	708.4	836.4	744.8	845.1	726.2	838.9	718.8	832.5	715.0	829.9	709.8	828.2	690.9	771.6	610.2	718.4
O	756.2	755.6	823.6	763.5	848.2	738.1	843.1	731.0	837.3	721.2	836.0	711.4	826.6	696.5	813.4	667.0	745.4	625.9
P		848.6	797.8	844.9	767.9	842.7	729.4	836.4	716.7	826.0	713.0	825.4	697.9	821.9	683.8	783.3	690.1	
Q			874.1	801.2	834.9	750.5	846.0	712.1	813.4	699.4	814.6	724.8	817.5	684.3	788.9	708.1		
R				842.2	763.4	840.9	718.1	815.0	711.9	806.2	705.8	797.1	739.0	768.5	694.1			
S					761.7	733.1	832.1	783.8	851.5	779.2	840.2	743.5	760.9	646.3				

Figure 8-21 Bundle Power Distribution (kW) at Bundle Position 8
(Optimised 284-Channel Core – Time-Average Model, 2-BS Fuelling Scheme)

	1	2	3	4	5	6	7	8	9	10	11	12	13	14	15	16	17	18
A					524.7	689.8	650.8	766.9	648.9	748.4	684.4	778.5	645.1	676.6				
B				564.7	667.5	643.6	755.1	612.8	733.6	600.2	773.7	635.2	789.4	655.5	766.9			
C			603.9	689.1	571.2	770.8	640.8	783.2	596.6	761.6	628.2	822.7	667.3	782.6	703.7	846.0		
D		600.1	717.8	583.4	763.7	614.6	806.4	634.6	795.0	630.7	823.3	657.5	833.6	680.9	819.4	735.9	835.8	
E	550.1	691.7	586.5	775.2	614.7	810.0	640.6	827.8	650.6	831.3	663.6	845.1	671.3	845.8	696.2	824.8	704.1	745.2
F	672.4	538.5	749.8	617.2	811.8	641.1	828.8	650.6	836.2	656.7	845.4	665.0	852.4	680.8	842.1	649.9	761.6	659.9
G	583.3	714.8	600.6	801.0	638.2	829.7	650.4	838.4	654.7	842.4	660.9	848.6	670.1	846.7	666.2	808.1	605.8	756.4
H	735.3	576.4	779.5	638.9	822.1	647.6	837.6	655.5	841.9	658.3	846.0	661.6	843.9	656.0	830.9	637.4	759.1	639.6
J	628.4	747.1	623.5	818.3	644.9	835.4	656.0	843.2	657.8	843.6	659.2	843.1	655.7	832.5	653.4	797.5	597.3	764.1
K	764.3	597.4	797.7	653.5	832.7	655.8	843.2	659.2	843.6	657.8	843.2	656.0	835.3	644.8	818.2	623.4	746.9	628.3
L	639.7	759.3	637.5	831.0	656.0	844.0	661.6	846.0	658.2	841.9	655.5	837.5	647.5	821.9	638.7	779.3	576.2	735.0
M	756.5	605.8	808.2	666.3	846.7	670.1	848.6	660.8	842.3	654.6	838.3	650.3	829.5	638.0	800.8	600.4	714.6	583.1
N	660.0	761.7	650.0	842.2	680.8	852.4	664.9	845.4	656.6	836.1	650.5	828.7	641.0	811.6	617.0	749.6	538.3	672.2
O	745.3	704.2	824.8	696.2	845.8	671.2	845.0	663.6	831.2	650.5	827.6	640.5	809.8	614.6	774.9	586.3	691.4	549.9
P		835.8	735.9	819.4	680.9	833.6	657.5	823.2	630.6	794.8	634.5	806.2	614.4	763.5	583.2	717.5	599.9	
Q			846.0	703.6	782.6	667.2	822.6	628.2	761.5	596.5	783.0	640.7	770.5	571.0	688.9	603.7		
R				766.8	655.5	789.3	635.1	773.5	600.1	733.4	612.6	754.9	643.4	667.3	564.5			
S					676.6	645.0	778.4	684.3	748.2	648.7	766.6	650.6	689.6	524.5				

Figure 8-22 Bundle Power Distribution (kW) at Bundle Position 9
(Optimised 284-Channel Core – Time-Average Model, 2-BS Fuelling Scheme)

	1	2	3	4	5	6	7	8	9	10	11	12	13	14	15	16	17	18
A					416.3	580.7	530.5	652.4	526.7	635.8	562.3	670.4	532.8	584.1				
B				446.6	556.5	525.4	656.1	501.0	638.4	489.9	680.0	523.6	686.6	544.7	670.8			
C			482.1	573.5	459.0	669.6	527.7	694.6	490.2	676.6	520.4	731.8	555.1	696.9	591.1	750.6		
D		482.6	603.4	470.9	661.8	505.3	718.3	527.6	712.3	525.3	742.4	550.3	754.0	570.1	736.9	624.3	743.8	
E	445.0	584.4	477.0	674.5	506.1	722.2	534.6	746.5	546.2	753.3	558.8	768.8	565.3	769.6	586.8	745.3	598.7	661.1
F	571.3	438.8	658.6	509.9	723.6	535.9	750.2	548.0	762.0	555.0	772.8	562.4	778.5	575.0	766.2	546.9	690.3	557.7
G	478.3	629.6	497.3	715.2	533.8	750.7	548.6	765.9	554.7	772.2	560.6	777.7	567.7	773.4	562.3	733.1	507.5	671.3
H	640.3	477.0	696.8	534.9	745.2	546.4	765.2	556.0	772.7	559.4	777.2	561.7	773.2	554.5	754.7	535.8	683.6	534.0
J	521.1	667.2	521.5	739.0	543.6	763.1	556.4	774.2	559.4	775.5	560.4	773.4	555.6	759.9	550.5	719.5	498.2	672.4
K	672.6	498.3	719.6	550.6	760.0	555.6	773.4	560.4	775.5	559.4	774.2	556.4	763.0	543.5	738.9	521.4	667.0	521.0
L	534.1	683.7	535.9	754.8	554.5	773.2	561.7	777.2	559.4	772.7	556.0	765.1	546.3	745.0	534.8	696.6	476.9	640.1
M	671.4	507.6	733.2	562.3	773.5	567.7	777.7	560.6	772.1	554.6	765.8	548.5	750.6	533.7	715.1	497.2	629.5	478.2
N	557.8	690.4	547.0	766.2	575.0	778.5	562.4	772.8	554.9	761.9	547.9	750.1	535.8	723.4	509.8	658.4	438.7	571.0
O	661.1	598.7	745.3	586.8	769.6	565.2	768.7	558.8	753.2	546.1	746.3	534.5	722.1	506.0	674.3	476.9	584.2	444.8
P		743.9	624.4	736.9	570.1	753.9	550.2	742.4	525.3	712.1	527.5	718.1	505.2	661.6	470.7	603.1	482.4	
Q			750.6	591.1	696.8	555.0	731.7	520.3	676.5	490.1	694.4	527.5	669.4	458.8	573.3	481.9		
R				670.8	544.7	686.5	523.5	679.9	489.8	638.2	500.9	655.9	525.2	556.3	446.4			
S					584.1	532.7	670.3	562.2	635.6	526.6	652.2	530.3	580.5	416.1				

Figure 8-23 Bundle Power Distribution (kW) at Bundle Position 10
(Optimised 284-Channel Core - Time-Average Model, 2-BS Fuelling Scheme)

	1	2	3	4	5	6	7	8	9	10	11	12	13	14	15	16	17	18
A					314.4	428.6	377.0	488.2	403.3	503.2	409.5	497.0	388.5	471.0				
B				333.0	427.9	376.1	486.1	360.3	504.2	368.7	515.5	373.2	517.0	418.2	536.2			
C			336.5	434.1	336.5	497.2	372.7	524.8	364.7	533.4	373.7	548.0	399.8	552.1	447.7	564.8		
D		328.8	430.5	334.7	496.5	355.4	533.2	374.6	547.2	381.8	560.2	389.8	570.3	416.9	567.0	446.7	546.2	
E	301.2	411.1	326.9	490.7	354.2	533.0	374.4	556.1	387.1	565.8	395.1	575.0	399.6	581.0	416.3	552.4	421.6	479.3
F	400.7	298.6	474.6	352.4	531.3	373.7	555.5	384.5	568.1	390.6	577.3	395.3	581.0	405.2	569.5	381.1	508.7	388.3
G	325.6	453.1	341.4	521.7	371.6	554.0	383.5	569.7	389.2	575.6	393.8	579.5	398.3	576.0	392.7	539.2	351.4	484.8
H	455.8	327.0	506.0	370.7	550.6	381.4	567.7	389.8	575.4	392.5	579.5	393.8	575.1	388.3	556.6	371.1	499.5	367.6
J	356.9	484.2	359.7	542.2	379.6	565.8	389.6	576.6	392.4	577.7	393.2	575.2	388.8	564.0	382.9	525.8	343.2	481.9
K	482.1	343.2	525.9	382.9	564.0	388.8	575.2	393.2	577.7	392.4	576.6	389.5	565.8	379.5	542.1	359.7	484.1	356.8
L	367.7	499.5	371.2	556.6	388.3	575.1	393.8	579.5	392.5	575.4	389.8	567.7	381.3	550.5	370.6	505.8	326.9	455.6
M	484.9	351.4	539.3	392.7	576.0	398.3	579.5	393.8	575.6	389.1	569.6	383.4	553.9	371.5	521.6	341.3	453.0	325.5
N	388.4	508.7	381.2	569.6	405.2	581.0	395.3	577.3	390.5	568.1	384.4	555.4	373.6	531.2	352.3	474.4	298.6	400.6
O	479.4	421.6	552.4	416.3	581.0	399.6	575.0	395.1	565.7	387.0	556.0	374.3	532.9	354.1	490.5	326.8	410.9	301.1
P		546.3	446.7	567.0	416.9	570.2	389.7	560.1	381.7	547.1	374.5	533.0	355.3	496.3	334.6	430.3	328.6	
Q			564.7	447.7	552.0	399.7	547.9	373.6	533.3	364.6	524.7	372.6	497.1	336.4	433.9	336.3		
R				536.2	418.2	516.9	373.2	515.4	368.7	504.1	360.2	486.0	376.0	427.8	332.9			
S					471.0	388.5	497.0	409.4	503.1	403.2	488.0	376.8	428.4	314.3				

Figure 8-24 Bundle Power Distribution (kW) at Bundle Position 11
(Optimised 284-Channel Core - Time-Average Model, 2-BS Fuelling Scheme)

	1	2	3	4	5	6	7	8	9	10	11	12	13	14	15	16	17	18
A					124.3	172.8	149.5	197.3	161.3	205.0	163.1	201.5	155.2	192.3				
B				131.5	172.6	149.8	197.5	143.3	206.7	147.6	210.4	148.7	211.0	168.0	219.4			
C			131.5	174.4	133.1	201.7	148.0	214.0	145.7	219.1	148.7	223.8	159.6	226.4	179.6	229.2		
D		127.1	171.4	131.8	200.3	140.6	216.8	148.5	223.9	152.1	228.6	155.0	233.4	165.9	231.8	177.7	219.3	
E	115.8	162.3	127.8	197.1	139.3	215.9	148.1	225.8	153.6	230.9	156.6	234.6	158.6	236.8	165.1	224.1	166.1	190.8
F	157.2	115.9	190.0	138.3	214.0	147.4	225.4	151.8	231.3	154.7	234.7	156.5	236.6	160.1	231.3	150.2	204.9	151.5
G	125.6	180.4	133.5	210.0	146.0	224.3	151.4	231.0	153.9	234.3	155.5	235.7	157.4	233.5	154.8	217.9	137.4	192.4
H	179.6	127.2	203.2	145.6	222.2	150.4	230.4	153.7	233.9	155.2	235.2	155.6	233.6	152.8	225.1	145.7	200.2	142.4
J	137.9	193.4	141.0	218.7	149.2	229.4	153.8	233.8	155.1	234.9	155.1	233.6	153.4	228.1	150.6	211.7	133.8	190.5
K	190.5	133.8	211.8	150.6	228.1	153.4	233.6	155.1	234.9	155.1	233.8	153.8	229.4	149.2	218.7	140.9	193.3	137.9
L	142.5	200.2	145.7	225.1	152.9	233.6	155.6	235.2	155.2	233.9	153.7	230.4	150.3	222.2	145.5	203.1	127.2	179.6
M	192.5	137.4	217.9	154.8	233.5	157.4	235.7	155.5	234.2	153.9	231.0	151.4	224.2	145.9	209.9	133.5	180.4	125.5
N	151.5	204.9	150.2	231.3	160.1	236.6	156.5	234.7	154.7	231.3	151.8	225.4	147.3	214.0	138.2	190.0	115.9	157.2
O	190.8	166.2	224.1	165.1	236.8	158.6	234.6	156.6	230.8	153.6	225.8	148.0	215.9	139.3	197.0	127.8	162.2	115.8
P		219.3	177.7	231.8	165.9	233.4	155.0	228.6	152.1	223.8	148.5	216.7	140.6	200.2	131.7	171.4	127.1	
Q			229.2	179.6	226.3	159.5	223.8	148.7	219.0	145.6	214.0	148.0	201.7	133.0	174.4	131.4		
R				219.4	167.9	210.9	148.7	210.4	147.6	206.6	143.3	197.5	149.7	172.6	131.4			
S					192.3	155.2	201.5	163.0	204.9	161.2	197.3	149.5	172.7	124.3				

Figure 8-25 Bundle Power Distribution (kW) at Bundle Position 12
(Optimised 284-Channel Core – Time-Average Model, 2-BS Fuelling Scheme)

	1	2	3	4	5	6	7	8	9	10	11	12	13	14	15	16	17	18
A					0.88	0.22	0.04	0.34	0.64	0.24	0.38	0.72	0.30	0.12				
B				0.28	0.70	0.40	0.74	0.92	0.50	0.66	0.96	0.54	0.20	0.86	0.64			
C			0.58	0.84	0.42	0.60	0.94	0.52	0.78	0.58	0.32	0.90	0.48	0.82	0.24	0.66		
D		0.96	0.32	0.18	0.76	0.10	0.36	0.06	0.28	0.84	0.18	0.08	0.62	0.16	0.38	0.96	0.32	
E	0.72	0.54	0.90	0.08	0.46	0.68	0.14	0.88	0.70	0.42	0.76	0.26	0.44	0.22	0.72	0.54	0.90	0.08
F	0.30	0.20	0.48	0.62	0.44	0.98	0.56	0.22	0.40	0.60	0.10	0.68	0.98	0.80	0.30	0.20	0.48	0.62
G	0.12	0.86	0.82	0.16	0.02	0.80	0.56	0.04	0.74	0.94	0.36	0.24	0.56	0.46	0.12	0.86	0.82	0.16
H	0.34	0.64	0.24	0.38	0.72	0.30	0.12	0.34	0.92	0.52	0.06	0.88	0.22	0.04	0.34	0.64	0.24	0.38
J	0.92	0.50	0.66	0.96	0.54	0.20	0.86	0.64	0.50	0.78	0.28	0.70	0.40	0.74	0.92	0.50	0.66	0.96
K	0.52	0.78	0.58	0.32	0.90	0.48	0.82	0.24	0.66	0.58	0.84	0.42	0.60	0.94	0.52	0.78	0.58	0.32
L	0.06	0.28	0.84	0.18	0.08	0.62	0.16	0.38	0.96	0.32	0.18	0.76	0.10	0.36	0.06	0.28	0.84	0.18
M	0.88	0.70	0.42	0.76	0.26	0.44	0.12	0.72	0.54	0.90	0.08	0.36	0.68	0.14	0.88	0.70	0.42	0.76
N	0.22	0.40	0.60	0.10	0.68	0.98	0.80	0.30	0.20	0.48	0.62	0.44	0.98	0.56	0.22	0.40	0.60	0.10
O	0.04	0.74	0.94	0.36	0.24	0.56	0.46	0.12	0.86	0.82	0.16	0.12	0.80	0.56	0.04	0.74	0.94	0.36
P		0.92	0.52	0.06	0.88	0.22	0.04	0.34	0.64	0.24	0.38	0.72	0.30	0.22	0.34	0.92	0.52	
Q			0.78	0.28	0.70	0.40	0.74	0.92	0.50	0.66	0.96	0.54	0.20	0.86	0.64	0.50		
R				0.84	0.42	0.60	0.94	0.52	0.78	0.58	0.32	0.90	0.48	0.82	0.24			
S					0.76	0.10	0.36	0.06	0.28	0.84	0.18	0.08	0.62	0.16				

Figure 8-26 Typical Channel-Age Map
(Optimised 284-Channel Core – Patterned-Age-Model, 2-BS Fuelling Scheme)

	1	2	3	4	5	6	7	8	9	10	11	12	13	14	15	16	17	18
A					5881	6632	7139	7125	6853	6980	7097	6880	6627	6146				
B				6691	6500	7035	6612	6505	6523	6457	6499	6729	7130	6480	6597			
C			7045	6797	6761	6981	6890	6840	6506	6618	6982	6947	7068	6584	6998	7031		
D		6769	7137	7101	7017	7372	7268	7415	7121	6800	7354	7465	7081	7343	6993	6919	7039	
E	6179	6724	6667	7449	7222	7162	7533	7096	7123	7289	7171	7473	7320	7371	7101	6854	6651	6441
F	6517	6449	6803	7092	7365	7027	7294	7530	7347	7214	7599	7218	7024	7138	7278	6976	6320	6434
G	6631	6182	6649	7379	7623	7176	7341	7667	7126	6998	7430	7523	7313	7329	7403	6639	6205	6623
H	6659	6327	6965	7215	7100	7458	7609	7437	6991	7238	7612	7104	7495	7543	7246	6737	6550	6649
J	6460	6406	6711	6837	7162	7479	7101	7204	7229	7065	7431	7174	7322	7020	6835	6786	6317	6455
K	6647	6268	6765	7217	6963	7300	7122	7458	7140	7192	7081	7344	7190	6888	7065	6630	6362	6713
L	6789	6531	6637	7356	7527	7268	7581	7404	6978	7390	7542	7180	7556	7309	7392	6932	6208	6715
M	6303	6245	6861	7018	7462	7412	7624	7206	7263	7054	7634	7452	7235	7498	6933	6684	6375	6323
N	6518	6326	6712	7383	7216	7036	7150	7491	7492	7313	7280	7369	7009	7269	7299	6827	6199	6536
O	6413	6636	6614	7276	7355	7240	7359	7580	7053	7062	7538	7537	7075	7150	7475	6718	6569	6271
P		6757	7020	7144	6946	7316	7497	7260	6914	7146	7206	7041	7247	7304	7011	6910	6903	
Q			6928	6943	6616	7091	7014	6627	6666	6581	6610	7115	7218	6569	6871	7072		
R				6474	6566	6971	6531	6734	6431	6530	6854	6590	7053	6506	6742			
S					5908	6672	7042	7288	7031	6846	7255	7176	6559	6151				

Figure 8-27 Instantaneous Channel-Power Distribution (kW)
(Optimised 284-Channel Core - Patterned-Age-Model, 2-BS Fuelling Scheme)

	1	2	3	4	5	6	7	8	9	10	11	12	13	14	15	16	17	18
A					0.975	1.009	1.019	0.997	0.980	0.998	0.993	0.982	1.009	1.020				
B				1.006	0.985	0.998	0.971	0.954	0.981	0.971	0.953	0.988	1.012	0.982	0.992			
C			0.992	0.983	1.005	0.990	0.963	0.988	0.965	0.981	1.008	0.971	1.003	0.979	1.013	0.991		
D		0.970	1.007	1.029	0.987	1.041	1.017	1.040	1.015	0.969	1.032	1.045	1.000	1.034	1.014	0.977	1.009	
E	0.984	0.993	0.972	1.040	1.013	0.993	1.041	0.977	0.985	1.008	0.987	1.033	1.015	1.034	0.991	1.000	0.982	1.026
F	1.010	1.023	1.003	1.000	1.015	0.967	1.004	1.035	1.012	0.994	1.044	0.994	0.967	0.984	1.027	1.028	1.003	0.997
G	1.023	0.967	0.974	1.037	1.056	0.985	1.008	1.053	0.980	0.962	1.020	1.033	1.004	1.016	1.041	0.973	0.970	1.022
H	1.001	0.978	1.015	1.012	0.989	1.029	1.045	1.020	0.960	0.994	1.044	0.976	1.035	1.051	1.017	0.982	1.013	1.000
J	0.959	0.984	0.975	0.958	0.998	1.033	0.975	0.987	0.992	0.970	1.019	0.986	1.011	0.979	0.958	0.987	0.971	0.958
K	0.987	0.963	0.983	1.012	0.971	1.008	0.978	1.022	0.980	0.987	0.971	1.009	0.993	0.960	0.990	0.964	0.978	0.997
L	1.021	1.010	0.967	1.032	1.049	1.003	1.041	1.015	0.958	1.015	1.034	0.986	1.043	1.019	1.037	1.011	0.960	1.010
M	0.972	0.976	1.005	0.986	1.034	1.018	1.047	0.989	0.999	0.970	1.048	1.023	0.993	1.039	0.975	0.979	0.997	0.975
N	1.010	1.004	0.989	1.041	0.994	0.969	0.985	1.030	1.032	1.008	1.001	1.015	0.965	1.002	1.030	1.007	0.984	1.013
O	1.022	0.980	0.965	1.016	1.032	1.004	1.017	1.043	0.976	0.977	1.038	1.042	0.981	1.003	1.044	0.980	0.970	0.999
P		0.968	0.991	1.036	0.978	1.033	1.050	1.019	0.986	1.019	1.011	0.986	1.024	1.028	1.017	0.976	0.990	
Q			0.976	1.005	0.984	1.006	0.980	0.957	0.989	0.976	0.955	0.994	1.024	0.977	0.994	0.997		
R				0.973	0.995	0.990	0.959	0.988	0.968	0.983	1.006	0.968	1.001	0.986	1.014			
S					0.980	1.016	1.005	1.020	1.005	0.979	1.015	1.024	0.999	1.021				

Figure 8-28 Channel-Power Ripple Map
(Optimised 284-Channel Core - Patterned-Age-Model, 2-BS Fuelling Scheme)

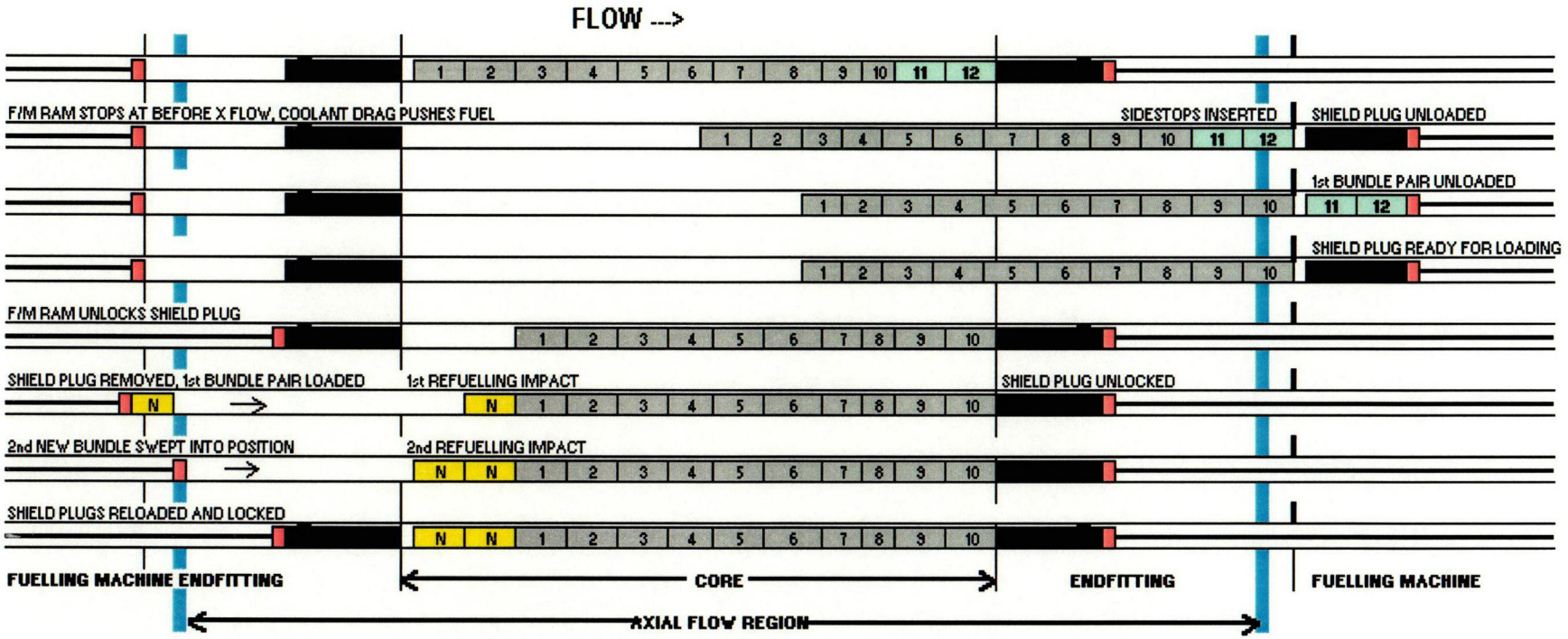

Figure 8-29 ACR Reference 2-Bundle-Shift Fuelling Scheme

C17

Appendix A
WIMS-IST Standard Model for ACR Lattice Calculations

```
*************************************************************************
*                Standard WIMS model for ACR calculations
*************************************************************************
* TITLE         : ACR NEGATIVE-VOID-REACTIVITY CANFLEX FUEL-BUNDLE DESIGN
* AUTHOR(S)     : M. OVANES/P. CHAN/D. ALTIPARMAKOV, 2002, June
* FILE          : ACRstd_seu20dy46_cv.dat
*                 Associated PROC16 case is: ACRstd_seu20dy46_e6.pin
* CODE VERSION : WIMS-IST (WIMS-AECL version 2-5d-3)
* LIBRARY       : ENDF/B-VI version 1a1
*
* PROJECT       : ACR CORE PHYSICS DESIGN
* DESCRIPTION   : CANFLEX fuel bundle using 2.0 SEU fuel, with the central element
replaced
*                 by an element containing 95.4% natural uranium and 4.6 wt% dysprosium
(in total U)
*
* REFERENCES: 1) D.V. Altiparmakov, "The Best WIMS-AECL Model for ACR Lattice
Calculations",
*                 108-131630-440-XXX, Jun 2002
*             2) A. Manzer and S. Pallek, "ACR-700 Fuel for Negative Void Reactivity",
*                 108-37000-DCD-002, Jun 2002
*             3) F. Ardeshiri, "Standard WIMS-AECL Models for 37-element and CANFLEX
Fuel Bundles",
*                 FFC-RCP-006, Jan 2002
*             4) J.V. Donnelly, "Application of WIMS-AECL to CANDU Latice-Cell
Analysis",
*                 FFC-RCP-003, Apr 1999
*
* CANFLEX BUNDLE DESIGN
*
* Lattice pitch (cm)              =    22.0
* Bundle length (cm)              =    49.53
* Fuel-stack length (cm)          =    48.11
* End-Region Thickness (cm)       =    1.42
* Estimated Bundle U Mass (kg)    =    17.98
* Estimated Bundle Zr Mass (kg)   =    2.3
* Inner & Centre Pins (13.5 mm OD)
*       Sheath Outer Radius (mm)  =    6.750
*       Sheath Thickness (mm)     =    0.44
*       UO2 Mass Per Pin (G)      =    638
* Outer & Intermediate Pins (11.5 mm OD)
*       Sheath Outer Radius (MM)  =    5.750
*       Sheath Thickness (mm)     =    0.39
*       UO2 Mass Per Pin (G)      =    439
* PT Inner Radius (cm)            =    5.1689
* Pressure Tube Thickness (mm)    =    6.5
* CT Outer Radius (cm)            =    7.8
* Calandria Tube Thickness (mm)   =    2.5
*
* NOMINAL PARAMETERS FOR CANFLEX CLUSTER
*
* UO2 average fuel temp(K)         =   960.16
* Coolant temperature (K)          =   573.16
```

```
* Moderator temperature (K)        =   353.16
* UO2 density (g/cm3) inner fuel   =   10.298
* UO2 density (g/cm3) outer fuel   =   9.820
* Coolant purity H2O (at%)         =   99.999
* Moderator purity D2O (at%)       =   99.90
* Coolant density (g/cm3)          =   0.71273
* Moderator density (g/cm3)        =   1.07801
* Boron concentration (ppm)        =   0.0
*
* GENERAL REMARKS:
* ------------------------------------------------
* 1. "COOLANT" SPECTRAL TYPE REGION
*    The radius of this region is equal to the outermost cladding point,
*    which for the CANFLEX fuel bundle is 4.96 cm. The rest of the
*    coolant is declared as having the spectral type MOderator
*
* 2. ALTERNATIVE CROSS-SECTION SETS
*    The combination U238 data and unshielded zirconium cross sections
*    is used. The results of front-end burnup calculations are in good
*    agreement with MCNP. In back-end burnup calculations the void
*    reactivity is underestimated by 1-3 mk.
*
* 3. GROUP CONDENSATION: 50-group structure
*    Groups  1 to 24 (fast) condensed to 5 groups as in 33-group structure
*    Groups 25 to 53 (resonance + a few thermal) without condensation
*    Groups 54 to 89 (thermal) condensed to 22 groups as in 33-group structure
*
* 4. THE HYBRID LATTICE CELL MODEL
*    Two-dimensional representation is applied to the "coolant" spectral
*    type region. The rest of the lattice cell is treated in one-dimensional
*    annular geometry
*
* 5. NUMBER OF LINES AND ANGLES
*    One set of lines and angles is used; 100 lines (ray spacing of 0.5mm)
*    and 7 angles
*
* 6. ANNULAR CELL SUBDIVISION
*    65 coolant annuli, 14 moderator annuli and 3 PT annuli
*
* 7. FUEL ROD SUBDIVISION
*    Two annuli into two radially opposite sectors (90 and 270 degrees)
*
* 8. BURNUP TIME STEP
*    The burnup time step is 10 days and the main transport solution is
*    recalculated at each step, except at the beginning of the
*    irradiation, when the time step is 1 day.
*
* 9. ZERO PRESSURE-TUBE CREEP
*
* NOTE: The input file contains a 59-step burnup calculation,
*       followed by 59 coolant voiding calculations
*************************************************************************
*
PRELUDE
Title "FUEL46SC   -  Standard WIMS Model for ACR Calculations"
*
CELL cluster
```

```
SEQUENCE Pij
SCAN
NDAS
NRODS  43 -14 100 7 4 3 2 1   * One set of lines and angles
PREOUT

LINES 0.  4.96     100  5
LINES 4.96 5.1689   4   1
*
*  common MAIN DATA GROUP for cell calculation
*
ANNULUS # 0.750 Cool          * Fine mesh coolant annuli
ANNULUS # 0.820 Cool
ANNULUS # 0.890 Cool
ANNULUS # 0.960 Cool
ANNULUS # 1.010 Cool
ANNULUS # 1.080 Cool
ANNULUS # 1.150 Cool
ANNULUS # 1.220 Cool
ANNULUS # 1.290 Cool
ANNULUS # 1.360 Cool
ANNULUS # 1.430 Cool
ANNULUS # 1.500 Cool
ANNULUS # 1.570 Cool
ANNULUS # 1.640 Cool
ANNULUS # 1.710 Cool
ANNULUS # 1.780 Cool
ANNULUS # 1.850 Cool
ANNULUS # 1.920 Cool
ANNULUS # 1.990 Cool
ANNULUS # 2.060 Cool
ANNULUS # 2.130 Cool
ANNULUS # 2.200 Cool
ANNULUS # 2.270 Cool
ANNULUS # 2.340 Cool
ANNULUS # 2.410 Cool
ANNULUS # 2.480 Cool
ANNULUS # 2.550 Cool
ANNULUS # 2.620 Cool
ANNULUS # 2.690 Cool
ANNULUS # 2.760 Cool
ANNULUS # 2.830 Cool
ANNULUS # 2.900 Cool
ANNULUS # 2.970 Cool
ANNULUS # 3.040 Cool
ANNULUS # 3.110 Cool
ANNULUS # 3.180 Cool
ANNULUS # 3.250 Cool
ANNULUS # 3.320 Cool
ANNULUS # 3.490 Cool
ANNULUS # 3.560 Cool
ANNULUS # 3.630 Cool
ANNULUS # 3.700 Cool
ANNULUS # 3.770 Cool
ANNULUS # 3.840 Cool
ANNULUS # 3.910 Cool
ANNULUS # 3.980 Cool
```

```
ANNULUS # 4.050 Cool
ANNULUS # 4.120 Cool
ANNULUS # 4.190 Cool
ANNULUS # 4.260 Cool
ANNULUS # 4.330 Cool
ANNULUS # 4.400 Cool
ANNULUS # 4.470 Cool
ANNULUS # 4.540 Cool
ANNULUS # 4.610 Cool
ANNULUS # 4.680 Cool
ANNULUS # 4.750 Cool
ANNULUS # 4.820 Cool
ANNULUS # 4.890 Cool
ANNULUS # 4.960 Cool      * End of the spectral coolant region
NPIJAN #                  * 2D cell model
ANNULUS # 5.030  Cool_Mod * Coolant of spectral type moderator
ANNULUS # 5.100  Cool_Mod
ANNULUS # 5.1689 Cool_Mod
*
ANNULUS # 5.37   PT
ANNULUS # 5.57   PT
ANNULUS # 5.8169 PT
ANNULUS # 7.55   Gap
ANNULUS # 7.80   CT
*
ANNULUS #  8.13 Moder     * Moderator annuli specified explicitly
ANNULUS #  8.46 Moder
ANNULUS #  8.79 Moder
ANNULUS #  9.12 Moder
ANNULUS #  9.45 Moder
ANNULUS #  9.78 Moder
ANNULUS # 10.11 Moder
ANNULUS # 10.44 Moder
ANNULUS # 10.77 Moder
ANNULUS # 11.10 Moder
ANNULUS # 11.43 Moder
ANNULUS # 11.76 Moder
ANNULUS # 12.09 Moder
ANNULUS # 12.412171 Moder * Outer cell boundary
*
ARRAY # 1 1 0 0
RODSUB # # 0.3200 Fuel1a                    * 2 rod annuli of different
RODSUB # # 0.6310 Fuel1b                    * materials
RODSUB # # 0.6750 Clad
*
ARRAY # 1 7 1.73 0
RODSUB # # 0.3200 Fuel2a1 90d Fuel2a2 270d  * 2 rods x 2 sectors each
RODSUB # # 0.6310 Fuel2b1 90d Fuel2b2 270d  * of different materials
RODSUB # # 0.6750 Clad    90d Clad    270d
*
ARRAY # 1 14 3.075 12.857143d
RODSUB # # 0.2700 Fuel3a1 90d Fuel3a2 270d
RODSUB # # 0.5360 Fuel3b1 90d Fuel3b2 270d
RODSUB # # 0.5750 Clad    90d Clad    270d
*
ARRAY # 1 21 4.384 0
RODSUB # # 0.2700 Fuel4a1 90d Fuel4a2 270d
```

```
RODSUB # # 0.5360 Fuel4b1 90d Fuel4b2 270d
RODSUB # # 0.5750 Clad    90d Clad    270d
*
*  50-energy-group structure
*
TOLERANCE 1E-6
NEWRES
Buckling  1.075061E-04 8.204787E-05 1.075061E-04  8.204787E-05  * critical buckling
search
*
FEWGROUPS  4  8 12 16 20 22                                    $ 50 energy groups; 5 fast
groups;
          24 26 28 29 30 31 32 33 34 35 36 37 38 39 40     $
          41 42 43 44 45 46 47 48 49 50 51 52 53           $ Resonance
          56 59 62 65 67 69 71 73 75 77 79 81 83 85 87 89 * 12 thermal groups below
0.625eV
SUPPRESS  1  1 1 1 1  1 1 1 1 1  1 0 1  0  1 -1            * x-sections, leakage,
reaction rates & burnup data
*
*  Define core initial conditions and material compositions
*
*
*  Initial conditions and material compositions
*
WATER    Cool      0.    573.16  CO  DD2O=0.001
WATER    Cool_Mod  0.    573.16  MO  DD2O=0.001
*
WATER    Moder1     0.    353.16  MO  DD2O=99.9
Material Boron 1.08579 353.16 MO b10=199.259  b11=881.821
Material Gad   0.32878 353.16 MO gd155=2292.860 gd157=2455.861
Mixture  Moder Moder1 1.00 boron=1.e-9 gad 0.0 353.16 Moder
*
noburn Moder  *-------------- to stop burning the Gd in moderator -----
*
MATERIAL PT     6.5041 573.16  MO  $
         B10    =  0.00002431   $
         CR50   =  0.0003375    $
         CR52   =  0.0067697    $
         CR53   =  0.0007823    $
         CR54   =  0.0001984    $
         FE54   =  0.0026659    $
         FE56   =  0.0429768    $
         FE57   =  0.0010016    $
         FE58   =  0.0001359    $
         NI58   =  0.0023587    $
         NI60   =  0.0009328    $
         NI61   =  0.000041     $
         NI62   =  0.0001325    $
         NI64   =  0.0000346    $
         ZR90   =  49.47178     $
         ZR91   =  10.90855     $
         ZR92   =  16.85707     $
         ZR94   =  17.20341     $
         ZR96   =  2.87179      $
         NB93   =  2.58
*
MATERIAL Gap  -1        353.16 MO  $
         O16    =  27.11        $
```

```
         C       =  72.89
*
MATERIAL CT      6.4003   353.16 MO  $
         B10     =  0.00005962   $
         CR50    =  0.0041734    $
         CR52    =  0.0837008    $
         CR53    =  0.0096724    $
         CR54    =  0.0024534    $
         FE54    =  0.0076934    $
         FE56    =  0.1240245    $
         FE57    =  0.0028903    $
         FE58    =  0.0003921    $
         NI58    =  0.0370665    $
         NI60    =  0.0146594    $
         NI61    =  0.0006452    $
         NI62    =  0.0020835    $
         NI64    =  0.0005451    $
         ZR90    =  49.798483    $
         ZR91    =  10.9806701   $
         ZR92    =  16.9684301   $
         ZR94    =  17.5704469   $
         ZR96    =  2.890958
*
MATERIAL Clad    7.48    573.16  CL  $ * (effective density
         B10     =  0.00005962   $    *  to give 2.3 kgZr/bundle)
         CR50    =  0.0041737    $
         CR52    =  0.0837008    $
         CR53    =  0.0096726    $
         CR54    =  0.0024534    $
         FE54    =  0.0119675    $
         FE56    =  0.1929267    $
         FE57    =  0.0044963    $
         FE58    =  0.0006100    $
         NI58    =  0.0047175    $
         NI60    =  0.0018657    $
         NI61    =  0.0000821    $
         NI62    =  0.0002651    $
         NI64    =  0.0000693    $
         ZR90    =  49.784792    $
         ZR91    =  10.977651    $
         ZR92    =  16.963765    $
         ZR94    =  17.565616    $
         ZR96    =  2.890163
*
*------------------- NU & Dy Mixture in Central Pin-------------------------
MATERIAL Fuel1a    10.298     960.16  FU  $
         O16     =  13.4529      $
         DY160   =  0.1061       $
         DY161   =  0.8623       $
         DY162   =  1.1708       $
         DY163   =  1.1502       $
         DY164   =  1.3106       $
         U235    =  0.710971     $
         U238    =  99.290
*
*--------------------- SEU Fuel ------------------------------------
MATERIAL Fuel2a1  10.298     960.16  FU  O16=13.4529  U235=2.00  U238=98.00
```

```
MATERIAL Fuel3a1   9.820    960.16  FU  O16=13.4529  U235=2.00  U238=98.00
MATERIAL Fuel4a1   9.820    960.16  FU  O16=13.4529  U235=2.00  U238=98.00
*
MATERIAL Fuel1b  = Fuel1a      * The same initial composition
MATERIAL Fuel2a2 = Fuel2a1     * in all fuel annuli/sectors
MATERIAL Fuel2b1 = Fuel2a1
MATERIAL Fuel2b2 = Fuel2a1
MATERIAL Fuel3a2 = Fuel3a1
MATERIAL Fuel3b1 = Fuel3a1
MATERIAL Fuel3b2 = Fuel3a1
MATERIAL Fuel4a2 = Fuel4a1
MATERIAL Fuel4b1 = Fuel4a1
MATERIAL Fuel4b2 = Fuel4a1
*
* -------------- End Region ----------------------------------------
* END REGION VOLUME is 30.45% Zircaloy-4, 49.14% H20 coolant
* the 20.41% gap (10%air+90%He) is modelled as void
* Mixture  Endreg clad=.3044725 coolant=.4914372  573.16 -cool
*
*  EDIT GROUP
*
* Day 0 to day1
write 1                        * Initial material composition
POWER 1 32.34  1  1   0.00001
BEGIN
*
BENOIST 1
BEEONE  1
BUCKLING  1.075061E-04  8.204787E-05 1.075061E-04  8.204787E-05
LEAKAGE -6
CELLAV
PRINT -2 -2 1 1  1 0
* isotope set for ENDF/B-VI library
REACTION U235=0 U238=0                                  $
         NP239=0                                        $
         PU239=0 PU240=0 PU241=0                        $
         RH105=0                                        $
         CD113=0                                        $
         I135=0  XE135=0                                $
         ND145=0 ND146=0 ND147=0  ND148=0               $
         PM147=0 PM148=0 PM148m=0 PM149=0 PM151=0       $
         SM147=0 SM149=0 SM150=0  SM151=0 SM152=0       $
         EU153=0 EU154=0 EU155=0  EU156=0               $
         GD157=0
PARTITION 4  8 12 16 20 22 24 26 28                     $
         29 30 31 32 33 34 35 36 37 38 39 40            $
         41 42 43 44 45 46 47 48 49 50 51 52 53         $
         56 59 62 65 67 69 71 73 75 77 79 81 83 85 87 89
MATERIAL 0
Suppress 1 1 1 1 1  1 1 1 1 1  1 1 1 -1 1  -1
BEGIN
   POWER   1 32.34 1 1
   write 2
BEGIN
BEGIN
   POWER   1 32.34 1 1
   write 3
```

```
BEGIN
BEGIN
   POWER   1 32.34 1 1
   write 4
BEGIN
BEGIN
   POWER   1 32.34 1 1
   write 5
BEGIN
BEGIN
   POWER   1 32.34 1 1
   write 6
BEGIN
BEGIN
   POWER   1 32.34 1 1
   write 7
BEGIN
BEGIN
   POWER   1 32.34 1 1
   write 8
BEGIN
BEGIN
   POWER   1 32.34 1 1
   write 9
BEGIN
BEGIN
   POWER   1 32.34 1 1
   write 10
BEGIN
BEGIN
   POWER   1 32.34 1 1
   write 11
BEGIN
BEGIN
   POWER   1 32.34 10 1
   write 12
BEGIN
BEGIN
   POWER   1 32.34 10 1
   write 13
BEGIN
BEGIN
   POWER   1 32.34 10 1
   write 14
BEGIN
BEGIN
   POWER   1 32.34 10 1
   write 15
BEGIN
BEGIN
   POWER   1 32.34 20 1
   write 16
BEGIN
BEGIN
   POWER   1 32.34 20 1
   write 17
BEGIN
```

```
BEGIN
   POWER   1 32.34 20 1
   write 18
BEGIN
BEGIN
   POWER   1 32.34 20 1
   write 19
BEGIN
BEGIN
   POWER   1 32.34 20 1
   write 20
BEGIN
BEGIN
   POWER   1 32.34 20 1
   write 21
BEGIN
BEGIN
   POWER   1 32.34 20 1
   write 22
BEGIN
BEGIN
   POWER   1 32.34 20 1
   write 23
BEGIN
BEGIN
   POWER   1 32.34 20 1
   write 24
BEGIN
BEGIN
   POWER   1 32.34 20 1
   write 25
BEGIN
BEGIN
   POWER   1 32.34 20 1
   write 26
BEGIN
BEGIN
   POWER   1 32.34 20 1
   write 27
BEGIN
BEGIN
   POWER   1 32.34 20 1
   write 28
BEGIN
BEGIN
   POWER   1 32.34 20 1
   write 29
BEGIN
BEGIN
   POWER   1 32.34 20 1
   write 30
BEGIN
BEGIN
   POWER   1 32.34 20 1
   write 31
BEGIN
BEGIN
```

```
   POWER   1 32.34 20 1
   write 32
BEGIN
BEGIN
   POWER   1 32.34 20 1
   write 33
BEGIN
BEGIN
   POWER   1 32.34 20 1
   write 34
BEGIN
BEGIN
   POWER   1 32.34 20 1
   write 35
BEGIN
BEGIN
   POWER   1 32.34 20 1
   write 36
BEGIN
BEGIN
   POWER   1 32.34 20 1
   write 37
BEGIN
BEGIN
   POWER   1 32.34 20 1
   write 38
BEGIN
BEGIN
   POWER   1 32.34 20 1
   write 39
BEGIN
BEGIN
   POWER   1 32.34 20 1
   write 40
BEGIN
BEGIN
   POWER   1 32.34 20 1
   write 41
BEGIN
BEGIN
   POWER   1 32.34 20 1
   write 42
BEGIN
BEGIN
   POWER   1 32.34 20 1
   write 43
BEGIN
BEGIN
   POWER   1 32.34 20 1
   write 44
BEGIN
BEGIN
   POWER   1 32.34 20 1
   write 45
BEGIN
BEGIN
   POWER   1 32.34 20 1
```

```
   write 46
BEGIN
BEGIN
   POWER   1 32.34 20 1
   write 47
BEGIN
BEGIN
   POWER   1 32.34 20 1
   write 48
BEGIN
BEGIN
   POWER   1 32.34 20 1
   write 49
BEGIN
BEGIN
   POWER   1 32.34 20 1
   write 50
BEGIN
BEGIN
   POWER   1 32.34 20 1
   write 51
BEGIN
BEGIN
   POWER   1 32.34 20 1
   write 52
BEGIN
BEGIN
   POWER   1 32.34 20 1
   write 53
BEGIN
BEGIN
   POWER   1 32.34 20 1
   write 54
BEGIN
BEGIN
   POWER   1 32.34 20 1
   write 55
BEGIN
BEGIN
   POWER   1 32.34 20 1
   write 56
BEGIN
BEGIN
   POWER   1 32.34 20 1
   write 57
BEGIN
BEGIN
   POWER   1 32.34 20 1
   write 58
BEGIN
BEGIN
   POWER   1 32.34 20 1
   write 59
BEGIN
BEGIN
* ============== voided case ====================
    read 1
```

```
    Power 1 32.34 0.001 1
    density  0.001  0.001
BEGIN
BEGIN
   read 2
   Power 1 32.34 0.001 1
   density  0.001  0.001
BEGIN
BEGIN
   read 3
   Power 1 32.34 0.001 1
   density  0.001  0.001
BEGIN
BEGIN
   read 4
   Power 1 32.34 0.001 1
   density  0.001  0.001
BEGIN
BEGIN
   read 5
   Power 1 32.34 0.001 1
   density  0.001  0.001
BEGIN
BEGIN
   read 6
   Power 1 32.34 0.001 1
   density  0.001  0.001
BEGIN
BEGIN
   read 7
   Power 1 32.34 0.001 1
   density  0.001  0.001
BEGIN
BEGIN
   read 8
   Power 1 32.34 0.001 1
   density  0.001  0.001
BEGIN
BEGIN
   read 9
   Power 1 32.34 0.001 1
   density  0.001  0.001
BEGIN
BEGIN
   read 10
   Power 1 32.34 0.001 1
   density  0.001  0.001
BEGIN
BEGIN
   read 11
   Power 1 32.34 0.001 1
   density  0.001  0.001
BEGIN
BEGIN
   read 12
   Power 1 32.34 0.001 1
   density  0.001  0.001
```

```
BEGIN
BEGIN
   read 13
   Power 1 32.34 0.001 1
   density  0.001  0.001
BEGIN
BEGIN
   read 14
   Power 1 32.34 0.001 1
   density  0.001  0.001
BEGIN
BEGIN
   read 15
   Power 1 32.34 0.001 1
   density  0.001  0.001
BEGIN
BEGIN
   read 16
   Power 1 32.34 0.001 1
   density  0.001  0.001
BEGIN
BEGIN
   read 17
   Power 1 32.34 0.001 1
   density  0.001  0.001
BEGIN
BEGIN
   read 18
   Power 1 32.34 0.001 1
   density  0.001  0.001
BEGIN
BEGIN
   read 19
   Power 1 32.34 0.001 1
   density  0.001  0.001
BEGIN
BEGIN
   read 20
   Power 1 32.34 0.001 1
   density  0.001  0.001
BEGIN
BEGIN
   read 21
   Power 1 32.34 0.001 1
   density  0.001  0.001
BEGIN
BEGIN
   read 22
   Power 1 32.34 0.001 1
   density  0.001  0.001
BEGIN
BEGIN
   read 23
   Power 1 32.34 0.001 1
   density  0.001  0.001
BEGIN
BEGIN
```

```
   read 24
   Power 1 32.34 0.001 1
   density  0.001  0.001
BEGIN
BEGIN
   read 25
   Power 1 32.34 0.001 1
   density  0.001  0.001
BEGIN
BEGIN
   read 26
   Power 1 32.34 0.001 1
   density  0.001  0.001
BEGIN
BEGIN
   read 27
   Power 1 32.34 0.001 1
   density  0.001  0.001
BEGIN
BEGIN
   read 28
   Power 1 32.34 0.001 1
   density  0.001  0.001
BEGIN
BEGIN
   read 29
   Power 1 32.34 0.001 1
   density  0.001  0.001
BEGIN
BEGIN
   read 30
   Power 1 32.34 0.001 1
   density  0.001  0.001
BEGIN
BEGIN
   read 31
   Power 1 32.34 0.001 1
   density  0.001  0.001
BEGIN
BEGIN
   read 32
   Power 1 32.34 0.001 1
   density  0.001  0.001
BEGIN
BEGIN
   read 33
   Power 1 32.34 0.001 1
   density  0.001  0.001
BEGIN
BEGIN
   read 34
   Power 1 32.34 0.001 1
   density  0.001  0.001
BEGIN
BEGIN
   read 35
   Power 1 32.34 0.001 1
```

```
   density  0.001  0.001
BEGIN
BEGIN
   read 36
   Power 1 32.34 0.001 1
   density  0.001  0.001
BEGIN
BEGIN
   read 37
   Power 1 32.34 0.001 1
   density  0.001  0.001
BEGIN
BEGIN
   read 38
   Power 1 32.34 0.001 1
   density  0.001  0.001
BEGIN
BEGIN
   read 39
   Power 1 32.34 0.001 1
   density  0.001  0.001
BEGIN
BEGIN
   read 40
   Power 1 32.34 0.001 1
   density  0.001  0.001
BEGIN
BEGIN
   read 41
   Power 1 32.34 0.001 1
   density  0.001  0.001
BEGIN
BEGIN
   read 42
   Power 1 32.34 0.001 1
   density  0.001  0.001
BEGIN
BEGIN
   read 43
   Power 1 32.34 0.001 1
   density  0.001  0.001
BEGIN
BEGIN
   read 44
   Power 1 32.34 0.001 1
   density  0.001  0.001
BEGIN
BEGIN
   read 45
   Power 1 32.34 0.001 1
   density  0.001  0.001
BEGIN
BEGIN
   read 46
   Power 1 32.34 0.001 1
   density  0.001  0.001
BEGIN
```

```
BEGIN
   read 47
   Power 1 32.34 0.001 1
   density  0.001  0.001
BEGIN
BEGIN
   read 48
   Power 1 32.34 0.001 1
   density  0.001  0.001
BEGIN
BEGIN
   read 49
   Power 1 32.34 0.001 1
   density  0.001  0.001
BEGIN
BEGIN
   read 50
   Power 1 32.34 0.001 1
   density  0.001  0.001
BEGIN
BEGIN
   read 51
   Power 1 32.34 0.001 1
   density  0.001  0.001
BEGIN
BEGIN
   read 52
   Power 1 32.34 0.001 1
   density  0.001  0.001
BEGIN
BEGIN
   read 53
   Power 1 32.34 0.001 1
   density  0.001  0.001
BEGIN
BEGIN
   read 54
   Power 1 32.34 0.001 1
   density  0.001  0.001
BEGIN
BEGIN
   read 55
   Power 1 32.34 0.001 1
   density  0.001  0.001
BEGIN
BEGIN
   read 56
   Power 1 32.34 0.001 1
   density  0.001  0.001
BEGIN
BEGIN
   read 57
   Power 1 32.34 0.001 1
   density  0.001  0.001
BEGIN
BEGIN
   read 58
```

```
   Power 1 32.34 0.001 1
   density  0.001  0.001
BEGIN
BEGIN
   read 59
   Power 1 32.34 0.001 1
   density  0.001  0.001
BEGIN
BEGIN
STOP
```

Appendix B
Nuclide Densities of Fresh, Mid-Burnup and Discharged Fuel

B.1 Nuclide Number Densities (Atom/Barn-cm) of Fresh Fuel

1 barn = 10xE-24 cm^2

TIME= 1.001 DAYS BURNUP= 32.344 MWD/(T.INITIAL)

BURNUPS (MWD/T.INITIAL)	Central Pin 5.601	Ring1 21.891	Ring2 28.911	Ring3 41.474
Ring 1 (Central Pin)				
O16	4.41947E-02	KR83	6.72235E-10	ZR93	8.17256E-09
MO95	8.43173E-09	MO97	7.96803E-09	MO100	8.52649E-09
TC99	8.37591E-09	RU101	7.36070E-09	RU102	6.55251E-09
RU103	5.25158E-09	RH103	4.64601E-11	RH105	1.91284E-09
PD105	4.86132E-10	PD107	5.78796E-10	PD108	2.74460E-10
AG109	1.22433E-10	CD113	2.68904E-11	IN115	2.34173E-11
I129	1.04210E-09	I135	3.17782E-09	XE131	3.97568E-09
XE133	8.51603E-09	XE135	1.54542E-09	CS133	5.75180E-10
CS134	5.71705E-14	CS135	1.55917E-09	LA139	8.71189E-09
CE141	7.69337E-09	CE142	7.74153E-09	CE144	7.18311E-09
PR141	8.23085E-11	PR143	7.56124E-09	ND143	1.94889E-10
ND144	1.05605E-11	ND145	5.37231E-09	ND146	4.26906E-09
ND147	3.13020E-09	ND148	2.48353E-09	PM147	9.90841E-11
PM148	1.46112E-14	PM148M	9.05220E-15	PM149	1.45616E-09
PM151	5.38018E-10	SM147	2.40186E-14	SM149	2.32253E-10
SM150	9.80185E-12	SM151	1.72327E-10	SM152	4.60564E-10
EU153	3.01505E-10	EU154	1.31763E-13	EU155	7.62302E-11
EU156	3.61027E-11	GD157	1.77515E-11	DY160	3.48259E-05
DY161	2.81211E-04	DY162	3.79890E-04	DY163	3.70856E-04
DY164	4.19183E-04	HO165	1.01424E-06	ER166	1.69540E-10
ER167	3.68402E-15	U233	2.03603E-20	U234	7.60776E-12
U235	1.58771E-04	U236	2.33407E-08	U238	2.19102E-02
NP237	1.28165E-09	NP238	3.12230E-13	NP239	2.28522E-07
PU236	7.77466E-18	PU238	3.49899E-14	PU239	3.52596E-08
PU240	4.39519E-11	PU241	5.46888E-14	PU242	8.12007E-18
AM241	1.70468E-18	AM242M	1.08555E-22	AM243	8.44642E-22
PFP	1.56736E-10	PFP2	2.17657E-08		
Ring 2 (Inner Fuel Pins)					
O16	4.59869E-02	KR83	2.77861E-09	ZR93	3.34756E-08
MO95	3.41424E-08	MO97	3.16910E-08	MO100	3.36554E-08
TC99	3.27952E-08	RU101	2.75554E-08	RU102	2.34272E-08
RU103	1.78124E-08	RH103	1.57600E-10	RH105	5.23992E-09
PD105	1.33335E-09	PD107	1.28415E-09	PD108	5.85128E-10
AG109	2.54307E-10	CD113	7.43330E-11	IN115	6.45674E-11
I129	3.69040E-09	I135	1.24173E-08	XE131	1.52758E-08
XE133	3.38140E-08	XE135	4.21318E-09	CS133	2.28420E-09
CS134	3.28619E-13	CS135	4.55020E-09	LA139	3.45622E-08
CE141	3.08846E-08	CE142	3.12975E-08	CE144	2.88399E-08
PR141	3.30469E-10	PR143	3.06938E-08	ND143	7.91173E-10

ND144	4.44528E-11	ND145	2.10468E-08	ND146	1.62182E-08
ND147	1.19130E-08	ND148	9.24977E-09	PM147	3.77104E-10
PM148	9.39080E-14	PM148M	6.49811E-14	PM149	5.20282E-09
PM151	1.82055E-09	SM147	9.14230E-14	SM149	8.10561E-10
SM150	5.82135E-11	SM151	5.81666E-10	SM152	1.55500E-09
EU153	9.62134E-10	EU154	5.71357E-13	EU155	2.10883E-10
EU156	9.31987E-11	GD157	4.10345E-11	U233	7.74260E-20
U234	2.53983E-11	U235	4.64516E-04	U236	1.03485E-07
U238	2.25025E-02	NP237	1.50776E-09	NP238	5.06008E-13
NP239	2.92808E-07	PU236	1.04204E-17	PU238	5.66680E-14
PU239	4.51579E-08	PU240	7.65887E-11	PU241	1.12583E-13
PU242	2.60714E-17	AM241	3.49760E-18	AM242M	2.36016E-22
AM243	3.20359E-21	PFP	5.99524E-10	PFP2	8.55096E-08
Ring 3 (Intermediate Fuel Pins)					
O16	4.38524E-02	KR83	3.49092E-09	ZR93	4.20244E-08
MO95	4.28151E-08	MO97	3.96734E-08	MO100	4.21018E-08
TC99	4.09928E-08	RU101	3.42886E-08	RU102	2.90106E-08
RU103	2.19284E-08	RH103	1.94020E-10	RH105	6.25873E-09
PD105	1.59422E-09	PD107	1.48514E-09	PD108	6.71645E-10
AG109	2.90448E-10	CD113	8.81147E-11	IN115	7.73785E-11
I129	4.56519E-09	I135	1.55174E-08	XE131	1.90581E-08
XE133	4.23219E-08	XE135	4.12843E-09	CS133	2.85914E-09
CS134	4.50249E-13	CS135	4.61976E-09	LA139	4.32571E-08
CE141	3.86981E-08	CE142	3.92423E-08	CE144	3.61366E-08
PR141	4.14102E-10	PR143	3.84987E-08	ND143	9.92363E-10
ND144	5.71046E-11	ND145	2.63089E-08	ND146	2.02118E-08
ND147	1.48469E-08	ND148	1.15058E-08	PM147	4.70001E-10
PM148	1.34202E-13	PM148M	9.57113E-14	PM149	6.43980E-09
PM151	2.24014E-09	SM147	1.13951E-13	SM149	9.83291E-10
SM150	9.54875E-11	SM151	7.14082E-10	SM152	1.91462E-09
EU153	1.17600E-09	EU154	8.35621E-13	EU155	2.52436E-10
EU156	1.11026E-10	GD157	4.58631E-11	U233	7.58153E-20
U234	2.45398E-11	U235	4.42768E-04	U236	1.26862E-07
U238	2.14579E-02	NP237	1.46010E-09	NP238	5.87147E-13
NP239	3.24793E-07	PU236	1.02196E-17	PU238	6.57334E-14
PU239	5.00728E-08	PU240	1.02190E-10	PU241	1.67462E-13
PU242	5.01011E-17	AM241	5.19421E-18	AM242M	3.92754E-22
AM243	6.70036E-21	PFP	7.33020E-10	PFP2	1.06920E-07
Ring 4 (Outermost Fuel Pins)					
O16	4.38524E-02	KR83	4.99179E-09	ZR93	6.00446E-08
MO95	6.11028E-08	MO97	5.65152E-08	MO100	5.99269E-08
TC99	5.82974E-08	RU101	4.85241E-08	RU102	4.08359E-08
RU103	3.06653E-08	RH103	2.71332E-10	RH105	8.43350E-09
PD105	2.15235E-09	PD107	1.92670E-09	PD108	8.62926E-10
AG109	3.70731E-10	CD113	1.17369E-10	IN115	1.04895E-10
I129	6.41864E-09	I135	2.20609E-08	XE131	2.70470E-08
XE133	6.02708E-08	XE135	4.22106E-09	CS133	4.07231E-09
CS134	7.21125E-13	CS135	4.90284E-09	LA139	6.16035E-08
CE141	5.51782E-08	CE142	5.59963E-08	CE144	5.15271E-08
PR141	5.90523E-10	PR143	5.49544E-08	ND143	1.41655E-09
ND144	8.48152E-11	ND145	3.74166E-08	ND146	2.86511E-08
ND147	2.10445E-08	ND148	1.62783E-08	PM147	6.66265E-10
PM148	2.25824E-13	PM148M	1.66154E-13	PM149	9.05741E-09
PM151	3.13048E-09	SM147	1.61552E-13	SM149	1.33807E-09

SM150	1.87703E-10	SM151	9.93460E-10	SM152	2.67974E-09
EU153	1.63131E-09	EU154	1.48109E-12	EU155	3.41514E-10
EU156	1.49665E-10	GD157	5.51177E-11	U233	6.93462E-20
U234	2.34645E-11	U235	4.42433E-04	U236	1.76879E-07
U238	2.14578E-02	NP237	1.40299E-09	NP238	7.15619E-13
NP239	4.15199E-07	PU236	9.37877E-18	PU238	8.00572E-14
PU239	6.39761E-08	PU240	1.65418E-10	PU241	3.10317E-13
PU242	1.27376E-16	AM241	9.62182E-18	AM242M	8.69379E-22
AM243	1.89566E-20	PFP	1.00274E-09	PFP2	1.52112E-07

B.2 Nuclide Number Densities (Atom/Barn-cm) of Mid-Burnup Fuel

TIME= 311.000 DAYS BURNUP= 10015.445 MWD/(T.INITIAL)

BURNUPS (MWD/T.INITIAL)	Central Pin 2518.655	Ring1 7059.828	Ring2 9132.266	Ring3 12534.697

Ring 1 (Central Pin)

O16	4.41947E-02	KR83	2.45433E-07	ZR93	3.17596E-06
MO95	3.42272E-06	MO97	3.45091E-06	MO100	3.88505E-06
TC99	3.64402E-06	RU101	3.32628E-06	RU102	3.16760E-06
RU103	6.79191E-07	RH103	2.10738E-06	RH105	1.80550E-08
PD105	1.69894E-06	PD107	7.91455E-07	PD108	5.08938E-07
AG109	3.01190E-07	CD113	1.77181E-09	IN115	1.15893E-08
I129	5.99204E-07	I135	6.22179E-09	XE131	1.77409E-06
XE133	1.25682E-07	XE135	2.97509E-09	CS133	3.85800E-06
CS134	5.39762E-08	CS135	1.40696E-06	LA139	3.68094E-06
CE141	5.99637E-07	CE142	3.27578E-06	CE144	2.07747E-06
PR141	2.73601E-06	PR143	2.41948E-07	ND143	2.77924E-06
ND144	9.73951E-07	ND145	2.15967E-06	ND146	1.81660E-06
ND147	8.59145E-08	ND148	1.08762E-06	PM147	1.07150E-06
PM148	2.25570E-09	PM148M	4.51210E-09	PM149	1.07715E-08
PM151	2.73598E-09	SM147	1.06738E-07	SM149	2.80133E-08
SM150	7.29276E-07	SM151	1.31772E-07	SM152	4.44418E-07
EU153	2.04713E-07	EU154	1.73792E-08	EU155	1.50275E-08
EU156	9.50192E-09	GD157	7.44629E-10	DY160	2.73287E-05
DY161	2.05729E-04	DY162	3.88326E-04	DY163	3.73963E-04
DY164	2.37258E-04	HO165	2.39078E-04	ER166	1.43000E-05
ER167	8.64066E-08	U233	1.88753E-15	U234	2.18694E-09
U235	1.21856E-04	U236	6.73724E-06	U238	2.18115E-02
NP237	4.61592E-07	NP238	8.46001E-10	NP239	1.01796E-06
PU236	8.25856E-13	PU238	3.70822E-08	PU239	5.78564E-05
PU240	7.69215E-06	PU241	2.29841E-06	PU242	1.34457E-07
AM241	2.44098E-08	AM242M	1.97242E-10	AM243	5.20811E-09
PFP	3.05862E-09	PFP2	9.93591E-06		

Ring 2 (Inner Fuel Pins)

O16	4.59869E-02	KR83	7.61001E-07	ZR93	9.92055E-06
MO95	1.03097E-05	MO97	1.00149E-05	MO100	1.09766E-05
TC99	1.02394E-05	RU101	9.00679E-06	RU102	8.15895E-06
RU103	1.40604E-06	RH103	4.99617E-06	RH105	3.03855E-08

PD105	3.26087E-06	PD107	1.34865E-06	PD108	8.51765E-07
AG109	4.79460E-07	CD113	2.08003E-09	IN115	2.15644E-08
I129	1.42873E-06	I135	1.44923E-08	XE131	4.67165E-06
XE133	2.95076E-07	XE135	4.91324E-09	CS133	1.09393E-05
CS134	3.03432E-07	CS135	2.80139E-06	LA139	1.07671E-05
CE141	1.51025E-06	CE142	9.75940E-06	CE144	6.12066E-06
PR141	8.25836E-06	PR143	6.10575E-07	ND143	8.21320E-06
ND144	3.44332E-06	ND145	6.29559E-06	ND146	5.23971E-06
ND147	2.02309E-07	ND148	3.01589E-06	PM147	2.80321E-06
PM148	1.06519E-08	PM148M	1.70460E-08	PM149	2.63079E-08
PM151	5.49150E-09	SM147	3.08690E-07	SM149	4.48320E-08
SM150	2.05247E-06	SM151	1.94486E-07	SM152	1.15008E-06
EU153	5.12183E-07	EU154	5.26352E-08	EU155	2.75718E-08
EU156	1.93534E-08	GD157	7.55261E-10	U233	6.20543E-15
U234	6.54080E-09	U235	3.09986E-04	U236	2.63755E-05
U238	2.23800E-02	NP237	1.01141E-06	NP238	2.42548E-09
NP239	1.26313E-06	PU236	1.74731E-12	PU238	9.18973E-08
PU239	6.26408E-05	PU240	1.14797E-05	PU241	3.61808E-06
PU242	3.27254E-07	AM241	3.91263E-08	AM242M	3.44138E-10
AM243	1.58566E-08	PFP	4.75074E-09	PFP2	2.78980E-05
Ring 3 (Intermediate Fuel Pins)					
O16	4.38524E-02	KR83	9.05025E-07	ZR93	1.20974E-05
MO95	1.25700E-05	MO97	1.22620E-05	MO100	1.34653E-05
TC99	1.24650E-05	RU101	1.09904E-05	RU102	9.97718E-06
RU103	1.71163E-06	RH103	6.03217E-06	RH105	3.68437E-08
PD105	3.97549E-06	PD107	1.72656E-06	PD108	1.10307E-06
AG109	6.19510E-07	CD113	1.90042E-09	IN115	2.52903E-08
I129	1.75943E-06	I135	1.71619E-08	XE131	5.64241E-06
XE133	3.50612E-07	XE135	4.33251E-09	CS133	1.33275E-05
CS134	4.43250E-07	CS135	2.59634E-06	LA139	1.31457E-05
CE141	1.80618E-06	CE142	1.19549E-05	CE144	7.43250E-06
PR141	1.01332E-05	PR143	7.22413E-07	ND143	9.69963E-06
ND144	4.60064E-06	ND145	7.62541E-06	ND146	6.42416E-06
ND147	2.38062E-07	ND148	3.69393E-06	PM147	3.29177E-06
PM148	1.48444E-08	PM148M	1.91952E-08	PM149	3.25990E-08
PM151	6.57032E-09	SM147	3.67701E-07	SM149	3.92953E-08
SM150	2.54879E-06	SM151	1.71644E-07	SM152	1.43804E-06
EU153	6.68977E-07	EU154	7.34147E-08	EU155	3.40609E-08
EU156	2.72173E-08	GD157	6.72023E-10	U233	5.38360E-15
U234	5.76954E-09	U235	2.55457E-04	U236	3.07344E-05
U238	2.13233E-02	NP237	1.17342E-06	NP238	3.43982E-09
NP239	1.41884E-06	PU236	1.94671E-12	PU238	1.23360E-07
PU239	6.06871E-05	PU240	1.42496E-05	PU241	4.68346E-06
PU242	5.90188E-07	AM241	5.00907E-08	AM242M	4.53496E-10
AM243	3.17432E-08	PFP	4.03459E-09	PFP2	3.41594E-05
Ring 4 (Outermost Fuel Pins)					
O16	4.38524E-02	KR83	1.15914E-06	ZR93	1.62573E-05
MO95	1.69065E-05	MO97	1.66203E-05	MO100	1.83542E-05
TC99	1.67850E-05	RU101	1.49055E-05	RU102	1.36143E-05
RU103	2.31385E-06	RH103	8.10653E-06	RH105	4.97767E-08
PD105	5.45389E-06	PD107	2.57429E-06	PD108	1.66941E-06
AG109	9.32461E-07	CD113	1.88391E-09	IN115	3.29637E-08
I129	2.43199E-06	I135	2.18508E-08	XE131	7.50792E-06
XE133	4.48544E-07	XE135	3.77210E-09	CS133	1.79995E-05

CS134	7.51159E-07	CS135	2.46914E-06	LA139	1.77512E-05
CE141	2.33444E-06	CE142	1.62190E-05	CE144	9.91588E-06
PR141	1.38053E-05	PR143	9.13626E-07	ND143	1.22891E-05
ND144	7.17337E-06	ND145	1.01623E-05	ND146	8.76370E-06
ND147	2.99864E-07	ND148	5.03961E-06	PM147	4.18452E-06
PM148	2.32834E-08	PM148M	2.34824E-08	PM149	4.46420E-08
PM151	8.62358E-09	SM147	4.81061E-07	SM149	3.58814E-08
SM150	3.53449E-06	SM151	1.54965E-07	SM152	1.98615E-06
EU153	1.00026E-06	EU154	1.20125E-07	EU155	4.99692E-08
EU156	4.69528E-08	GD157	6.58148E-10	U233	3.99648E-15
U234	4.71013E-09	U235	1.95361E-04	U236	3.88753E-05
U238	2.12878E-02	NP237	1.50008E-06	NP238	5.72680E-09
NP239	1.84907E-06	PU236	2.21126E-12	PU238	1.89801E-07
PU239	6.38447E-05	PU240	1.97465E-05	PU241	6.84237E-06
PU242	1.30474E-06	AM241	7.15353E-08	AM242M	6.50918E-10
AM243	8.01923E-08	PFP	3.39446E-09	PFP2	4.64335E-05

B.3 Nuclide Number Densities (Atom/Barn-cm) of Discharged Fuel

TIME= 631.000 DAYS BURNUP= 20276.684 MWD/(T.INITIAL)

BURNUPS (MWD/T.INITIAL)	Central Pin 6820.551	Ring1 15283.305	Ring2 18971.959	Ring3 24460.518

Ring 1 (Central Pin)

O16	4.41947E-02	KR83	5.65249E-07	ZR93	7.83494E-06
MO95	8.61724E-06	MO97	9.03626E-06	MO100	1.04365E-05
TC99	9.49982E-06	RU101	8.85018E-06	RU102	8.76668E-06
RU103	1.14856E-06	RH103	6.34705E-06	RH105	3.09491E-08
PD105	5.31001E-06	PD107	2.76879E-06	PD108	1.84390E-06
AG109	1.09623E-06	CD113	2.30071E-09	IN115	2.84357E-08
I129	1.75435E-06	I135	9.15012E-09	XE131	4.50906E-06
XE133	1.87186E-07	XE135	3.34561E-09	CS133	1.02147E-05
CS134	2.84589E-07	CS135	3.25961E-06	LA139	9.50945E-06
CE141	8.93496E-07	CE142	8.48285E-06	CE144	4.04650E-06
PR141	7.78955E-06	PR143	3.46112E-07	ND143	6.79501E-06
ND144	4.19643E-06	ND145	5.37382E-06	ND146	4.77938E-06
ND147	1.24676E-07	ND148	2.84758E-06	PM147	2.40992E-06
PM148	6.15230E-09	PM148M	1.00330E-08	PM149	1.72961E-08
PM151	4.30413E-09	SM147	4.69291E-07	SM149	3.11670E-08
SM150	2.01454E-06	SM151	1.81499E-07	SM152	1.30761E-06
EU153	7.21016E-07	EU154	9.15585E-08	EU155	3.77625E-08
EU156	2.42895E-08	GD157	9.56228E-10	DY160	2.05094E-05
DY161	1.38111E-04	DY162	3.72976E-04	DY163	3.76906E-04
DY164	1.29385E-04	HO165	3.90323E-04	ER166	5.43746E-05
ER167	5.90610E-07	U233	6.93138E-15	U234	3.92335E-09
U235	8.54726E-05	U236	1.29983E-05	U238	2.16934E-02
NP237	1.04056E-06	NP238	2.32008E-09	NP239	1.20206E-06
PU236	3.58518E-12	PU238	1.73185E-07	PU239	8.26391E-05
PU240	2.37727E-05	PU241	8.98016E-06	PU242	1.41994E-06
AM241	1.85158E-07	AM242M	1.98896E-09	AM243	1.23862E-07

PFP	3.26716E-09	PFP2	2.66146E-05		
Ring 2 (Inner Fuel Pins)					
O16	4.59869E-02	KR83	1.39770E-06	ZR93	2.00883E-05
MO95	2.10689E-05	MO97	2.12553E-05	MO100	2.38167E-05
TC99	2.13338E-05	RU101	1.94659E-05	RU102	1.85219E-05
RU103	1.84238E-06	RH103	1.18288E-05	RH105	4.35986E-08
PD105	8.67572E-06	PD107	4.20647E-06	PD108	2.77130E-06
AG109	1.51349E-06	CD113	2.40602E-09	IN115	4.16560E-08
I129	3.39269E-06	I135	1.60674E-08	XE131	9.26924E-06
XE133	3.29572E-07	XE135	4.33530E-09	CS133	2.29983E-05
CS134	1.24412E-06	CS135	5.54393E-06	LA139	2.26036E-05
CE141	1.65543E-06	CE142	2.05177E-05	CE144	9.25428E-06
PR141	1.89157E-05	PR143	6.47588E-07	ND143	1.55967E-05
ND144	1.25737E-05	ND145	1.26925E-05	ND146	1.14729E-05
ND147	2.21295E-07	ND148	6.46471E-06	PM147	4.69687E-06
PM148	2.02622E-08	PM148M	2.70499E-08	PM149	3.42712E-08
PM151	6.79634E-09	SM147	1.07735E-06	SM149	4.37380E-08
SM150	4.73314E-06	SM151	2.29208E-07	SM152	2.57876E-06
EU153	1.51500E-06	EU154	2.18350E-07	EU155	7.41473E-08
EU156	5.13971E-08	GD157	1.00496E-09	U233	1.96414E-14
U234	1.05429E-08	U235	1.86782E-04	U236	4.57769E-05
U238	2.22362E-02	NP237	2.81506E-06	NP238	8.03949E-09
NP239	1.47286E-06	PU236	9.12495E-12	PU238	5.14575E-07
PU239	8.16472E-05	PU240	3.12958E-05	PU241	1.13845E-05
PU242	2.70862E-06	AM241	2.33079E-07	AM242M	2.48715E-09
AM243	2.91753E-07	PFP	4.05599E-09	PFP2	6.03127E-05
Ring 3 (Intermediate Fuel Pins)					
O16	4.38524E-02	KR83	1.52614E-06	ZR93	2.33893E-05
MO95	2.45119E-05	MO97	2.49760E-05	MO100	2.81132E-05
TC99	2.47832E-05	RU101	2.28496E-05	RU102	2.19155E-05
RU103	2.11246E-06	RH103	1.35008E-05	RH105	4.99649E-08
PD105	1.02961E-05	PD107	5.26124E-06	PD108	3.49101E-06
AG109	1.86836E-06	CD113	2.07039E-09	IN115	4.56342E-08
I129	4.03865E-06	I135	1.74733E-08	XE131	1.05447E-05
XE133	3.59700E-07	XE135	3.46735E-09	CS133	2.67158E-05
CS134	1.75472E-06	CS135	4.97619E-06	LA139	2.64344E-05
CE141	1.81311E-06	CE142	2.41084E-05	CE144	1.05710E-05
PR141	2.22777E-05	PR143	6.96775E-07	ND143	1.66863E-05
ND144	1.65256E-05	ND145	1.46021E-05	ND146	1.36351E-05
ND147	2.38420E-07	ND148	7.61792E-06	PM147	5.04751E-06
PM148	2.61092E-08	PM148M	2.77362E-08	PM149	4.03238E-08
PM151	7.61289E-09	SM147	1.20377E-06	SM149	3.64557E-08
SM150	5.66193E-06	SM151	1.97791E-07	SM152	3.00388E-06
EU153	1.92066E-06	EU154	2.80871E-07	EU155	9.56901E-08
EU156	7.78692E-08	GD157	9.39674E-10	U233	1.44949E-14
U234	8.34601E-09	U235	1.26232E-04	U236	4.98457E-05
U238	2.11636E-02	NP237	3.22328E-06	NP238	1.14429E-08
NP239	1.67421E-06	PU236	9.75295E-12	PU238	6.80568E-07
PU239	7.17137E-05	PU240	3.50129E-05	PU241	1.27763E-05
PU242	4.39838E-06	AM241	2.47592E-07	AM242M	2.57169E-09
AM243	5.28916E-07	PFP	3.13419E-09	PFP2	7.08963E-05
Ring 4 (Outermost Fuel Pins)					
O16	4.38524E-02	KR83	1.68795E-06	ZR93	2.91947E-05
MO95	3.06094E-05	MO97	3.17894E-05	MO100	3.61460E-05

TC99	3.10384E-05	RU101	2.92126E-05	RU102	2.84580E-05
RU103	2.65310E-06	RH103	1.65261E-05	RH105	6.30488E-08
PD105	1.35491E-05	PD107	7.55349E-06	PD108	5.05532E-06
AG109	2.62048E-06	CD113	1.93918E-09	IN115	5.38159E-08
I129	5.30407E-06	I135	2.00970E-08	XE131	1.27815E-05
XE133	4.15184E-07	XE135	2.73702E-09	CS133	3.34110E-05
CS134	2.78677E-06	CS135	4.67620E-06	LA139	3.33703E-05
CE141	2.08296E-06	CE142	3.06563E-05	CE144	1.28137E-05
PR141	2.83423E-05	PR143	7.78428E-07	ND143	1.78883E-05
ND144	2.45346E-05	ND145	1.79268E-05	ND146	1.77323E-05
ND147	2.68793E-07	ND148	9.78867E-06	PM147	5.58270E-06
PM148	3.59020E-08	PM148M	2.97168E-08	PM149	5.14768E-08
PM151	9.27940E-09	SM147	1.41646E-06	SM149	3.15086E-08
SM150	7.32743E-06	SM151	1.80364E-07	SM152	3.79496E-06
EU153	2.69376E-06	EU154	4.05660E-07	EU155	1.40209E-07
EU156	1.40881E-07	GD157	1.03169E-09	U233	8.29959E-15
U234	5.73897E-09	U235	6.76901E-05	U236	5.60634E-05
U238	2.10842E-02	NP237	3.90667E-06	NP238	1.82592E-08
NP239	2.19518E-06	PU236	1.01154E-11	PU238	9.76884E-07
PU239	6.84062E-05	PU240	4.11710E-05	PU241	1.52983E-05
PU242	8.26503E-06	AM241	2.69461E-07	AM242M	2.68027E-09
AM243	1.14857E-06	PFP	2.39422E-09	PFP2	9.05149E-05

Appendix C
RFSP-IST Model for ACR-700 Core Calculations

```
*START    MICHAELA OVANES
ACR-700 100% FP, 2-GROUP RFSP TIME-AVERAGE MODEL, 284 CHANNELS, REFLECTOR 51 CM THICK
SEU 2.0 % CT 2.5 CM PT 6.5 CM 4.6 % DY NU CENTRAL PIN
$*******************************************************************************
$ TITLE        : ACR-700 284-CHANNELS EQUILIBRIUM CORE DESIGN
$ AUTHOR(S)    : M. OVANES/ 2002, May
$ FILE         : acr284_std_1982_73MW_mreg_cvr_tav.inp
$ CODE VERSION : RFSP-IST (RFSP-IST.REL_3-01HPL)
$
$ PROJECT      : 10810-03300 ACR-700 CORE PHYSICS DESIGN
$ DESCRIPTION  : Setup the WIMS-IST/DRAGON-Based RFSP-IST 2-Group Time-Average
$                for ACR-700 284-Channel Equilibrium Core
$
$ GENARAL REMARKS:
$ ---------------------------------------------
$ 1. CORE POWER
$    Total core thermal power is 1982.00 MW. Total fission power is 2095.14 MW.
$    A ratio of thermal power to coolant to fission power of 0.9460 is assumed.
$    Target maximum channel power is 7.3 MW.
$
$ 2. GROUP CONDENSATION: 2-energy group formalism
$
$ 3. FUEL DESIGN
$    43-element CANFLEX fuel bundle using 2.0 SEU fuel, with the central
$    element replaced by an element containing 95.4% natural uranium and
$    4.6 wt% dysprosium (in total U).
$
$ 3. NOMINAL PARAMETERS FOR CANFLEX CLUSTER
$    UO2 average fuel temp (K)      =   960.16
$    Coolant temperature (K)        =   573.16
$    Moderator temperature (K)      =   353.16
$    UO2 density (g/cm3) inner fuel =   10.298
$    UO2 density (g/cm3) outer fuel =   9.820
$    Coolant purity H2O (at%)       =   99.999
$    Moderator purity D2O (at%)     =   99.90
$    Coolant density (g/cm3)        =   0.71273
$    Moderator density (g/cm3)      =   1.07801
$    Boron concentration (ppm)      =   0.0
$
$ 4. FUEL PROPERTIES: based on the standard WIMS-IST model for ACR analysis,
$    ACRstd_seu2dy46_e6.pin.  This fuel design gives a -5 mk FULL-CORE CVR
```

```
$    and 20.0 MWd/kgU DISCHARGE BURNUP. Fuel and reflector properties are
$    representative of an equilibrium-core environment, equivalent of a
$    mid-burnup value of about 10 MWd/kgU.
$
$ 5. ZERO PRESSURE-TUBE CREEP
$
$*******************************************************************************
*READ TAPE284-73-tx
*MODEL    ACR-700 284 CHANNELS 2-GROUP RFSP TA MODEL, 2.0% SEU CENTRAL NU/DY4.6 WT%
NU/DY PIN, 50 CM REFLECTOR
$2-------1---------2---------3---------4---------5---------6---------7---------8
*DATA     GEOMETRY
$ dimensions of mesh arrays are:
A        50   50   26   18   18   12    0    0    0    0    0    0  284 3408  042
B              0.0            0.0            0.0
C             62.000         62.000         0.0
D             22.000         22.000         49.530
E  1 249 249 225
F  1 2 3 4 5 6 7 8 9101112131415161718
G  A B C D E F G H J K L M N O P Q R S
H  1 2 3 4 5 6 7 8 9101112
I  0 0 0 0 1 1 1 1 1 1 1 1 1 1 0 0 0 0
I  0 0 0 1 1 1 1 1 1 1 1 1 1 1 1 0 0 0
I  0 0 1 1 1 1 1 1 1 1 1 1 1 1 1 1 0 0
I  0 1 1 1 1 1 1 1 1 1 1 1 1 1 1 1 1 0
I  1 1 1 1 1 1 1 1 1 1 1 1 1 1 1 1 1 1
I  1 1 1 1 1 1 1 1 1 1 1 1 1 1 1 1 1 1
I  1 1 1 1 1 1 1 1 1 1 1 1 1 1 1 1 1 1
I  1 1 1 1 1 1 1 1 1 1 1 1 1 1 1 1 1 1
I  1 1 1 1 1 1 1 1 1 1 1 1 1 1 1 1 1 1
I  1 1 1 1 1 1 1 1 1 1 1 1 1 1 1 1 1 1
I  1 1 1 1 1 1 1 1 1 1 1 1 1 1 1 1 1 1
I  1 1 1 1 1 1 1 1 1 1 1 1 1 1 1 1 1 1
I  1 1 1 1 1 1 1 1 1 1 1 1 1 1 1 1 1 1
I  1 1 1 1 1 1 1 1 1 1 1 1 1 1 1 1 1 1
I  0 1 1 1 1 1 1 1 1 1 1 1 1 1 1 1 1 0
I  0 0 1 1 1 1 1 1 1 1 1 1 1 1 1 1 0 0
I  0 0 0 1 1 1 1 1 1 1 1 1 1 1 1 0 0 0
I  0 0 0 0 1 1 1 1 1 1 1 1 1 1 0 0 0 0
$-------------------------------------------------------------------
$  define burnup regions for time-average calculations
$-------------------------------------------------------------------
J           C 3  D 3 CORNER     P 3  Q 3 CORNER
J           C16  D16 CORNER     P16  Q16 CORNER
$-------------------------------------------------------------------
$  define data for notch array and mesh spacing
```

```
$-----------------------------------------------------------------
M            260.00     260.000   260.00
$ mesh spacing (cm) - X direction
X             9.000  249
X            11.000  447
$ mesh spacing (cm) - Y direction
Y             9.000  249
Y            11.000  447
$ mesh spacing (cm) - Z direction
Z            24.765  225
*PRINT    REGIONS
*PRINT    DIMENSIONS
*PRINT    MESH SPACE
$-----------------------------------------------------------------
$  read in WIMS-based 2-group incremental cross sections
$  to be added to the mesh volumes for reactivity devices
$-----------------------------------------------------------------
*DATA     2-GROUP
$
$ zone controller :  revised XS for a total worth of 9 mk; thickness=1.34
$ ( property name: ZCR01A)
$ ( device name  : ZCR***)
MODEL     MOVEPROPS2          ZCR01A    ZCR01A
2GTR1  5.2388459E-03
2GTR2  5.5274665E-03
2GSA1  8.8870525E-05
2GSA2  1.9517243E-03
2GS12 -1.3297889E-04
2GS21  2.9888324E-05
2GNF1 -4.5860652E-06
2GNF2  4.9045403E-04
2GF    1.2458622E-02
2GH1  -1.2910637E-04
2GH2   1.4412985E-02
$
$ zone controller guide tube
$ ( property name: ZCRGT01A)
$ ( device name  : ZCRGT***)
MODEL     MOVEPROPS2          ZCRGT01   ZCRGT01
2GTR1  1.0262430E-04
2GTR2 -8.7827444E-04
2GSA1  1.1026859E-05
2GSA2  5.0425529E-05
2GS12 -5.0528906E-05
2GS21  1.1664088E-06
```

```
2GNF1 -1.7260900E-06
2GNF2  2.4325214E-05
2GF    6.4146519E-04
2GH1  -4.9493698E-05
2GH2   7.1454793E-04
$
$ Shutoff rod & control absorbers
$ ( property name: SOR)
$ ( device name  : SOR**)
$ ( device name  : CAR**)
MODEL     MOVEPROPS2          SOR
2GTR1  2.2888333E-03
2GTR2  7.9998076E-03
2GSA1  5.2061680E-04
2GSA2  2.0300030E-02
2GS12 -2.1139067E-04
2GS21  9.9993384E-05
2GNF1 -6.8685040E-06
2GNF2  2.1973327E-09
2GF    5.0170124E-02
2GH1  -1.8886664E-04
2GH2   6.4747274E-02
$
$ Shutoff rods & control absorbers guide tube
$ ( property name: SRGT1)
$ ( device name  : SRGT**,SRGT**,
$                : CRGT**,CRGT**)
MODEL     MOVEPROPS2          SRGT1
2GTR1  1.0173023E-04
2GTR2 -8.7037683E-04
2GSA1  1.0877848E-05
2GSA2  4.9948692E-05
2GS12 -5.0115399E-05
2GS21  1.1548691E-06
2GNF1 -1.7117709E-06
2GNF2  2.4086796E-05
2GF    6.3544512E-04
2GH1  -4.9087561E-05
2GH2   7.0756971E-04
$-------------------------------------------------------------------
$  define movable devices
$-------------------------------------------------------------------
$ Zone controllers
MODEL     MOVE DEVS2          ZCR01A    ZCR01A   5
A           139.0000  161.0000  018.5000  260.0000  123.825   173.355
```

```
MODEL     MOVE DEVS2          ZCR01A    ZCR01B   8
A           139.0000  161.0000  260.0000  501.5000  123.825   173.355
MODEL     MOVE DEVS2          ZCR01A    ZCR04A   5
A           139.0000  161.0000  018.5000  260.0000  272.415   321.945
MODEL     MOVE DEVS2          ZCR01A    ZCR04B   8
A           139.0000  161.0000  260.0000  501.5000  272.415   321.945
MODEL     MOVE DEVS2          ZCR01A    ZCR07A   5
A           139.0000  161.0000  018.5000  260.0000  421.005   470.535
MODEL     MOVE DEVS2          ZCR01A    ZCR07B   8
A           139.0000  161.0000  260.0000  501.5000  421.005   470.535
MODEL     MOVE DEVS2          ZCR01A    ZCR02A   5
A           249.0000  271.0000  018.5000  260.0000  123.825   173.355
MODEL     MOVE DEVS2          ZCR01A    ZCR02B   8
A           249.0000  271.0000  260.0000  501.5000  123.825   173.355
MODEL     MOVE DEVS2          ZCR01A    ZCR05A   5
A           249.0000  271.0000  018.5000  260.0000  272.415   321.945
MODEL     MOVE DEVS2          ZCR01A    ZCR05B   8
A           249.0000  271.0000  260.0000  501.5000  272.415   321.945
MODEL     MOVE DEVS2          ZCR01A    ZCR08A   5
A           249.0000  271.0000  018.5000  260.0000  421.005   470.535
MODEL     MOVE DEVS2          ZCR01A    ZCR08B   8
A           249.0000  271.0000  260.0000  501.5000  421.005   470.535
MODEL     MOVE DEVS2          ZCR01A    ZCR03A   5
A           359.0000  381.0000  018.5000  260.0000  123.825   173.355
MODEL     MOVE DEVS2          ZCR01A    ZCR03B   8
A           359.0000  381.0000  260.0000  501.5000  123.825   173.355
MODEL     MOVE DEVS2          ZCR01A    ZCR06A   5
A           359.0000  381.0000  018.5000  260.0000  272.415   321.945
MODEL     MOVE DEVS2          ZCR01A    ZCR06B   8
A           359.0000  381.0000  260.0000  501.5000  272.415   321.945
MODEL     MOVE DEVS2          ZCR01A    ZCR09A   5
A           359.0000  381.0000  018.5000  260.0000  421.005   470.535
MODEL     MOVE DEVS2          ZCR01A    ZCR09B   8
A           359.0000  381.0000  260.0000  501.5000  421.005   470.535
$
$ Zone-controller guide tubes
MODEL     MOVE DEVS2          ZCRGT01   ZCRGT01
A           139.0000  161.0000    0.0000  520.0000  123.825   173.355
MODEL     MOVE DEVS2          ZCRGT01   ZCRGT04
A           139.0000  161.0000    0.0000  520.0000  272.415   321.945
MODEL     MOVE DEVS2          ZCRGT01   ZCRGT07
A           139.0000  161.0000    0.0000  520.0000  421.005   470.535
MODEL     MOVE DEVS2          ZCRGT01   ZCRGT02
A           249.0000  271.0000    0.0000  520.0000  123.825   173.355
MODEL     MOVE DEVS2          ZCRGT01   ZCRGT05
```

```
A          249.0000  271.0000    0.0000  520.0000  272.415   321.945
MODEL     MOVE DEVS2          ZCRGT01   ZCRGT08
A          249.0000  271.0000    0.0000  520.0000  421.005   470.535
MODEL     MOVE DEVS2          ZCRGT01   ZCRGT03
A          359.0000  381.0000    0.0000  520.0000  123.825   173.355
MODEL     MOVE DEVS2          ZCRGT01   ZCRGT06
A          359.0000  381.0000    0.0000  520.0000  272.415   321.945
MODEL     MOVE DEVS2          ZCRGT01   ZCRGT09
A          359.0000  381.0000    0.0000  520.0000  421.005   470.535
$
$ Shutoff rods
$ (Short type = 451 cm SOR01, SOR05, SOR06, SOR010, SOR11, SOR15, SOR16, SOR20)
$ (Long type  = 493 cm SOR02, SOR03, SOR04, SOR07, SOR08, SOR09,
$                      SOR12, SOR13, SOR14, SOR17, SOR18, SOR19)
$  Travelling distance = & 485.5 cm (S) & 506.5 cm (L)
$-------------------------------------------------
MODEL     MOVE DEVS2          SOR       SOR01    2
A          117.0000  139.0000 -451.0000    0.00     49.530    99.060
MODEL     MOVE DEVS2          SOR       SOR06    2
A          117.0000  139.0000 -451.0000    0.00    198.120   247.650
MODEL     MOVE DEVS2          SOR       SOR11    2
A          117.0000  139.0000 -451.0000    0.00    346.710   396.240
MODEL     MOVE DEVS2          SOR       SOR16    2
A          117.0000  139.0000 -451.0000    0.00    495.300   544.830
MODEL     MOVE DEVS2          SOR       SOR05    2
A          381.0000  403.0000 -451.0000    0.00     49.530    99.060
MODEL     MOVE DEVS2          SOR       SOR10    2
A          381.0000  403.0000 -451.0000    0.00    198.120   247.650
MODEL     MOVE DEVS2          SOR       SOR15    2
A          381.0000  403.0000 -451.0000    0.00    346.710   396.240
MODEL     MOVE DEVS2          SOR       SOR20    2
A          381.0000  403.0000 -451.0000    0.00    495.300   544.830
$
MODEL     MOVE DEVS2          SOR       SOR02    2
A          183.0000  205.0000 -493.0000    0.0      49.530    99.060
MODEL     MOVE DEVS2          SOR       SOR07    2
A          183.0000  205.0000 -493.0000    0.0     198.120   247.650
MODEL     MOVE DEVS2          SOR       SOR12    2
A          183.0000  205.0000 -493.0000    0.0     346.710   396.240
MODEL     MOVE DEVS2          SOR       SOR17    2
A          183.0000  205.0000 -493.0000    0.0     495.300   544.830
MODEL     MOVE DEVS2          SOR       SOR03    2
A          249.0000  271.0000 -493.0000    0.0      49.530    99.060
MODEL     MOVE DEVS2          SOR       SOR08    2
A          249.0000  271.0000 -493.0000    0.0     198.120   247.650
```

```
MODEL     MOVE DEVS2          SOR       SOR13    2
A           249.0000  271.0000 -493.0000    0.0     346.710   396.240
MODEL     MOVE DEVS2          SOR       SOR18    2
A           249.0000  271.0000 -493.0000    0.0     495.300   544.830
MODEL     MOVE DEVS2          SOR       SOR04    2
A           315.0000  337.0000 -493.0000    0.0      49.530    99.060
MODEL     MOVE DEVS2          SOR       SOR09    2
A           315.0000  337.0000 -493.0000    0.0     198.120   247.650
MODEL     MOVE DEVS2          SOR       SOR14    2
A           315.0000  337.0000 -493.0000    0.0     346.710   396.240
MODEL     MOVE DEVS2          SOR       SOR19    2
A           315.0000  337.0000 -493.0000    0.0     495.300   544.830
$
$ SOR guide tubes
$-------------------------------------------------
MODEL     MOVE DEVS2          SRGT1     SRGT01   2
A           117.0000  139.0000   0.0000   506.5000   49.530    99.060
MODEL     MOVE DEVS2          SRGT1     SRGT06   2
A           117.0000  139.0000   0.0000   506.5000  198.120   247.650
MODEL     MOVE DEVS2          SRGT1     SRGT11   2
A           117.0000  139.0000   0.0000   506.5000  346.710   396.240
MODEL     MOVE DEVS2          SRGT1     SRGT16   2
A           117.0000  139.0000   0.0000   506.5000  495.300   544.830
MODEL     MOVE DEVS2          SRGT1     SRGT05   2
A           381.0000  403.0000   0.0000   506.5000   49.530    99.060
MODEL     MOVE DEVS2          SRGT1     SRGT10   2
A           381.0000  403.0000   0.0000   506.5000  198.120   247.650
MODEL     MOVE DEVS2          SRGT1     SRGT15   2
A           381.0000  403.0000   0.0000   506.5000  346.710   396.240
MODEL     MOVE DEVS2          SRGT1     SRGT20   2
A           381.0000  403.0000   0.0000   506.5000  495.300   544.830
$
MODEL     MOVE DEVS2          SRGT1     SRGT02   2
A           183.0000  205.0000   0.0000   520.0000   49.530    99.060
MODEL     MOVE DEVS2          SRGT1     SRGT07   2
A           183.0000  205.0000   0.0000   520.0000  198.120   247.650
MODEL     MOVE DEVS2          SRGT1     SRGT12   2
A           183.0000  205.0000   0.0000   520.0000  346.710   396.240
MODEL     MOVE DEVS2          SRGT1     SRGT17   2
A           183.0000  205.0000   0.0000   520.0000  495.300   544.830
MODEL     MOVE DEVS2          SRGT1     SRGT03   2
A           249.0000  271.0000   0.0000   520.0000   49.530    99.060
MODEL     MOVE DEVS2          SRGT1     SRGT08   2
A           249.0000  271.0000   0.0000   520.0000  198.120   247.650
MODEL     MOVE DEVS2          SRGT1     SRGT13   2
```

```
A          249.0000  271.0000   0.0000   520.0000  346.710   396.240
MODEL     MOVE DEVS2          SRGT1     SRGT18   2
A          249.0000  271.0000   0.0000   520.0000  495.300   544.830
MODEL     MOVE DEVS2          SRGT1     SRGT04   2
A          315.0000  337.0000   0.0000   520.0000   49.530    99.060
MODEL     MOVE DEVS2          SRGT1     SRGT09   2
A          315.0000  337.0000   0.0000   520.0000  198.120   247.650
MODEL     MOVE DEVS2          SRGT1     SRGT14   2
A          315.0000  337.0000   0.0000   520.0000  346.710   396.240
MODEL     MOVE DEVS2          SRGT1     SRGT19   2
A          315.0000  337.0000   0.0000   520.0000  495.300   544.830
$
$ Mechanical control absorber rods
$-----------------------------------------------
MODEL     MOVE DEVS2          SOR       CAR01    2
A          183.0000  205.0000 -493.0000    0.0     123.825   173.355
MODEL     MOVE DEVS2          SOR       CAR02    2
A          315.0000  337.0000 -493.0000    0.0     123.825   173.355
MODEL     MOVE DEVS2          SOR       CAR03    2
A          183.0000  205.0000 -493.0000    0.0     421.005   470.535
MODEL     MOVE DEVS2          SOR       CAR04    2
A          315.0000  337.0000 -493.0000    0.0     421.005   470.535
$
$ Control absorber guide tubes
$-----------------------------------------------
MODEL     MOVE DEVS2          SRGT1     CRGT01   2
A          183.0000  205.0000    0.0000  520.0000  123.825   173.355
MODEL     MOVE DEVS2          SRGT1     CRGT02   2
A          315.0000  337.0000    0.0000  520.0000  123.825   173.355
MODEL     MOVE DEVS2          SRGT1     CRGT03   2
A          183.0000  205.0000    0.0000  520.0000  421.005   470.535
MODEL     MOVE DEVS2          SRGT1     CRGT04   2
A          315.0000  337.0000    0.0000  520.0000  421.005   470.535
$
$-----------------------------------------------------------------
$  read in 2-group fuel properties for CANFLEX type SEU20DY46
$-----------------------------------------------------------------
*READ CARD
BLOCK     LATPROPS2GFUEL46SC
FORMAT    (-A10)
READ      fuel46sc          1         1
FORMAT    (2I10)
READ      fuel46sc          3         4
FORMAT    (6E20.11)
READ      fuel46sc          5      1952
```

```
BLOCK     XENONPROP2FUEL46SC
FORMAT    (-A10)
READ      fuel46sc          1         1
FORMAT    (2I10)
READ      fuel46sc          3         4
FORMAT    (6E20.11)
READ      fuel46sc          5       536
BLOCK     LATPROPS2GFUEL46SV
FORMAT    (-A10)
READ      fuel46sv          1         1
FORMAT    (2I10)
READ      fuel46sv          3         4
FORMAT    (6E20.11)
READ      fuel46sv          5      1952
$
BLOCK     LATPROPS2GSEU2DY46SC
FORMAT    (-A10)
READ      seu2dy46sc        1         1
FORMAT    (2I10)
READ      seu2dy46sc        3         4
FORMAT    (6E20.11)
READ      seu2dy46sc        5      1952
BLOCK     XENONPROP2SEU2DY46SC
FORMAT    (-A10)
READ      seu2dy46sc        1         1
FORMAT    (2I10)
READ      seu2dy46sc        3         4
FORMAT    (6E20.11)
READ      seu2dy46sc        5       536
$-----------------------------------------------------------------
$  read in 2-group reflector properties
$-----------------------------------------------------------------
*READ CARD
BLOCK     LATPROPS2GREFLECTOR
FORMAT    (2I10)
READ      ngrefl2o          1         2
FORMAT    (6E20.11)
READ      ngrefl2o          3        13
$
$-----------------------------------------------------------------
$  define core loading
$-----------------------------------------------------------------
*DATA     GEOMETRY
K                   FUEL46SC
L                   20011015  1
```

```
$
*PRINT    LATPROPS2G
*PRINT    DEVPROPS2G
$---------------------------------------------------------------------
$  set up a bi-directional 2 bundle-shift fuelling scheme
$---------------------------------------------------------------------
*DATA     IRRADIATON
C          A  5        +2
$
$---------------------------------------------------------------------
$  define time-average exit irradiations by burnup region (n/kb)
$---------------------------------------------------------------------
*DATA     IRRADIATON
B         REG1T              2
B         REG1B              2
B         REG2T0             2
B         REG2B0             2
B         REG2T              2
B         REG2B              2
B         REG3T              2
B         REG3B              2
B         REG3T0             2
B         REG3B0             2
B         REG4T              2
B         REG4B              2
B         REG4T1             2
B         REG4B1             2
B         REG4T0             2
B         REG4B0             2
B         REG5T              2
B         REG5B              2
B         REG5T0             2
B         REG5B0             2
B         REG6T              2
B         REG6B              2
B         CORNER             2
A         CORNER         2.365
A         REG1T          2.291
A         REG1B          2.291
A         REG2T0         3.007
A         REG2B0         3.007
A         REG2T          3.575
A         REG2B          3.575
A         REG3T          4.057
A         REG3B          4.057
```

```
A          REG3T0         4.200
A          REG3B0         4.200
A          REG4T          4.057
A          REG4B          4.057
A          REG4T1         4.248
A          REG4B1         4.248
A          REG4T0         4.176
A          REG4B0         4.176
A          REG5T          4.367
A          REG5B          4.367
A          REG5T0         4.345
A          REG5B0         4.345
A          REG6T          4.399
A          REG6B          4.399
$-------------------------------------------------------------------
$  time-average flux and power distribution with uniform xenon distribution
$-------------------------------------------------------------------
*DATA      FLUX/POWER
A    2  10 1982000.0    0.9460  0.00001   1.10       1.0       .05       0  00 500
B          1.0
*TIME-AVER  .0001      15        0.80
2-GROUP
E    2  10 1982000.0    0.9460  0.00001   1.10       1.0       .05       0  00 300
$ Nominal core configuration : zone controllers inserted at 50%
C          ZCR***        0.500
$
*SUMMARY
2-GROUP
*PRINT     POWERS
$
$-------------------------------------------------------------------
$  time-average flux and power distribution with distributed xenon
$-------------------------------------------------------------------
*TIME-AVER  .0001      15        0.80
2-GROUP
S              0.29239E-04    0.21158E-04    1.81755E-18
XE                  1  0.0     1.0       1.0        0.0001           12
E    2  10 1982000.0    0.9460  0.00001   1.30       1.0       .05       0  00 300
$ Nominal core configuration : all zone controllers inserted at 50%
C          ZCR***        0.500
$
*SUMMARY
2-GROUP
*PRINT     POWERS
*PRINT     CELL PHI
```

```
*PRINT    SLOW FLUX
$-----------------------------------------------------------------
$ write out CP/BP data from the direct-access file
$-----------------------------------------------------------------
*RITE TAPE284-73-tax
TITLE     ACR-700 284-CHANNELS CANFLEX SEU20DY46S 2G RFSP TIME-AVERAGE WITH
DISTRIBUTED XENON, 7.3MW MAX CHANNEL POWER
$
*RITE CARD
FORMAT    (F10.4)
BLOCK     FLUX/POWERPOWERS    CHANNEL
W         284-73-cp           1       284
*RITE CARD
FORMAT    (12F10.4)
BLOCK     FLUX/POWERPOWERS    BUNDLE
W         284-73-bp           1      3408
*PRINT    CHN BURNUP
*RITE CARD
FORMAT    (F6.4)
BLOCK     IRRADIATONCHN BURNUP
W         284-73-cb           1       284
*PRINT    EXIT IRRAD
*RITE CARD
FORMAT    (F6.4)
BLOCK     IRRADIATONEXIT IRRAD
W         284-73-w            1       284
*PRINT    TIMAVEXITW
*RITE CARD
FORMAT    (F6.4)
BLOCK     IRRADIATONTIMAVEXITW
W         284-73-tw           1       284
*PRINT    DWELL TIME
*RITE CARD
FORMAT    (F7.5)
BLOCK     IRRADIATONDWELL TIME
W         284-73-dt           1       284
$
*DELETE   SIMULDATA
*STORE
FROM      GEOMETRY  SERIAL NUM
TO        SIMULDATA TIMAV              0         0SERIAL NUM
*STORE
FROM      GEOMETRY  FUEL TYPES
TO        SIMULDATA TIMAV              0         0FUEL TYPES
*STORE
FROM      FLUX/POWERSLOW FLUX CELL PHI
```

```
TO        SIMULDATA TIMAV              0          0CELL PHI
*STORE
FROM      IRRADIATONDELTA RHO
TO        SIMULDATA TIMAV              0          0DELTA RHO
*STORE
FROM      IRRADIATONCHN BURNUP
TO        SIMULDATA TIMAV              0          0CHN BURNUP
*STORE
FROM      FLUX/POWERPOWERS    CHANNEL
TO        SIMULDATA TIMAV              0          0CHANNEL
*STORE
FROM      FLUX/POWERPOWERS    BUNDLE
TO        SIMULDATA TIMAV              0          0BUNDLE
*STORE
FROM      PHYS PARMS2GFFACTOR
TO        SIMULDATA TIMAV              0          02GFFACTOR
*STORE
FROM      PHYS PARMS2GH1FACTOR
TO        SIMULDATA TIMAV              0          02GH1FACTOR
*STORE
FROM      PHYS PARMS2GH2FACTOR
TO        SIMULDATA TIMAV              0          02GH2FACTOR
$
$-------------------------------------------------------------------
$  time-average calculation for the voided core
$-------------------------------------------------------------------
*DATA     GEOMETRY
K                     FUEL46SV
$
*TIME-AVER  .0001      01      0.8                          1
2-GROUP
E    2  10 1982000.0    0.9460  0.00001   1.10       1.0      .05      0  00 300
C         ZCR***       0.500
$
*SUMMARY
2-GROUP
*PRINT    POWERS
*PRINT    CELL PHI
$
*RITE CARD
FORMAT    (F10.4)
BLOCK     FLUX/POWERPOWERS    CHANNEL
W         284-73-cv          1       284
$
*CLOSE    NORMAL TERMINATION
```

Appendix D
Fuel Burnup Distribution in ACR-700

	1	2	3	4	5	6	7	8	9	10	11	12	13	14	15	16	17	18
A					1.0	16.0	1.0	16.0	1.0	16.1	0.9	16.0	0.9	15.9				
B				1.1	16.3	1.0	16.3	1.0	17.2	1.1	17.1	0.9	16.3	0.9	15.9			
C			0.9	17.1	1.1	21.2	1.6	23.8	1.6	23.9	1.5	23.8	1.3	17.2	0.9	14.4		
D		0.9	17.1	1.1	21.2	1.6	23.8	1.6	23.8	1.6	23.8	1.5	23.8	1.3	17.2	0.9	14.4	
E	0.9	14.8	1.4	21.2	1.6	23.8	1.6	23.8	1.6	23.8	1.5	23.8	1.5	23.8	1.2	21.2	0.7	14.4
F	14.5	1.0	21.2	1.6	23.8	1.6	23.8	1.6	24.4	1.6	24.4	1.5	23.8	1.5	23.8	1.2	17.1	0.7
G	0.8	17.1	1.5	23.8	1.6	23.8	1.6	24.4	1.6	24.4	1.6	24.4	1.5	23.8	1.5	23.8	0.9	14.5
H	20.5	1.3	23.8	1.5	23.8	1.6	24.4	1.6	24.4	1.6	24.4	1.6	24.4	1.5	23.8	1.4	20.9	1.2
J	1.2	20.9	1.5	23.8	1.5	24.4	1.6	24.4	1.6	24.4	1.6	24.4	1.6	23.8	1.5	23.8	1.2	20.5
K	20.5	1.2	23.8	1.5	23.8	1.6	24.4	1.6	24.4	1.6	24.4	1.6	24.4	1.5	23.8	1.5	20.9	1.2
L	1.2	20.9	1.4	23.8	1.5	24.4	1.6	24.4	1.6	24.4	1.6	24.4	1.6	23.8	1.5	23.8	1.3	20.5
M	14.5	0.9	23.8	1.5	23.8	1.5	24.4	1.6	24.4	1.6	24.4	1.6	23.8	1.6	23.8	1.5	17.1	0.8
N	0.7	17.1	1.2	23.8	1.5	23.8	1.5	24.4	1.6	24.4	1.6	23.8	1.6	23.8	1.6	21.2	1.0	14.5
O	14.4	0.7	21.2	1.2	23.8	1.5	23.8	1.5	23.8	1.6	23.8	1.6	23.8	1.6	21.2	1.4	14.8	0.9
P		14.4	0.9	17.2	1.3	23.8	1.5	23.8	1.6	23.8	1.6	23.8	1.6	21.2	1.1	17.1	0.9	
Q			14.4	0.9	17.2	1.3	23.8	1.5	23.9	1.6	23.8	1.6	21.2	1.1	17.1	0.9		
R				15.9	0.9	16.3	0.9	17.1	1.1	17.2	1.0	16.3	1.0	16.3	1.1			
S					15.9	0.9	16.0	0.9	16.1	1.0	16.0	1.0	16.0	1.0				

Figure D-1 Fuel Burnup (MWd/kgU) Distribution in Bundle Position 1
(ACR-700 284-Channel TAVEQUIV Model – 2-BS Fuelling Scheme)

	1	2	3	4	5	6	7	8	9	10	11	12	13	14	15	16	17	18
A					2.6	16.0	2.4	16.0	2.4	16.1	2.3	16.0	2.2	15.9				
B				2.6	16.3	2.5	16.3	2.6	17.2	2.6	17.1	2.3	16.3	2.2	15.9			
C			2.3	17.1	2.7	21.2	3.8	23.8	3.9	23.9	3.7	23.8	3.1	17.2	2.3	14.4		
D		2.2	17.1	2.7	21.2	3.9	23.8	3.8	23.8	3.8	23.8	3.6	23.8	3.1	17.2	2.2	14.4	
E	2.2	14.8	3.4	21.2	3.9	23.8	3.8	23.8	3.8	23.8	3.7	23.8	3.6	23.8	3.0	21.2	1.9	14.4
F	14.5	2.6	21.2	3.9	23.8	3.8	23.8	4.0	24.4	3.9	24.4	3.7	23.8	3.6	23.8	3.0	17.1	1.9
G	2.1	17.1	3.8	23.8	3.8	23.8	4.0	24.4	3.9	24.4	3.9	24.4	3.7	23.8	3.6	23.8	2.4	14.5
H	20.5	3.2	23.8	3.8	23.8	3.9	24.4	4.0	24.4	3.9	24.4	3.9	24.4	3.7	23.8	3.6	20.9	3.0
J	3.0	20.9	3.7	23.8	3.8	24.4	3.9	24.4	4.0	24.4	3.9	24.4	3.9	23.8	3.7	23.8	3.1	20.5
K	20.5	3.1	23.8	3.7	23.8	3.9	24.4	3.9	24.4	4.0	24.4	3.9	24.4	3.8	23.8	3.7	20.9	3.0
L	3.0	20.9	3.6	23.8	3.7	24.4	3.9	24.4	3.9	24.4	4.0	24.4	3.9	23.8	3.8	23.8	3.2	20.5
M	14.5	2.4	23.8	3.6	23.8	3.7	24.4	3.9	24.4	3.9	24.4	4.0	23.8	3.8	23.8	3.8	17.1	2.1
N	1.9	17.1	3.0	23.8	3.6	23.8	3.7	24.4	3.9	24.4	4.0	23.8	3.8	23.8	3.9	21.2	2.6	14.5
O	14.4	1.9	21.2	3.0	23.8	3.6	23.8	3.7	23.8	3.8	23.8	3.8	23.8	3.9	21.2	3.4	14.8	2.2
P		14.4	2.2	17.2	3.1	23.8	3.6	23.8	3.8	23.8	3.8	23.8	3.9	21.2	2.7	17.1	2.2	
Q			14.4	2.3	17.2	3.1	23.8	3.7	23.9	3.9	23.8	3.8	21.2	2.7	17.1	2.3		
R				15.9	2.2	16.3	2.3	17.1	2.6	17.2	2.6	16.3	2.5	16.3	2.6			
S					15.9	2.2	16.0	2.3	16.1	2.4	16.0	2.4	16.0	2.6				

Figure D-2 Fuel Burnup (MWd/kgU) Distribution in Bundle Position 2 (ACR-700 284-Channel TAVEQUIV Model — 2-BS Fuelling Scheme)

	1	2	3	4	5	6	7	8	9	10	11	12	13	14	15	16	17	18
A					4.2	15.3	4.1	15.3	4.0	15.3	3.9	15.3	3.8	15.2				
B				4.3	15.5	4.3	15.6	4.4	16.4	4.3	16.4	4.0	15.6	3.8	15.3			
C			3.9	16.3	4.5	20.2	6.6	22.7	6.4	22.8	6.3	22.8	5.4	16.5	3.9	13.8		
D		3.9	16.3	4.6	20.2	6.7	22.7	6.6	22.8	6.5	22.8	6.3	22.8	5.3	16.5	4.0	13.9	
E	3.8	14.1	5.9	20.2	6.7	22.7	6.7	22.7	6.6	22.7	6.5	22.8	6.3	22.8	5.3	20.4	3.4	13.8
F	13.9	4.6	20.2	6.7	22.7	6.7	22.7	6.9	23.3	6.8	23.4	6.5	22.8	6.3	22.8	5.3	16.5	3.4
G	3.7	16.4	6.7	22.7	6.7	22.7	6.9	23.3	6.9	23.3	6.8	23.4	6.5	22.8	6.3	22.8	4.2	13.9
H	19.6	5.6	22.8	6.6	22.7	6.9	23.3	6.9	23.3	6.8	23.3	6.8	23.4	6.5	22.8	6.4	20.1	5.3
J	5.4	20.0	6.5	22.8	6.6	23.4	6.8	23.3	6.9	23.3	6.8	23.4	6.8	22.8	6.5	22.8	5.5	19.6
K	19.6	5.5	22.8	6.5	22.8	6.8	23.4	6.8	23.3	6.9	23.3	6.8	23.4	6.6	22.8	6.5	20.0	5.4
L	5.3	20.1	6.4	22.8	6.5	23.4	6.8	23.3	6.8	23.3	6.9	23.3	6.9	22.7	6.6	22.8	5.6	19.6
M	13.9	4.2	22.8	6.3	22.8	6.5	23.4	6.8	23.3	6.9	23.3	6.9	22.7	6.7	22.8	6.7	16.4	3.7
N	3.4	16.5	5.3	22.8	6.3	22.8	6.5	23.4	6.8	23.3	6.9	22.7	6.7	22.7	6.7	20.2	4.6	13.9
O	13.8	3.4	20.4	5.3	22.8	6.3	22.8	6.5	22.7	6.6	22.7	6.7	22.7	6.7	20.2	5.9	14.1	3.8
P		13.9	4.0	16.5	5.3	22.8	6.3	22.8	6.5	22.8	6.6	22.7	6.7	20.2	4.6	16.3	3.9	
Q			13.8	3.9	16.5	5.4	22.8	6.3	22.8	6.4	22.7	6.6	20.2	4.5	16.3	3.9		
R				15.3	3.8	15.6	4.0	16.4	4.3	16.4	4.4	15.6	4.3	15.5	4.3			
S					15.2	3.8	15.3	3.9	15.3	4.0	15.3	4.1	15.3	4.2				

Figure D-3 Fuel Burnup (MWd/kgU) Distribution in Bundle Position 3
(ACR-700 284-Channel TAVEQUIV Model — 2-BS Fuelling Scheme)

	1	2	3	4	5	6	7	8	9	10	11	12	13	14	15	16	17	18
A					6.1	14.1	6.0	14.2	5.9	14.2	5.7	14.3	5.6	14.2				
B				6.3	14.3	6.2	14.4	6.4	15.2	6.3	15.3	5.8	14.6	5.6	14.3			
C			5.6	15.0	6.6	18.8	9.4	21.2	9.3	21.3	9.1	21.3	7.7	15.4	5.9	13.0		
D		5.6	15.0	6.6	18.7	9.4	21.2	9.3	21.2	9.2	21.2	9.0	21.3	7.7	15.4	5.8	13.0	
E	5.5	13.0	8.4	18.7	9.5	21.1	9.4	21.1	9.3	21.2	9.2	21.3	9.0	21.4	7.7	19.1	5.0	13.0
F	12.8	6.6	18.8	9.5	21.1	9.4	21.1	9.6	21.7	9.5	21.8	9.1	21.3	9.0	21.4	7.7	15.4	5.0
G	5.4	15.2	9.4	21.2	9.4	21.1	9.6	21.7	9.6	21.7	9.5	21.8	9.1	21.3	9.0	21.4	6.1	13.0
H	18.3	8.0	21.2	9.3	21.2	9.6	21.7	9.6	21.7	9.6	21.7	9.5	21.8	9.2	21.3	9.1	18.7	7.6
J	7.7	18.6	9.2	21.2	9.3	21.7	9.6	21.7	9.6	21.7	9.6	21.7	9.5	21.2	9.2	21.3	7.9	18.3
K	18.3	7.9	21.3	9.2	21.2	9.5	21.7	9.6	21.7	9.6	21.7	9.6	21.7	9.3	21.2	9.2	18.6	7.7
L	7.6	18.7	9.1	21.3	9.2	21.8	9.5	21.7	9.6	21.7	9.6	21.7	9.6	21.2	9.3	21.2	8.0	18.3
M	13.0	6.1	21.4	9.0	21.3	9.1	21.8	9.5	21.7	9.6	21.7	9.6	21.1	9.4	21.2	9.4	15.2	5.4
N	5.0	15.4	7.7	21.4	9.0	21.3	9.1	21.8	9.5	21.7	9.6	21.1	9.4	21.1	9.5	18.8	6.6	12.8
O	13.0	5.0	19.1	7.7	21.4	9.0	21.3	9.2	21.2	9.3	21.1	9.4	21.1	9.5	18.7	8.4	13.0	5.5
P		13.0	5.8	15.4	7.7	21.3	9.0	21.2	9.2	21.2	9.3	21.2	9.4	18.7	6.6	15.0	5.6	
Q			13.0	5.9	15.4	7.7	21.3	9.1	21.3	9.3	21.2	9.4	18.8	6.6	15.0	5.6		
R				14.3	5.6	14.6	5.8	15.3	6.3	15.2	6.4	14.4	6.2	14.3	6.3			
S					14.2	5.6	14.3	5.7	14.2	5.9	14.2	6.0	14.1	6.1				

Figure D-4 Fuel Burnup (MWd/kgU) Distribution in Bundle Position 4 (ACR-700 284-Channel TAVEQUIV Model — 2-BS Fuelling Scheme)

	1	2	3	4	5	6	7	8	9	10	11	12	13	14	15	16	17	18
A					8.2	12.7	7.9	12.8	7.9	12.9	7.7	12.9	7.5	13.0				
B				8.3	12.9	8.2	13.0	8.4	13.8	8.4	13.8	7.7	13.2	7.6	13.1			
C			7.4	13.5	8.7	16.9	12.2	19.2	12.2	19.3	11.9	19.4	10.3	14.0	7.9	11.8		
D		7.4	13.4	8.7	16.9	12.3	19.1	12.1	19.2	12.0	19.2	11.8	19.4	10.3	14.0	7.8	11.8	
E	7.3	11.5	10.9	16.8	12.3	19.0	12.1	19.1	12.0	19.1	11.9	19.2	11.8	19.4	10.2	17.3	6.7	11.7
F	11.4	8.6	16.8	12.3	19.0	12.2	19.0	12.4	19.6	12.3	19.6	11.9	19.2	11.7	19.4	10.1	13.9	6.7
G	7.1	13.6	12.2	19.0	12.1	19.0	12.4	19.5	12.4	19.6	12.3	19.7	11.9	19.2	11.8	19.4	8.1	11.7
H	16.5	10.5	19.1	12.1	19.0	12.4	19.5	12.4	19.6	12.3	19.6	12.3	19.7	11.9	19.2	11.8	16.9	10.0
J	10.2	16.8	12.0	19.1	12.0	19.6	12.4	19.6	12.4	19.6	12.3	19.6	12.3	19.1	11.9	19.2	10.3	16.5
K	16.5	10.3	19.2	11.9	19.1	12.3	19.6	12.3	19.6	12.4	19.6	12.4	19.6	12.0	19.1	12.0	16.8	10.2
L	10.0	16.9	11.8	19.2	11.9	19.7	12.3	19.6	12.3	19.6	12.4	19.5	12.4	19.0	12.1	19.1	10.5	16.5
M	11.7	8.1	19.4	11.8	19.2	11.9	19.7	12.3	19.6	12.4	19.5	12.4	19.0	12.1	19.0	12.2	13.6	7.1
N	6.7	13.9	10.1	19.4	11.7	19.2	11.9	19.6	12.3	19.6	12.4	19.0	12.2	19.0	12.3	16.8	8.6	11.4
O	11.7	6.7	17.3	10.2	19.4	11.8	19.2	11.9	19.1	12.0	19.1	12.1	19.0	12.3	16.8	10.9	11.5	7.3
P		11.8	7.8	14.0	10.3	19.4	11.8	19.2	12.0	19.2	12.1	19.1	12.3	16.9	8.7	13.4	7.4	
Q			11.8	7.9	14.0	10.3	19.4	11.9	19.3	12.2	19.2	12.2	16.9	8.7	13.5	7.4		
R				13.1	7.6	13.2	7.7	13.8	8.4	13.8	8.4	13.0	8.2	12.9	8.3			
S					13.0	7.5	12.9	7.7	12.9	7.9	12.8	7.9	12.7	8.2				

Figure D-5 Fuel Burnup (MWd/kgU) Distribution in Bundle Position 5 (ACR-700 284-Channel TAVEQUIV Model — 2-BS Fuelling Scheme)

	1	2	3	4	5	6	7	8	9	10	11	12	13	14	15	16	17	18
A					9.7	11.0	9.6	11.2	9.4	11.3	9.3	11.4	9.2	11.5				
B				9.8	11.1	9.8	11.3	10.2	12.0	10.0	12.1	9.5	11.6	9.2	11.6			
C			8.9	11.7	10.4	14.8	14.7	16.9	14.4	17.1	14.3	17.2	12.4	12.3	9.6	10.5		
D		8.9	11.6	10.5	14.8	14.7	16.8	14.5	16.9	14.4	17.0	14.3	17.2	12.4	12.3	9.6	10.5	
E	8.8	10.0	13.2	14.7	14.7	16.7	14.6	16.8	14.4	16.9	14.3	17.0	14.2	17.2	12.4	15.4	8.3	10.4
F	9.9	10.4	14.7	14.7	16.7	14.6	16.8	14.9	17.3	14.8	17.4	14.3	17.1	14.2	17.2	12.4	12.3	8.3
G	8.7	11.8	14.7	16.8	14.6	16.8	14.9	17.3	14.8	17.3	14.8	17.4	14.3	17.0	14.2	17.2	10.0	10.3
H	14.5	12.7	16.8	14.6	16.8	14.9	17.3	14.9	17.3	14.8	17.3	14.8	17.4	14.3	17.0	14.3	14.9	12.2
J	12.4	14.8	14.5	16.9	14.5	17.3	14.9	17.3	14.8	17.3	14.8	17.4	14.8	16.9	14.4	17.0	12.5	14.6
K	14.6	12.5	17.0	14.4	16.9	14.8	17.4	14.8	17.3	14.8	17.3	14.9	17.3	14.5	16.9	14.5	14.8	12.4
L	12.2	14.9	14.3	17.0	14.3	17.4	14.8	17.3	14.8	17.3	14.9	17.3	14.9	16.8	14.6	16.8	12.7	14.5
M	10.3	10.0	17.2	14.2	17.0	14.3	17.4	14.8	17.3	14.8	17.3	14.9	16.8	14.6	16.8	14.7	11.8	8.7
N	8.3	12.3	12.4	17.2	14.2	17.1	14.3	17.4	14.8	17.3	14.9	16.8	14.6	16.7	14.7	14.7	10.4	9.9
O	10.4	8.3	15.4	12.4	17.2	14.2	17.0	14.3	16.9	14.4	16.8	14.6	16.8	14.7	14.7	13.2	10.0	8.8
P		10.5	9.6	12.3	12.4	17.2	14.3	17.0	14.4	16.9	14.5	16.8	14.7	14.8	10.5	11.6	8.9	
Q			10.5	9.6	12.3	12.4	17.2	14.3	17.1	14.4	16.9	14.6	14.8	10.4	11.7	8.9		
R				11.6	9.2	11.6	9.5	12.1	10.0	12.0	10.2	11.3	9.8	11.1	9.8			
S					11.5	9.2	11.4	9.3	11.3	9.4	11.2	9.6	11.0	9.7				

Figure D-6 Fuel Burnup (MWd/kgU) Distribution in Bundle Position 6
(ACR-700 284-Channel TAVEQUIV Model — 2-BS Fuelling Scheme)

	1	2	3	4	5	6	7	8	9	10	11	12	13	14	15	16	17	18
A					11.5	9.2	11.4	9.3	11.3	9.4	11.2	9.6	11.0	9.7				
B				11.6	9.2	11.6	9.5	12.1	10.0	12.0	10.2	11.3	9.8	11.1	9.8			
C			10.5	9.6	12.3	12.4	17.2	14.3	17.1	14.4	16.9	14.6	14.8	10.4	11.7	8.9		
D		10.5	9.6	12.3	12.4	17.2	14.3	17.0	14.4	16.9	14.5	16.8	14.7	14.8	10.5	11.6	8.9	
E	10.4	8.3	15.4	12.4	17.2	14.2	17.0	14.3	16.9	14.4	16.8	14.6	16.8	14.7	14.7	13.2	10.0	8.8
F	8.3	12.3	12.4	17.2	14.2	17.1	14.3	17.4	14.8	17.3	14.9	16.8	14.6	16.7	14.7	14.7	10.4	9.9
G	10.3	10.0	17.2	14.2	17.0	14.3	17.4	14.8	17.3	14.8	17.3	14.9	16.8	14.6	16.8	14.7	11.8	8.7
H	12.2	14.9	14.3	17.0	14.3	17.4	14.8	17.4	14.8	17.3	14.9	17.3	14.9	16.8	14.6	16.8	12.7	14.5
J	14.6	12.5	17.0	14.4	16.9	14.8	17.4	14.8	17.3	14.8	17.3	14.9	17.3	14.5	16.9	14.5	14.8	12.4
K	12.4	14.8	14.5	16.9	14.5	17.3	14.9	17.3	14.8	17.3	14.8	17.4	14.8	16.9	14.4	17.0	12.5	14.6
L	14.5	12.7	16.8	14.6	16.8	14.9	17.3	14.9	17.3	14.8	17.3	14.8	17.4	14.3	17.0	14.3	14.9	12.2
M	8.7	11.8	14.7	16.8	14.6	16.8	14.9	17.3	14.8	17.3	14.8	17.4	14.3	17.0	14.2	17.2	10.0	10.3
N	9.9	10.4	14.7	14.7	16.7	14.6	16.8	14.9	17.3	14.8	17.4	14.3	17.1	14.2	17.2	12.4	12.3	8.3
O	8.8	10.0	13.2	14.7	14.7	16.8	14.6	16.8	14.4	16.9	14.3	17.0	14.2	17.2	12.4	15.4	8.3	10.4
P		8.9	11.6	10.5	14.8	14.7	16.8	14.5	16.9	14.4	17.0	14.3	17.2	12.4	12.3	9.6	10.5	
Q			8.9	11.7	10.4	14.8	14.6	16.9	14.4	17.1	14.3	17.2	12.4	12.3	9.6	10.5		
R				9.8	11.1	9.8	11.3	10.2	12.0	10.0	12.1	9.5	11.6	9.2	11.6			
S					9.7	11.0	9.6	11.2	9.4	11.3	9.3	11.4	9.2	11.5				

Figure D-7 Fuel Burnup (MWd/kgU) Distribution in Bundle Position 7 (ACR-700 284-Channel TAVEQUIV Model — 2-BS Fuelling Scheme)

	1	2	3	4	5	6	7	8	9	10	11	12	13	14	15	16	17	18
A					13.0	7.5	12.9	7.7	12.9	7.9	12.8	7.9	12.7	8.2				
B				13.1	7.6	13.2	7.7	13.8	8.4	13.8	8.4	13.0	8.2	12.9	8.3			
C			11.8	7.9	14.0	10.3	19.4	11.9	19.3	12.2	19.2	12.2	16.9	8.7	13.5	7.4		
D		11.8	7.8	14.0	10.2	19.4	11.8	19.2	12.0	19.2	12.1	19.1	12.3	16.9	8.7	13.4	7.4	
E	11.7	6.7	17.3	10.2	19.4	11.8	19.2	11.9	19.1	12.0	19.1	12.1	19.0	12.3	16.8	10.9	11.5	7.3
F	6.7	13.9	10.1	19.4	11.7	19.2	11.9	19.6	12.3	19.6	12.4	19.0	12.2	19.0	12.3	16.8	8.6	11.4
G	11.7	8.1	19.4	11.7	19.2	11.9	19.7	12.3	19.6	12.4	19.5	12.4	19.0	12.1	19.0	12.2	13.6	7.1
H	10.0	16.9	11.8	19.2	11.9	19.7	12.3	19.6	12.3	19.6	12.4	19.5	12.4	19.0	12.1	19.1	10.5	16.5
J	16.5	10.3	19.2	11.9	19.1	12.3	19.6	12.3	19.6	12.4	19.6	12.4	19.6	12.0	19.1	12.0	16.8	10.2
K	10.2	16.8	12.0	19.1	12.0	19.6	12.4	19.6	12.4	19.6	12.3	19.6	12.3	19.1	11.9	19.2	10.3	16.5
L	16.5	10.5	19.1	12.1	19.0	12.4	19.5	12.4	19.6	12.3	19.6	12.3	19.7	11.9	19.2	11.8	16.9	10.0
M	7.1	13.6	12.2	19.0	12.1	19.0	12.4	19.5	12.4	19.6	12.3	19.7	11.9	19.2	11.8	19.4	8.1	11.7
N	11.4	8.6	16.8	12.3	19.0	12.2	19.0	12.4	19.6	12.3	19.6	11.9	19.2	11.7	19.4	10.1	13.9	6.7
O	7.3	11.5	10.9	16.8	12.3	19.0	12.1	19.1	12.0	19.1	11.9	19.2	11.8	19.4	10.2	17.3	6.7	11.7
P		7.4	13.4	8.7	16.9	12.3	19.1	12.1	19.2	12.0	19.2	11.8	19.4	10.3	14.0	7.8	11.8	
Q			7.4	13.5	8.7	16.9	12.2	19.2	12.2	19.3	11.9	19.4	10.3	14.0	7.9	11.8		
R				8.3	12.9	8.2	13.0	8.4	13.8	8.4	13.8	7.7	13.2	7.6	13.1			
S					8.2	12.7	7.9	12.8	7.9	12.9	7.7	12.9	7.5	13.0				

Figure D-8 Fuel Burnup (MWd/kgU) Distribution in Bundle Position 8 (ACR-700 284-Channel TAVEQUIV Model — 2-BS Fuelling Scheme)

	1	2	3	4	5	6	7	8	9	10	11	12	13	14	15	16	17	18
A					14.2	5.6	14.3	5.7	14.2	5.9	14.2	6.0	14.1	6.1				
B				14.3	5.6	14.6	5.8	15.3	6.3	15.2	6.4	14.4	6.2	14.3	6.3			
C			13.0	5.9	15.4	7.7	21.3	9.1	21.3	9.3	21.2	9.4	18.8	6.6	15.0	5.6		
D		13.0	5.8	15.4	7.7	21.3	9.0	21.2	9.2	21.2	9.3	21.2	9.4	18.7	6.6	15.0	5.6	
E	13.0	5.0	19.1	7.7	21.4	9.0	21.3	9.2	21.2	9.3	21.1	9.4	21.1	9.5	18.7	8.4	13.0	5.5
F	5.0	15.4	7.7	21.4	9.0	21.3	9.1	21.8	9.5	21.7	9.6	21.1	9.4	21.1	9.5	18.8	6.6	12.8
G	13.0	6.1	21.4	9.0	21.3	9.1	21.8	9.5	21.7	9.6	21.7	9.6	21.1	9.4	21.2	9.4	15.2	5.4
H	7.6	18.7	9.1	21.3	9.2	21.8	9.5	21.7	9.6	21.7	9.6	21.7	9.6	21.2	9.3	21.2	8.0	18.3
J	18.3	7.9	21.3	9.2	21.2	9.5	21.7	9.6	21.7	9.6	21.7	9.6	21.7	9.3	21.2	9.2	18.6	7.7
K	7.7	18.6	9.2	21.2	9.3	21.7	9.6	21.7	9.6	21.7	9.6	21.7	9.5	21.2	9.2	21.3	7.9	18.3
L	18.3	8.0	21.2	9.3	21.2	9.6	21.7	9.6	21.7	9.6	21.7	9.5	21.8	9.2	21.3	9.1	18.7	7.6
M	5.4	15.2	9.4	21.2	9.4	21.1	9.6	21.7	9.6	21.7	9.5	21.8	9.1	21.3	9.0	21.4	6.1	13.0
N	12.8	6.6	18.8	9.5	21.1	9.4	21.1	9.6	21.7	9.5	21.8	9.1	21.3	9.0	21.4	7.7	15.4	5.0
O	5.5	13.0	8.4	18.7	9.5	21.1	9.4	21.1	9.3	21.2	9.2	21.3	9.0	21.4	7.7	19.1	5.0	13.0
P		5.6	15.0	6.6	18.7	9.4	21.2	9.3	21.2	9.2	21.2	9.0	21.3	7.7	15.4	5.8	13.0	
Q			5.6	15.0	6.6	18.8	9.4	21.2	9.3	21.3	9.1	21.3	7.7	15.4	5.9	13.0		
R				6.3	14.3	6.2	14.4	6.4	15.2	6.3	15.3	5.8	14.6	5.6	14.3			
S					6.1	14.1	6.0	14.2	5.9	14.2	5.7	14.3	5.6	14.2				

Figure D-9 Fuel Burnup (MWd/kgU) Distribution in Bundle Position 9
(ACR-700 284-Channel TAVEQUIV Model — 2-BS Fuelling Scheme)

	1	2	3	4	5	6	7	8	9	10	11	12	13	14	15	16	17	18
A					15.2	3.8	15.3	3.9	15.3	4.0	15.3	4.1	15.3	4.2				
B				15.3	3.8	15.6	4.0	16.4	4.3	16.4	4.4	15.6	4.3	15.5	4.3			
C			13.8	3.9	16.5	5.4	22.8	6.3	22.8	6.4	22.7	6.6	20.2	4.5	16.3	3.9		
D		13.9	4.0	16.5	5.3	22.8	6.3	22.8	6.5	22.8	6.6	22.7	6.7	20.2	4.6	16.3	3.9	
E	13.8	3.4	20.4	5.3	22.8	6.3	22.8	6.5	22.7	6.6	22.7	6.7	22.7	6.7	20.2	5.9	14.1	3.8
F	3.4	16.5	5.3	22.8	6.3	22.8	6.5	23.4	6.8	23.3	6.9	22.7	6.7	22.7	6.7	20.2	4.6	13.9
G	13.9	4.2	22.8	6.3	22.8	6.5	23.4	6.8	23.3	6.9	23.3	6.9	22.7	6.7	22.8	6.7	16.4	3.7
H	5.3	20.1	6.4	22.8	6.5	23.4	6.8	23.3	6.8	23.3	6.9	23.3	6.9	22.7	6.6	22.8	5.6	19.6
J	19.6	5.5	22.8	6.5	22.8	6.8	23.4	6.8	23.3	6.9	23.3	6.8	23.4	6.6	22.8	6.5	20.0	5.4
K	5.4	20.0	6.5	22.8	6.6	23.4	6.8	23.3	6.9	23.3	6.8	23.4	6.8	22.8	6.5	22.8	5.5	19.6
L	19.6	5.6	22.8	6.6	22.7	6.9	23.3	6.9	23.3	6.8	23.3	6.8	23.4	6.5	22.8	6.4	20.1	5.3
M	3.7	16.4	6.7	22.8	6.7	22.7	6.9	23.3	6.9	23.3	6.8	23.4	6.5	22.8	6.3	22.8	4.2	13.9
N	13.9	4.6	20.2	6.7	22.7	6.7	22.7	6.9	23.3	6.8	23.4	6.5	22.8	6.3	22.8	5.3	16.5	3.4
O	3.8	14.1	5.9	20.2	6.7	22.7	6.7	22.7	6.6	22.7	6.5	22.8	6.3	22.8	5.3	20.4	3.4	13.8
P		3.9	16.3	4.6	20.2	6.7	22.7	6.6	22.8	6.5	22.8	6.3	22.8	5.3	16.5	4.0	13.9	
Q			3.9	16.3	4.5	20.2	6.6	22.7	6.4	22.8	6.3	22.8	5.4	16.5	3.9	13.8		
R				4.3	15.5	4.3	15.6	4.4	16.4	4.3	16.4	4.0	15.6	3.8	15.3			
S					4.2	15.3	4.1	15.3	4.0	15.3	3.9	15.3	3.8	15.2				

Figure D-10 Fuel Burnup (MWd/kgU) Distribution in Bundle Position 10 (ACR-700 284-Channel TAVEQUIV Model — 2-BS Fuelling Scheme)

	1	2	3	4	5	6	7	8	9	10	11	12	13	14	15	16	17	18
A					15.9	2.2	16.0	2.3	16.1	2.4	16.0	2.4	16.0	2.6				
B				15.9	2.2	16.3	2.3	17.1	2.6	17.2	2.6	16.3	2.5	16.3	2.6			
C			14.4	2.3	17.2	3.1	23.8	3.7	23.9	3.9	23.8	3.8	21.2	2.7	17.1	2.3		
D		14.4	2.2	17.2	3.1	23.8	3.6	23.8	3.8	23.8	3.8	23.8	3.9	21.2	2.7	17.1	2.2	
E	14.4	1.9	21.2	3.0	23.8	3.6	23.8	3.7	23.8	3.8	23.8	3.8	23.8	3.9	21.2	3.4	14.8	2.2
F	1.9	17.1	3.0	23.8	3.6	23.8	3.7	24.4	3.9	24.4	4.0	23.8	3.8	23.8	3.9	21.2	2.6	14.5
G	14.5	2.4	23.8	3.6	23.8	3.7	24.4	3.9	24.4	3.9	24.4	4.0	23.8	3.8	23.8	3.8	17.1	2.1
H	3.0	20.9	3.6	23.8	3.7	24.4	3.9	24.4	3.9	24.4	4.0	24.4	3.9	23.8	3.8	23.8	3.2	20.5
J	20.5	3.1	23.8	3.7	23.8	3.9	24.4	3.9	24.4	4.0	24.4	3.9	24.4	3.8	23.8	3.7	20.9	3.0
K	3.0	20.9	3.7	23.8	3.8	24.4	3.9	24.4	4.0	24.4	3.9	24.4	3.9	23.8	3.7	23.8	3.1	20.5
L	20.5	3.2	23.8	3.8	23.8	3.9	24.4	4.0	24.4	3.9	24.4	3.9	24.4	3.7	23.8	3.6	20.9	3.0
M	2.1	17.1	3.8	23.8	3.8	23.8	4.0	24.4	3.9	24.4	3.9	24.4	3.7	23.8	3.6	23.8	2.4	14.5
N	14.5	2.6	21.2	3.9	23.8	3.8	23.8	4.0	24.4	3.9	24.4	3.7	23.8	3.6	23.8	3.0	17.1	1.9
O	2.2	14.8	3.4	21.2	3.9	23.8	3.8	23.8	3.8	23.8	3.7	23.8	3.6	23.8	3.0	21.2	1.9	14.4
P		2.2	17.1	2.7	21.2	3.9	23.8	3.8	23.8	3.8	23.8	3.6	23.8	3.1	17.2	2.2	14.4	
Q			2.3	17.1	2.7	21.2	3.8	23.8	3.9	23.9	3.7	23.8	3.1	17.2	2.3	14.4		
R				2.6	16.3	2.5	16.3	2.6	17.2	2.6	17.1	2.3	16.3	2.2	15.9			
S					2.6	16.0	2.4	16.0	2.4	16.1	2.3	16.0	2.2	15.9				

Figure D-11 Fuel Burnup (MWd/kgU) Distribution in Bundle Position 11 (ACR-700 284-Channel TAVEQUIV Model — 2-BS Fuelling Scheme)

	1	2	3	4	5	6	7	8	9	10	11	12	13	14	15	16	17	18
A					15.9	0.9	16.0	0.9	16.1	1.0	16.0	1.0	16.0	1.0				
B				15.9	0.9	16.3	0.9	17.1	1.1	17.2	1.0	16.3	1.0	16.3	1.1			
C			14.4	0.9	17.2	1.3	23.8	1.5	23.9	1.6	23.8	1.6	21.2	1.1	17.1	0.9		
D		14.4	0.9	17.2	1.3	23.8	1.5	23.8	1.6	23.8	1.6	23.8	1.6	21.2	1.1	17.1	0.9	
E	14.4	0.7	21.2	1.2	23.8	1.5	23.8	1.5	23.8	1.6	23.8	1.6	23.8	1.6	21.2	1.4	14.8	0.9
F	0.7	17.1	1.2	23.8	1.5	23.8	1.5	24.4	1.6	24.4	1.6	23.8	1.6	23.8	1.6	21.2	1.0	14.5
G	14.5	0.9	23.8	1.5	23.8	1.5	24.4	1.6	24.4	1.6	24.4	1.6	23.8	1.6	23.8	1.5	17.1	0.8
H	1.2	20.9	1.4	23.8	1.5	24.4	1.6	24.4	1.6	24.4	1.6	24.4	1.6	23.8	1.5	23.8	1.3	20.5
J	20.5	1.2	23.8	1.5	23.8	1.6	24.4	1.6	24.4	1.6	24.4	1.6	24.4	1.5	23.8	1.5	20.9	1.2
K	1.2	20.9	1.5	23.8	1.5	24.4	1.6	24.4	1.6	24.4	1.6	24.4	1.6	23.8	1.5	23.8	1.2	20.5
L	20.5	1.3	23.8	1.5	23.8	1.6	24.4	1.6	24.4	1.6	24.4	1.6	24.4	1.5	23.8	1.4	20.9	1.2
M	0.8	17.1	1.5	23.8	1.6	23.8	1.6	24.4	1.6	24.4	1.6	24.4	1.5	23.8	1.5	23.8	0.9	14.5
N	14.5	1.0	21.2	1.6	23.8	1.6	23.8	1.6	24.4	1.6	24.4	1.5	23.8	1.5	23.8	1.2	17.1	0.7
O	0.9	14.8	1.4	21.2	1.6	23.8	1.6	23.8	1.6	23.8	1.5	23.8	1.5	23.8	1.2	21.2	0.7	14.4
P		0.9	17.1	1.1	21.2	1.6	23.8	1.6	23.8	1.6	23.8	1.5	23.8	1.3	17.2	0.9	14.4	
Q			0.9	17.1	1.1	21.2	1.6	23.8	1.6	23.9	1.5	23.8	1.3	17.2	0.9	14.4		
R				1.1	16.3	1.0	16.3	1.0	17.2	1.1	17.1	0.9	16.3	0.9	15.9			
S					1.0	16.0	1.0	16.0	1.0	16.1	0.9	16.0	0.9	15.9				

Figure D-12 Fuel Burnup (MWd/kgU) Distribution in Bundle Position 12 (ACR-700 284-Channel TAVEQUIV Model — 2-BS Fuelling Scheme)